A STUDY OF DIAGONAL TENSION FAILURE IN REINFORCED CONCRETE BEAMS

SEPT. 1964

NO. 24

by

W. N. HARVEY

Joint Highway Research Project

PURDUE UNIVERSITY
LAFAYETTE INDIANA

Final Report

A STUDY OF DIAGONAL TENSION FAILURE IN REINFORCED CONCRETE BEAMS

TO: K. B. Woods, Director
Joint Highway Research Project

April 22, 1964

FROM: H. L. Michael, Associate Director
Joint Highway Research Project

Project: C-36-56J
File: 7-4-10

Attached is a Final Report "A Study of Diagonal Tension Failure in Reinforced Concrete Beams". The report has been authored by Mr. William N. Harvey, Graduate Assistant on our staff, and is the final report on the research approved by the Board on May 8, 1963 under a title similar to the title of the Final Report. Professor M. J. Gutzwiller directed the study and Mr. Harvey also used the report for a thesis for the MSCE degree.

The report contains a great amount of information from the literature and from experiments conducted as part of this study on the problem of diagonal tension in reinforced concrete beams. The report is presented for the record.

Respectfully submitted,

H. L. Michael

H. L. Michael, Secretary

HLM:bc

Attachment

cc: F. L. Ashbaucher
J. R. Cooper
W. L. Dolch
W. H. Goetz
F. F. Havey
F. S. Hill
G. A. Leonards
J. F. McLaughlin
R. D. Miles
R. E. Mills
M. B. Scott
E. J. Yoder
J. V. Smythe

Final Report

A STUDY OF DIAGONAL TENSION FAILURE IN REINFORCED CONCRETE BEAMS

by

William N. Harvey
Graduate Assistant

Joint Highway Research Project

Project: C-36-56J

File: 7-4-10

Purdue University

Lafayette, Indiana

April 22, 1964

ACKNOWLEDGMENTS

Acknowledgment is first made to the members of the board of the Joint Highway Research Project and to Professor K. B. Woods, Director, for providing funds for the project.

Special thanks is given to Professor M. J. Gutzwiller, major professor, and to Mr. R. H. Lee for their patient guidance and advice.

The author also wishes to express his appreciation to Mr. G. W. Foster and Mr. G. P. McClure, laboratory technicians, and to Mr. J. D. Pounds for their generous assistance in the laboratory.

TABLE OF CONTENTS

Table of Contents (Continued)

Table of Contents (Continued)

LIST OF TABLES

LIST OF TABLES (CONTINUED)

LIST OF FIGURES

Figure | Page

List of Figures (Continued)

List of Figures(Continued)

ABSTRACT

Harvey, William N., MSCE, Purdue University, August, 1964. "A Study of Diagonal Tension Failure in Reinforced Concrete Beams." Major Professor: M. J. Gutzwiller.

This research is an experimental study of the ultimate load behavior of reinforced concrete beams which fail in shear. Specifically, the objectives of the investigation were:

1) to compare the strengths and modes of failure of companion beams with and without shear reinforcement (vertical stirrups),
2) to determine how the shear strength is affected when part of the longitudinal tension steel is terminated within the tension zone.

Twenty beams of 6" x 13" rectangular cross-section were loaded to simulate a portion of a continuous girder subjected to concentrated loads. The beams were designed so that the critical region for failure was the length between the point of zero moment and the point of maximum negative moment - commonly called the shear span.

The major variables were the shear span to depth ratio and the amount of vertical stirrups within the shear span. Beams with nominal shear span to depth ratios of 2.2, 2.4, 2.9,

4.0, 4.4 were tested. In seven of the beams the negative tension steel was provided by four bars in two layers. All other beams contained two larger bars in a single layer. In addition, four beams were cast with the longitudinal tension bars cut off at the points where they were no longer required to resist tension. In all other specimens the longitudinal steel was extended throughout the full length of the beam.

It was found that the location of the critical diagonal tension crack relative to the support had a large influence on the mode ofshear failure and ultimate shear strength. The location of the critical diagonal crack, in turn, was dependent upon the length of shear span, the amount of web reinforcement, and upon local weakness induced by cutting off the longitudinal steel in the tension zone.

Detailed discussion of the failure patterns and individual beam behavior are presented along with the summary of test results.

LIST OF SYMBOLS

A_s	nominal area of tension steel
A'_s	nominal area of compression steel
A_v	cross-sectional area of one stirrup
a	length of critical shear span (distance from section of maximum moment to point of inflection)
b	width of beam section
C	total internal compression force in concrete
d	effective depth (measured to centroid of tension steel)
d'	distance from compression face to centroid of compression steel
jd	internal moment arm, straight-line theory
E_s	modulus of elasticity of steel
E_c	initial tangent modulus of concrete
f'_c	concrete compressive strength, 6" x 12" standard cylinder
f'_t	split-tension strength, 6" x 12" standard cylinder
f_v	stress in stirrup
f_{vy}	yield strength of stirrup steel
f_s	stress in longitudinal tension steel
f'_s	stress in longitudinal compression steel
f_{su}	stress in tension steel at failure of beam

LIST OF SYMBOLS (CONTINUED)

f_y		yield strength of longitudinal steel
M_s		ultimate shear-compression moment
M_u		ultimate flexural moment
M_x		maximum negative moment
M_y		maximum positive moment
n	E_s/E_c	modular ratio
p	A_s/bd	percentage longitudinal tension steel
P		total load
P_1, P_2		load on the overhang and load between supports, respectively
P_c		total load at formation of diagonal tension crack
P_u		total load at failure
r	$\frac{A_v}{bs}$	- web reinforcement ratio
s		horizontal spacing of stirrups
T		total force in tension steel
V		total shear at any section
V_a		shear in critical shear span
V_c		shear assigned to concrete (working stress design)
V'		shear assigned to stirrups (working stress design)
v		nominal shearing stress = $\frac{V}{bjd}$ or $\frac{V}{bd}$ as defined in text
v_c		portion of total shearing stress assigned to concrete or average shear at diagonal cracking
v_s		portion of total shearing stress assigned to stirrups

v_a	allowable nominal shearing stress ($\frac{V}{bjd}$)
v_u	ultimate shear strength
α	inclination of stirrups with respect to longitudinal axis
θ	inclination of diagonal crack with respect to longitudinal axis
ϵ_{cu}	strain at outermost compression fiber at failure
ϵ_{su}	strain in tension steel at failure
S.C.	shear-compression failure
D.T.	diagonal tension failure
F.T.	flexural tension failure
MII	strain in micro-inches per inch

INTRODUCTION

The Problem

In an effort to depart from the limitations imposed by the assumptions of elastic behavior, investigators for several years have studied the ultimate load behavior of reinforced concrete structures. While reasonable limits for design can be obtained from the basic fundamentals of mechanics, it is well known that the actual behavior of reinforced concrete beams does not conform with the standard theories of practice.

One result of this research effort is the ability to predict with reasonable accuracy the ultimate resistance of a beam section subjected to pure bending. Most flexural members are subjected to the combined action of bending and shearing forces which may seriously limit the moment capacity of a beam.

To establish the general conditions under which the strength of a beam will be affected or controlled by shear, one might consider the case of a simply-supported beam under two symmetrical concentrated loads. In this case the region between loads is in a state of pure bending; while the length

from the load to the support, commonly called the shear span, is subjected to a combination of shearing and bending forces.

When the length of the shear span is large (6 to 7 times the beam depth and greater), the pure bending forces developed at mid-span are large. As the load is increased, typical vertical tension cracks appear on the bottom side of the beam. Collapse of the beam will occur by crushing of the concrete in compression. For beams with normal amounts of tension reinforcement this is usually preceded by yielding of the steel. The presence of shear in the outer spans has no effect on the load carrying capacity.

However, if the loads are moved closer to the supports, the ratio of shear to moment is higher. The combination of shearing stresses and bending tensile stresses produces a principle tension acting at the inclination of approximately 45° at the neutral axis of the beam and nearly horizontal at the bottom of the beam. Evidence of this inclined tension is seen by the gradual change in inclination of the tension cracks as they approach the neutral axis of the beam. Before sufficient bending moment is developed to produce failure in flexure under the load point or in the middle span, a distinct diagonal tension crack appears and penetrates well into the compression zone. While this crack is usually an extension of the inclined portion of a flexural tension crack and cannot really be considered a separate one, it is distinct from the latter in that it penetrates deeply into the compression zone

at increasingly flatter slope, causing a significant redistribution of the internal stresses.

In general, it is the ability of the beam to accept this stress redistribution that determines the ultimate strength of the beam after formation of this diagonal crack. For beams without web reinforcement the strength beyond diagonal cracking seems to be dependent mainly upon the shear span to depth ratio. Provision of web reinforcement or stirrups, in general terms, has the effect of containing this crack, preventing its deep penetration into the compression zone, delaying the stress redistribution, and thereby increasing the strength.

A rational approach to the problem of predicting the load at which the inclined crack will form and penetrate into the compression zone would seem to be an analysis of the principle tension developed from a system of combined stresses. However, one can readily see that the distribution of shearing and normal bending stresses below the neutral axis is highly indeterminate. Cracking in the extreme tension fibers takes place at very early stages of loading. At sections coincident with these cracks the stress originally taken by the concrete is transferred to the tension steel. At sections between the cracks some degree of tension must be carried by the concrete, providing the bond between the steel and concrete is maintained. In addition, the shear once carried by the concrete must be zero across the crack. As a result there is probably a concentration of shearing stress at the top of the crack.

Standard Design Procedures

To establish a basis for design early investigators used as a measure of the diagonal tension a nominal unit shear derived on the basis that the concrete below the neutral axis carries no tension. The assumptions involved are illustrated in Figure 1.

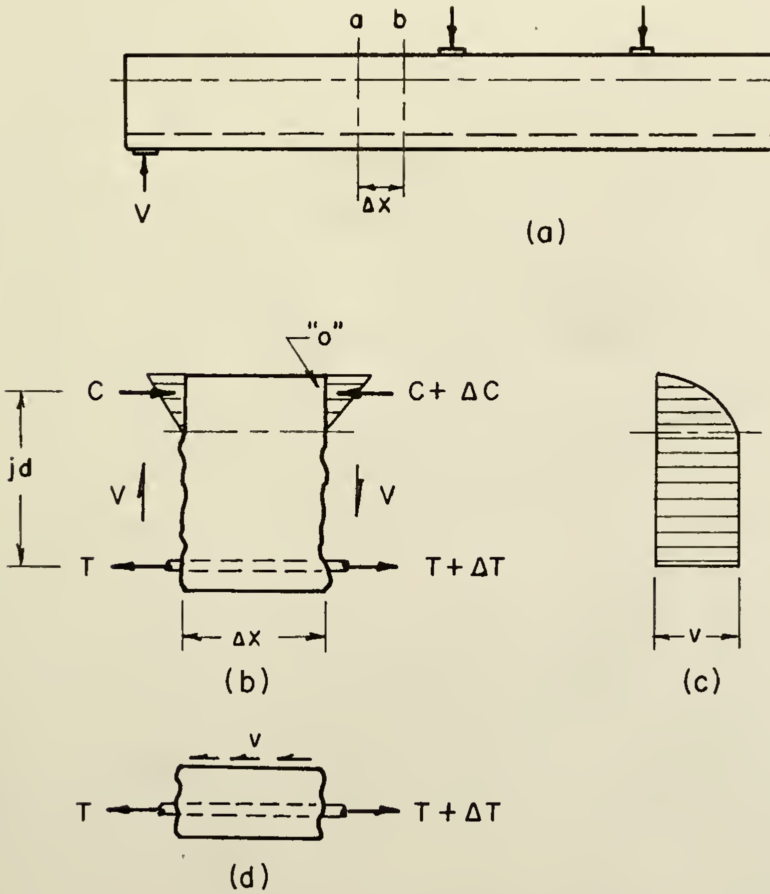

FIGURE 1. CONVENTIONAL SHEAR EQUATION

Considering a length, Δx, of a beam with fully developed flexural tension cracks (Figure 1b), the sum of the moments about point "0" must be zero:

$$\Delta T \, jd = V \, \Delta x$$

From Figure 1d summing horizontal forces yields:

$$\Delta T = vb \quad \Delta x$$

Combining these equations:

$$v = \frac{V}{bjd} \qquad \text{(Eq'n. 1)}$$

The shear distribution assumed in this derivation varies parabolically in the compression zone and is of constant magnitude below the neutral axis. (See Figure 1c) Since at the neutral axis the principle tension equals the unit shear, it was reasoned that $v = \frac{V}{bjd}$ could be used as a measure of the diagonal tension producing the critical inclined crack. The use of this equation as the basis for design with respect to shear has been almost universal. Most design codes have established allowable shearing stresses as a constant percentage of the concrete cylinder strength. American standards in the past have allowed a unit shear of .03 f'_c for beams without web reinforcement.

When this allowable shearing stress is exceeded, shear reinforcement in some form is required. The method used to design the shear reinforcement is based on the so-called "truss analogy".

Stresses in the stirrups are assessed by summation of vertical forces with the assumption that the uncracked compression zone carries a shear corresponding to $v_c = .03\ f'_c$. Included also is the assumption that the diagonal tension crack penetrates to a depth jd above the tension steel (that is, to the centroid of compression). Figure 2. On this basis the strength of beams with web reinforcement is derived in the following way.

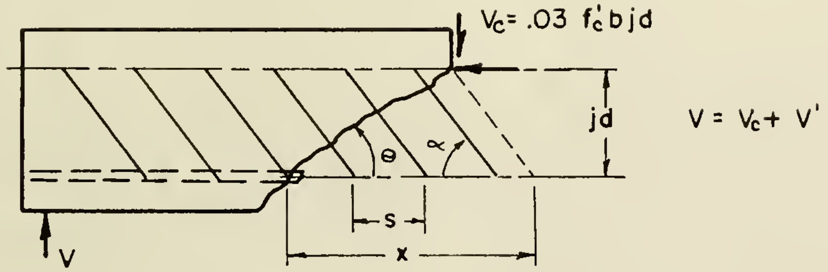

FIGURE 2. BASIS FOR TRUSS ANALOGY

θ = inclination of the diagonal tension crack

α = inclination of the stirrups

s = horizontal spacing of the stirrups

V = total shear

V_c = shear assumed to be carried by the concrete

V' = shear assumed to be carried by stirrups = $V - V_c$

A_v = cross-sectional area of one stirrup

f_v = stress in a stirrup

The number of stirrups crossed by the crack can be expressed as (See Figure 2)

$$N = \frac{x}{s} \text{ where } x = jd\,(\cot\theta + \cot\alpha)$$

The force in one stirrup is $A_v f_v$. Equating the vertical component of the forces in all stirrups crossed by the diagonal crack to the shear assigned to them gives

$$N\,A_v f_v \sin\alpha = V'$$

or

$$A_v f_v = \frac{V'}{\sin\alpha} \; \frac{s}{jd} \; \frac{1}{(\cot\theta + \cot\alpha)}$$

The usual assumption is that $\theta = 45^\circ$. Thus

$$A_v f_v = V' \frac{s}{jd} \left(\frac{1}{\sin\alpha + \cos\alpha} \right) \qquad \text{(Eq'n. 2)}$$

or

$$A_v f_v = V' \frac{s}{jd} \frac{1}{K}$$

where

$$K = \sin\alpha + \cos\alpha$$

Writing the portion of the total unit shear carried by the stirrups as $v_s = \frac{V'}{bjd}$ and the stirrup ratio as $r = \frac{A_v}{bs}$, the total shear strength of beams with stirrups is

$$v = v_c + v_s = .03 f'_c + Krf_v \qquad \text{(Eq'n. 5)}$$

Probably the largest source of error in this analysis is the arbitrary assignment of the portion of the total shear to be carried by the concrete. The penetration of the crack and, in turn, the capacity of the concrete for carrying shear would certainly depend on the amount and spacing of stirrups. The shear rigidity of the longitudinal steel, a quantity neglected in this procedure, is greatly increased by closely spaced stirrups.

The design method described above has been in use since the early 1900's. While it has withstood the tests of time and practice, it does not offer a rational explanation of beam behavior. Safe designs have resulted primarily through the selection of low allowable stresses. Beam tests through the years have yielded a wide variation in safety factors with respect to the strengths predicted by this method. In a recent report of the ACI-ASCE Committee on Shear and Diagonal Tension (1)*, evaluation of data from some 400 test beams showed no well-defined relation between concrete cylinder strength and the nominal shearing stresses at diagonal cracking.

* Numbers in parentheses refer to the BIBLIOGRAPHY at end of thesis.

Although the number of investigations involving shear behavior has been tremendous over the last two decades, it has been only within the last 3 to 4 years that enough information could be assembled to offer a departure from the conventional method of design. Major changes were made with respect to shear in the latest revision (1963) of the ACI Building Code. Even then, the revision was restricted to the method for determining the average shearing stress at diagonal cracking for beams without web reinforcement. Available information on the behavior of beams with stirrups was not sufficient to allow a departure from the conventional "truss analogy" concept.

Review of the Literature

A rational explanation of the basic distribution of internal stresses after diagonal cracking is still lacking. However, intensified efforts over the last several years have brought about a much better understanding of the general mechanism of shear failure. It is the purpose of the following discussion to point out some of the significant findings available in the literature. No attempt is made to present a historical development, as several excellent reviews are already available. (1), (19), (21)

Beams without Web Reinforcement

With the acceptance of the use of unit shear as a design criterion, it seems that the fundamentals of the problem were forgotten for a number of years. Early investigators were well aware that the unit shear at which diagonal cracking occurred was not a function of concrete strength alone. As more and more test results became available, investigators, still adhering to the idea of a limiting unit shear, began noticing that the average shearing stress at diagonal cracking was dependent on three major variables, instead of one.

These are:

1) the concrete compressive strength,

2) the percentage of longitudinal reinforcement, and

3) the magnitude of normal bending stress relative to the average shearing stress at the critical section.

The distinct effect of the third of these caused a return in the early 1950's to the basic consideration that the problem was one of combined stresses.

While a reasonable value of the principle tension stress after cracking cannot be calculated, the effect of bending stresses on the average shearing stress at diagonal cracking can be expressed by the dimensionless quantity M/Vd. For the simple beam under concentrated loads (Figure 3) the M/Vd ratio at the critical section is the shear span-to-depth ratio, a/d.

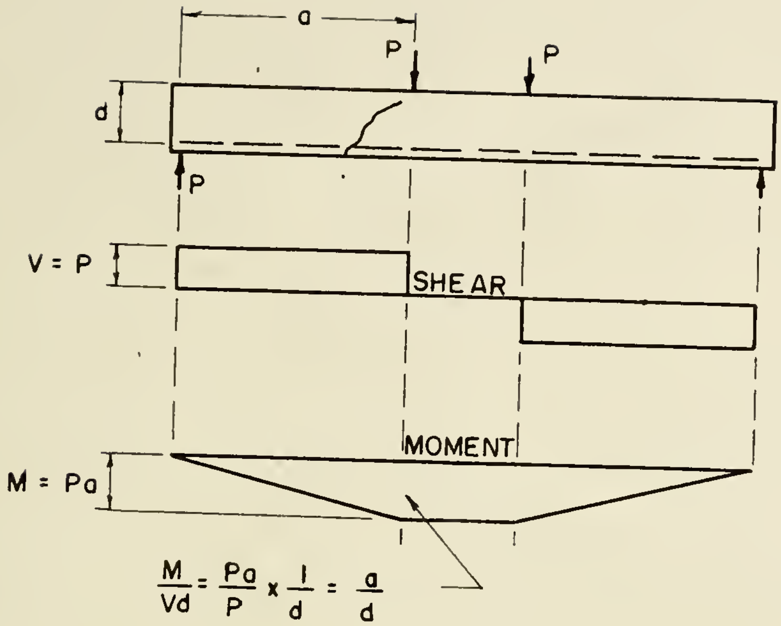

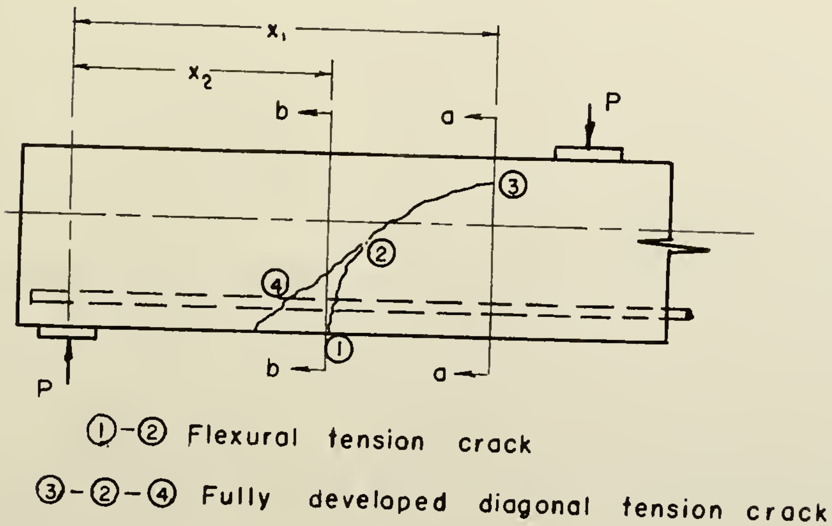

FIGURE 3. FORMATION OF DIAGONAL TENSION CRACK

It has definitely been shown that, as the length of shear span is increased, the average unit shear at diagonal cracking decreases. (6), (9), (13), (25), (28). That is, for increasing a/d ratios the normal bending stress component of the resultant diagonal tension is increasingly greater. Further evidence of this interaction of moment and shear is the fact that above a certain a/d ratio failure in flexure will occur before the diagonal tension stresses are high enough to develop the critical inclined crack. This limiting ratio seems to vary with the percentage of longitudinal steel, the number of loads in the span, and the axial load. (6), (10), (13), (21), (25).

Often the diagonal tension crack is an extension into the compression zone of the inclined portion of an existing flexural tension crack. (Figure 3 pt. 2 to pt. 3). The crack has also been noted to form near middepth (pt. 2), and extend both into the compression zone (pt. 3) and back towards the tension steel (pt. 3 to pt. 4), many times including the top of an existing flexural crack. In either case the diagonal crack almost always extends back to the tension steel (pt. 2 to pt. 4) nearly simultaneously with its appearance near mid-depth.

For beams without web reinforcement the strength beyond that at diagonal cracking seems to depend mainly upon the shear span to depth ratio (or M/Vd ratio). Beams with very short shear spans exhibit considerable reserve strength beyond

the formation of the initial diagonal crack. For relatively long shear spans the formation of the diagonal tension crack and complete failure often take place simultaneously.

Associated with these observations several investigators have reported two general modes of shear failure. Taking for example the simply-supported beam under a concentrated load, it has been noted for shear span-depth ratios below a certain value the crack generally stops at some point within the compression zone. With increasing load it gradually penetrates deeper. As the zone is greatly reduced, the compressive stress must be greatly increased. Ultimate failure is by crushing of the concrete in this reduced compression zone, generally adjacent to the load point. This type of failure is commonly called the shear-compression failure.

Distinct from this is the so-called sudden diagonal tension failure occurring in beams of longer shear span. Generally failure occurs as soon as the diagonal crack forms. If failure does not occur simultaneously, the crack penetrates rapidly into the compression zone, and very little increase in load is required to cause collapse.

Shown in Figure 4 is a plot of the shear at diagonal cracking and at ultimate load versus the shear span to depth ratio for a group of simply-supported beams reported by Morrow and Viest (25). For very short beams ($M/Vd = 1$) the ultimate failure load was about twice the diagonal cracking load. Other investigators have reported failure loads as much as 2.5 to 3 times the diagonal cracking loads for similar beams. As the

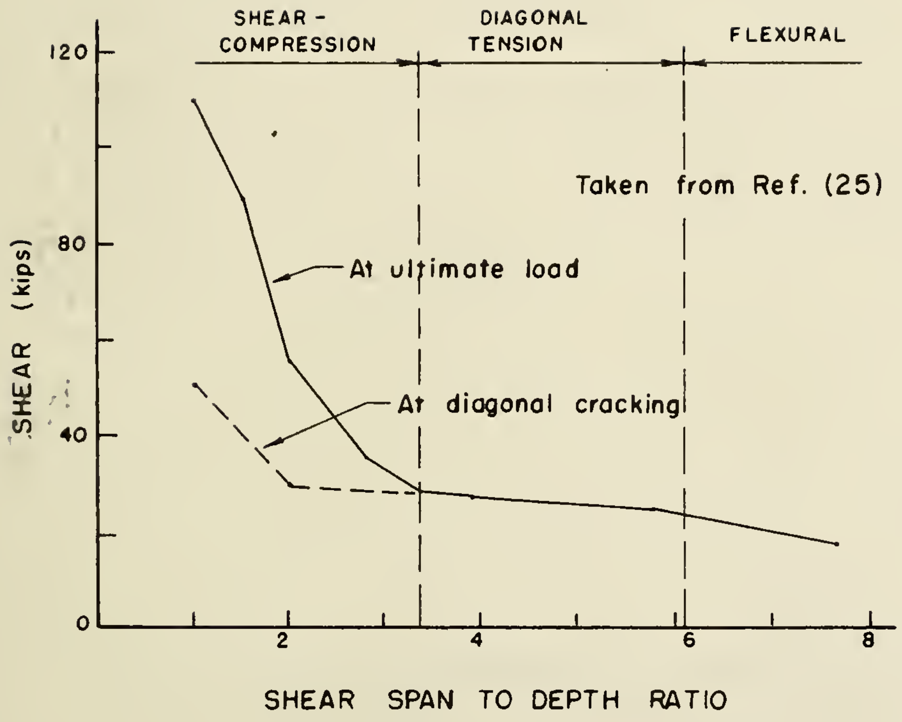

FIGURE 4. SHEAR STRENGTH VS. a/d RATIO

shear span is increased, this reserve strength becomes smaller. At a/d of approximately 3.4 the formation of the diagonal tension crack results in immediate failure. In addition, the mode of failure changes from shear-compression to the diagonal tension type. In the diagonal tension failure concrete strains remain low. Failure results from the crack's splitting entirely through the beam at increasingly flatter slope.

The reasons for the difference in behavior with length of shear span are not entirely clear. There is evidence that the M/Vd ratio is not the only controlling factor. The most significant influence seems to be the location of the diagonal crack. In Hanson's tests of simply-supported lightweight aggregate beams (17) all specimens had a shear span to depth ratio of 2.5. Some beams failed in sudden diagonal tension simultaneously with the formation of the diagonal crack. Others failed in shear-compression at loads substantially greater than the diagonal cracking load. In all beams failing in diagonal tension, the crack intersected the tension steel farther away from the concentrated load and was located much higher in the compression zone. Bower (6) reported similar findings in his tests of restrained beams with M/Vd = 2.5.

While in these two instances the crack location seemed to depend merely on chance, there is evidence that the crack is generally located farther from the section of maximum moment with increasing shear span. Several investigators have reported that the critical diagonal tension crack intersected the tension steel at a point generally midway between the points of maximum and zero moment. Ferguson (13) is of the opinion that the high local compression in the vicinity of the concentrated load is the factor explaining the increased resistance for short shear spans. He explains that crack development is restrained by this vertical compression,

and thus shear failure is delayed until the bending compression over the reduced section is high enough to result in crushing. In the case of the longer shear span, the crack develops farther out from the load point and local compression has little restraining effect upon the crack development. This hypothesis was supported by comparative tests of a beam, first, with loads concentrated at the top and, second, with the loads applied as shears to the sides. The M/Vd ratio was 1.35. In the first case failure was by shear compression; while in the latter failure was the sudden diagonal tension type at a greatly reduced load.

Looking more closely at the mechanism of shear failure, one can see the presence of other effects which will tend to modify the two general modes of failure. Once the diagonal crack begins to penetrate the compression zone, a substantial redistribution of internal stresses must occur. Because of the reduced concrete area, both the compressive and shearing forces in the region above the crack must be increased. Looking at a free-body of the portion of a beam outside the crack, (pts. 1-2-3) Figure 3, the summation of moments about the centroid of compression in the uncracked portion of the beam (Section a-a), shows that the steel at section b-b must carry an increased tension, corresponding to the greater external moment at section a-a. There is undoubtedly some amount of dowel action here, which would tend to relieve somewhat the shear carried by the uncracked compression zone and the tension

in the steel at this point. However, as the crack widens and rotation tends to concentrate about the uncracked portion at section a-a, the dowel forces are greatly increased and soon destroyed through the formation of the crack, pt. 2 to pt. 4. The increased steel tension, in addition, produces greatly increased bond stresses between the section at the crack and the sections closer to the support. This, combined with the dowel action, often leads to progressive destruction of bond throughout the shear span. Without sufficient anchorage by hook or by extension beyond the support immediate failure could result. When anchorage is provided, true beam action is lost, and behavior is then similar to that of a tied arch. (28), (29)

There has been some question as to whether the shear strength of a T-Section can be predicted from the results of tests on rectangular sections. There seems to be little information on direct comparisons of T-Beams and rectangular beams; however, indications are that the load at the formation of the diagonal crack in a T-Beam is comparable to that of a rectangular beam of the same width as the T-Beam stem. (31) The ultimate strength behavior of T-Beams seems to be somewhat different. Simple-span T-beams tested by Al-Alusi(5) indicate that the large compression area provided by the flange will not allow development of the shear-compression type failure. Shear span to depth ratios were varied from 2 to 7.8, and all failed by diagonal tension. All beams exhibited some reserve strength beyond diagonal cracking with increasingly greater

amounts for M/Vd ratios below four.

The shear behavior of a beam is also adversely affected by cutting off tension reinforcement in accordance with moment requirements. When bars are terminated -- say in the negative moment region of a continuous beam -- where they are no longer required to resist flexural tension, there occurs a discontinuity which has been noted in some cases to cause early formation of the diagonal tension crack. Ferguson (14) has reported that the load at diagonal cracking may be as low as 70 percent of that for the same beam with the steel fully extended. In addition, after formation of the diagonal crack, there occurs a large increase in steel tension at the point where the crack intersects the steel. If the steel has been reduced at this point, it is possible that premature yielding of the tension reinforcement could result.

While the shear at shear-compression failure generally decreases with increasing M/Vd ratios, Figure 4, the moment required to produce the ultimate crushing has been found to be reasonably constant. (6), (9), (21). This fact has led to various attempts to formulate a criterion of shear-compression failure based upon a limiting moment. The approach has been similar to the ultimate load analysis used for flexural failure. This involves the assumption of an ultimate compressive stress distribution, the parameters of which must be determined empirically. Upon writing the equations of equilibrium, the problem reduces to satisfying strain compatibility across the

section. While it has been shown that the distribution of strain in a flexural type failure is linear, this assumption cannot be made for the shear-compression failure because of the influence of the diagonal crack. As the crack widens, there tends to be concentrated rotation about the compression zone above the crack. This is further complicated when splitting along the steel occurs.

At least four different attempts have been made to establish a limiting moment equation. (21), (24), (25), (30). In each case, however, the assumed parameters have depended so heavily on empirical determination that it is doubtful whether they can be found to be generally applicable. Moody's equation, (24), developed from a series of simple-span and restrained beams, was found to give good results also for a series of two-span continuous beams under one and two loads (27). However, when extended to a series of two-span continuous beams under multiple point loads, the comparisons of test to calculated strengths were "poor and inconclusive" (8). In addition, there is some question as to whether such a strength criterion should be used, since the development of the shear-compression failure in beams without web reinforcement has been found to depend on how the load is transferred to the beam and in a few cases upon chance location of the diagonal crack.

Beams with Web Reinforcement

Research has been devoted primarily to the study of beams without web reinforcement. Of the few investigations

containing web reinforcement as a major variable, most have been restricted to beams of low M/Vd values.

In general the function of stirrups is to delay the sudden redistribution of stresses upon formation of the diagonal tension crack. Stirrups have no noticeable effect on beam behavior prior to formation of the diagonal crack. It has been found that stirrups carry little stress until they are crossed by an inclined crack.

Stirrups affect the mechanism of shear failure discussed above in several ways. First, they accept a major portion of the shear originally carried by the concrete, thus relieving the stress concentration in the concrete above the crack. This, in turn, prevents the deep penetration of the crack into the compression zone. Stirrups relieve the sudden increase in steel tension observed at the bottom of the crack in beams without stirrups. In addition, they hold the crack together and prevent the concentrated rotation about the top of the crack. The capacity of the tension steel for carrying shear by dowel action is substantially increased. Splitting along the tension steel is delayed and many times prevented, thus delaying the resulting loss in bond.

Beam action is effectively maintained until the yield strain of the stirrups is reached. Further behavior is similar to that of the beam without web reinforcement in which the diagonal crack has formed. For short shear spans ultimate failure is by shear-compression, following yielding

of the stirrups. (9), (16), (23). For longer shear spans there is evidence that the mode of failure is also shear-compression. (7), (16). Although this was shown (7) to be true for M/Vd ratios of 4, 5, and 7, the number of tests of shear-reinforced, long-span beams has been very limited. There is some speculation (1), that for beams with high M/Vd ratios and small amounts of web reinforcing, failure will still be of the sudden diagonal tension type with the stirrups yielding immediately upon diagonal cracking.

The strength of beams with web reinforcement has generally been found to be overly conservative with respect to that predicted by the conventional truss analogy. It is well accepted in this country that both the concrete compression zone and the web reinforcement contribute significantly to the shear capacity. The usual assumption is that the compression zone will carry the shear corresponding to the diagonal cracking strength of the beam without web reinforcement. Stirrups are proportioned to carry the shear in excess of this value. However, with the presence of stirrups the shear carrying capacity of the compression zone is greatly increased. This is primarily because of the restraint to penetration of the diagonal crack offered by the stirrups. In addition, stirrups greatly increase the dowel capacity of the longitudinal reinforcement -- a quantity neglected by the assumptions of the truss analogy.

Recent Changes in Design Procedures

Early in 1960, the ACI-ASCE Committee 326 on "Shear and Diagonal Tension" began correlating the vast amount of research data accumulated in the 1950's. Because a basic explanation of observed behavior could not be extracted, the results of this study were necessarily empirical. Primarily the recommended changes in design procedures were restricted to beams without web reinforcement. (1)

Recognizing the three major variables -- concrete strength, M/Vd ratio, and percentage of tension reinforcement -- the committee used a formulation proposed by I. M. Viest (1), (17) to obtain a relationship for the diagonal cracking load. This was based on the logical consideration that the problem was one of excessive principal tension produced by a combination of shearing and normal bending stresses. The formulation contains the following assumptions:

1) The shearing stress in the concrete is assumed proportional to the average shearing stress over the cross section; i.e.,

$$v = F_2 \frac{V}{bd}$$

2) The tensile bending stress (f_t) is proportional to the tensile steel stress (f_s) computed by use of the cracked section theory; i.e.,

$$f_t = F_1 \frac{M}{npbd^2}$$

3) The tensile strength of the concrete and its modulus of elasticity are linear functions of

$$\sqrt{f'_c}$$

On the basis of these assumptions, the equation for the principal stress at a point was used to derive an expression for the average shearing stress at diagonal cracking. Inclusion of the first two assumptions yields

$$v_c = \frac{V}{bd} = \left(A + B\,\frac{E_s}{E_c}\,\frac{V\,pd}{M}\right) f'_t$$

where

f'_t represents the resistance of the concrete to the principal tension stress.

This is further simplified with the third assumption to

$$v_c = \frac{V}{bd} = \left(A'\sqrt{f'_c} + B'\,\frac{V\,pd}{M}\right)$$

Originally, 194 test beams were used to empirically determine the values of the constants A' and B'. The parameters A' = 1.9 and B' = 2500 were chosen such that the equation yielded a conservative estimate for the majority of the beams included in the analysis. Although these 194 beams were of rectangular cross-section and were subjected only to one or two concentrated loads, the equation

$$v_c = \frac{V}{bd} = 1.9\sqrt{f'_c} + 2500\,\frac{V\,pd}{M} \qquad \text{(Eq'n. 4)}$$

was later extended to include data of over 400 test beams. These additional investigations indicated that the equation was also applicable to various loading and support conditions, to various shapes, and to beams with high strength reinforcement.

Although the equation is empirical and as such is limited to the conditions of the tests which define its parameters, it has a much more logical basis than the conventional shear design equation. The three variables which had previously been shown to affect the average shear at diagonal cracking are now included. This equation, as proposed by Committee 326 in their report (1), was later adopted in the ACI Building Code revision of 1963. (3)

The reserve strength of beams without web reinforcement in excess of the diagonal cracking load, experienced in beams of short shear span was not recognized by the committee. This was primarily due to the feeling that the conditions under which this excess strength could be fully utilized are not well defined. In addition, shear failures in the absence of web reinforcement are sudden and brittle in nature, generally giving very little warning. To be consistent with the ultimate strength design method, it was felt that shear reinforcement should be provided for loads in excess of that at diagonal cracking to insure a more ductile type failure.

Because of the lack of beam tests with shear reinforcement, the committee could not recommend any changes in existing

procedures for proportioning web reinforcement. Thus the old truss analogy method of assessing the shear carried by the stirrups still remains.

A second major change in the 1963 Code revision was the provision on tension steel cut-off. Tension steel now cannot be terminated within the tension zone, unless one of three requirements are met. This change arose from test results which indicated a definite reduction in shear strength in beams with bars cut off at the points where they were no longer needed to resist tension.

PURPOSE AND SCOPE

The objective of this study was to observe the behavior of beams of different shear span-to-depth ratios with varying amounts of web reinforcement. Of particular interest were:

1) The behavior of long-span beams with light and heavy amounts of web reinforcement;
2) The effect on shear strength of cutting-off the longitudinal reinforcement in the negative moment region of a continuous beam.

The tests were limited to beams of rectangular cross-section and to one set of loading conditions. Efforts were concentrated on relating the formation of the diagonal tension crack and the mode of failure to strains in the tension steel, concrete, and stirrups.

It was the intent that this particular laboratory study, combined with a review of recent findings in the area, would provide a basis for more comprehensive studies of diagonal tension failures.

TEST SPECIMENS AND PROCEDURES

Description of Specimens

All beams were simply-supported with one overhang. One concentrated load (P_1) was applied to the overhang and one (P_2) to the region between the supports. These loads were brought to the specimen as reactions from a steel wide flange beam. The point load to the steel beam was positioned to develop a specific ratio of maximum negative moment to maximum positive moment. The details and dimensions of the specimens, along with the applied shears and moments, are shown in Figure 5 and Table 1.

All beams had the same 6" x 13" rectangular cross-section. The major variables were the length of shear span "a", the arrangement of the longitudinal tension steel, and the amount of web reinforcement within the shear span. For control purposes companion specimens were tested with no shear reinforcement within the length "a". In four beams the longitudinal steel was cut off where it was no longer required to resist tension. In all other specimens, the steel was extended the full length of the beam.

To restrict failure to the shear span "a", an excessive amount of web reinforcement was provided in the overhang and

MOMENT

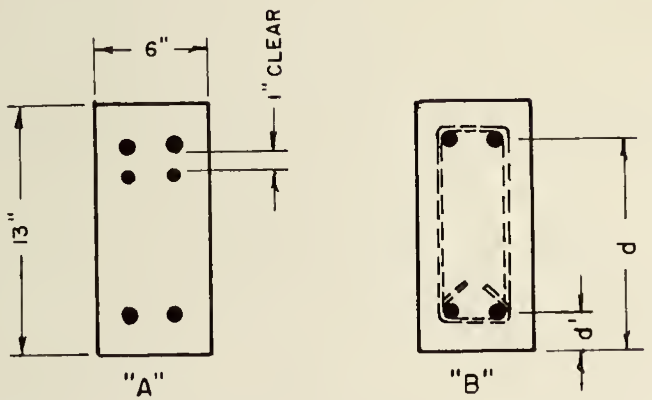

CROSS SECTION
(Negative Moment Region)

SERIES	I	II	III
M_x/M_y	1.5	2	2
V_a	.346 P	.310 P	.247 P
M_x	8.30 P	9.94 P	10.87 P

"A"- Beam: 2-No. 5 & 2-No. 4 Top

"B"- Beam: 2-No. 6 Top

All Beams: 2-No. 5 Bottom

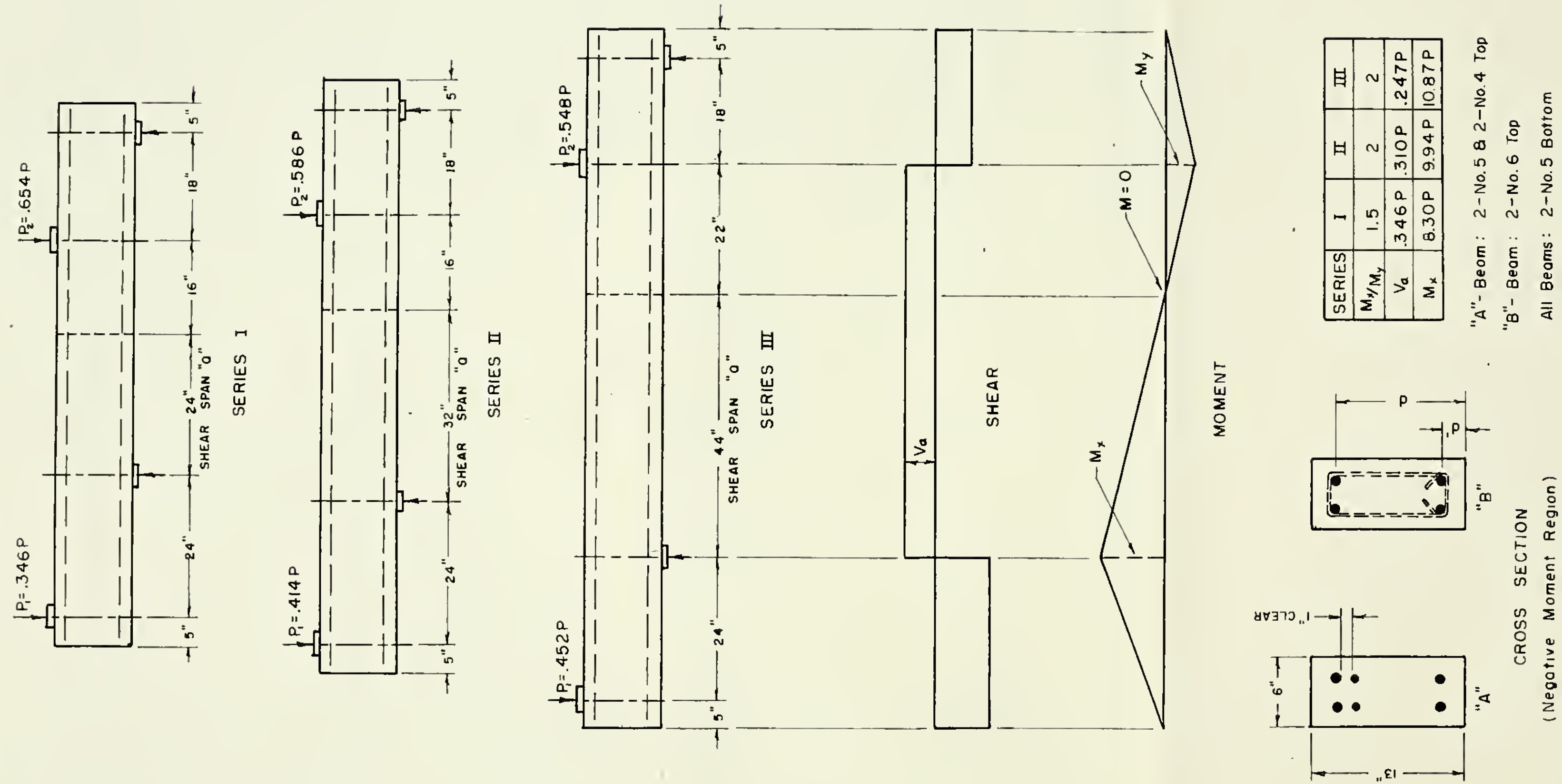

SERIES	I	II	III
M_x/M_y	1.5	2	2
V_a	.346P	.310P	.247P
M_x	8.30P	9.94P	10.87P

FIGURE 5. DETAILS OF SPECIMENS

TABLE 1.

PROPERTIES OF BEAM SPECIMENS

Beam Designation	Effective Depth to Negative Tension Steel d * (inches)	Distance from Bottom Face to Bottom Steel d' (inches)	Length of Shear Span a (inches)	Shear Span to Depth Ratio a/d	Longitudinal Reinforcement: Top (number of bars and sizes)	Longitudinal Reinforcement: Bottom (number of bars and sizes)	Ratio of Negative Tension Steel p (A_s/bd)	Web Reinforcement: Size and Spacing **	Web Reinforcement: r (A_v/bs)	Web Reinforcement: r f_{vy} *** (psi)	Concrete Compressive Strength f'_c (psi)	Concrete Split - Tensile Strength f'_t (psi)	Age (days)	Initial Tangent Modulus of Elasticity E_c (psi x 10^6)
IA-1	10.01	2.3	24	2.4	2-No.5 2-No.4	2-No.5	.0170	----	---	---	3087	410	14	2.65
-2	10.21	2.4	24	2.4	2-No.5 2-No.4	2-No.5	.0167	----	---	---	4032	366	14	2.83
-3	10.01	2.2	24	2.4	2-No.5 2-No.4	2-No.5	.0170	----	---	---	4207	422	14	2.94
-4	10.21	2.3	24	2.4	2-No.5 2-No.4	2-No.5	.0167	----	---	---	3957	404	14	3.05
IB-1	10.95	2.3	24	2.2	2-No.6	2-No.5	.0134	----	---	---	3557	497	14	2.67
-2	11.10	2.3	24	2.2	2-No.6	2-No.5	.0132	----	---	---	4240	355	7	2.73
IIB-1	11.20	2.35	32	2.9	2-No.6	2-No.5	.0131	----	---	---	4380	356	7	2.84
-2	11.15	2.3	32	2.9	2-No.6	2-No.5	.0132	No. 4 Wire at 6"	.00211	77.2	4310	412	7	2.86
-3	11.10	2.2	32	2.9	2-No.6	2-No.5	.0132	No. 4 Wire at 3 1/2"	.00362	132.5	4590	477	7	3.15
-4	11.10	2.3	32	2.9	2-No.6	2-No.5	.0132	No. 4 Wire at 3 1/2"	.00362	132.5	4210	379	7	3.24
-5	11.10	2.2	32	2.9	2-No.6	2-No.5	.0132	----	---	---	4360	416	7	3.25
IIIA-1	10.01	2.2	44	4.4	2-No.5 2-No.4	2-No.5	.0170	----	---	---	4260	461	14	3.31
-2	10.11	2.3	44	4.4	2-No.5 2-No.4	2-No.5	.0168	----	---	---	4095	402	14	2.87
-3	10.21	2.3	44	4.4	2-No.5 2-No.4	2-No.5	.0167	----	---	---	4155	483	14	3.18
IIIB-1	10.90	2.3	44	4.0	2-No.6	2-No.5	.0135	----	---	---	4210	436	14	2.85
-2	11.03	2.3	44	4.0	2-No.6	2-No.5	.0133	No. 4 Wire at 8"	.00158	57.8	4550	449	7	3.12
-3	11.15	2.3	44	4.0	2-No.6	2-No.5	.0132	No. 4 Wire at 5 1/2"	.00230	84.2	4460	391	7	3.08
-4	11.15	2.3	44	4.0	2-No.6	2-No.5	.0132	No. 4 Wire at 4"	.00316	115.8	4505	412	7	3.22
-5	11.10	2.3	44	4.0	2-No.6	2-No.5	.0132	No. 4 Wire at 4"	.00316	115.8	4425	429	7	2.98
-6	11.10	2.3	44	4.0	2-No.6	2-No.5	.0132	----	---	---	4550	380	7	3.19

* "d" - measured to center of gravity of negative tension steel; ** average diameter of the No. 4 Wire = 0.220"; *** Based on average f_{vy} = 36,600 psi. Width, b = 6" for all beams.

in the region outside the load P_2. In addition, the maximum negative moment, M_x, was maintained at 1 1/2 and 2 times the maximum positive moment, M_y.

The specimens are grouped into three series, according to the length of shear span, "a".

Series I a = 24" , $\frac{M_x}{M_y} = \frac{3}{2}$

Series II a = 32" , $\frac{M_x}{M_y} \doteq 2$

Series III a = 44" , $\frac{M_x}{M_y} = 2$

In addition, the beams are given the designation A or B denoting the amount and position of top steel.

A - 2-No. 5 and 2-No. 4 in two layers, d = 10"

B - 2-No. 6 in one layer, d = 11"

Two No. 5 bars were used for the bottom reinforcing in all beams.

Materials

Concrete Mix

All concrete was made with Type 1 portland cement. With the exception of two beams the concrete strengths throughout the tests were maintained to a range of 4000 to 4600 psi. The concrete for the first nine beams cast yielded strengths of

4000 to 4300 psi at 14 days. The proportions for this mix by saturated-surface-dry weight were 1:3.28:5.01 (cement: sand:gravel) with a water-cement ratio (w/c) of .660 by weight and a cement factor of 4.38 sacks/yd^3. The remaining beams had a shorter curing time. The mix was then changed to a 1:2.28:3.63 mix, w/c = .506, and cement factor 5.91 sacks/yd^3. This mix gave strengths of 4200 to 4600 psi at 7 days.

Aggregates

The aggregates used were purchased from Western Indiana Aggregates Corporation, Lafayette. The coarse aggregate was a natural gravel of 1 1/2" maximum size. At the laboratory it was separated into two sizes to minimize segregation during handling, and all larger than 1" was discarded. By weight, 48 percent of No. 4 to 1/2" size was combined with 52 percent of 1/2" to 1" size, according to Fuller's maximum density curve. Average properties of the fine and coarse aggregates are shown below.

	Sp. Gr.*	Absorption*	Fineness Modulus	
Sand	2.64	1.57 percent	2.74	
Gravel	2.69	1.26 percent	----	1" max. size

* Based on saturated-surface-dry weight.

TABLE 2.

GRADATION OF SAND

Sieve Size	Percent Retained
No. 4	0.8
8	9.8
16	31.2
30	50.9
50	87.2
100	94.3

Reinforcing Steel

The longitudinal reinforcing was a high strength steel with average properties as shown in Table 3. The Nos. 4, 5, and 6 deformed bars used were rolled from the same heat. The properties shown are the averages from four coupons selected at random. A representative stress-strain curve is shown in Figure 55 ., Appendix A . The deformations met the requirements of ASTM-A305.

TABLE 3.

PROPERTIES OF LONGITUDINAL STEEL

Yield Stress	75.4 ksi
Ultimate Strength	117.0 ksi
Modulus of Elasticity	30.4×10^6 psi
Elongation in 8"	14.3 %

The 1/4" diameter plain bars used for stirrups in the overhang and the 18" exterior span were of hard grade steel having an average yield point of 50,000 psi.

Stirrups in the critical shear span, "a", were a very soft No. 4 wire (dia. = .220") obtained from The Continental Steel Corporation, Kokomo, Indiana. A coupon of this steel was selected from the group of stirrups in each beam to determine the stress-strain properties. The average properties of these coupons are shown in Table 4. A representative stress-strain curve is shown in Figure 56, Appendix A.

TABLE 4.

PROPERTIES OF THE STIRRUP STEEL

Yield Stress	36.6 ksi
Ultimate Strength	52.9 ksi
Modulus of Elasticity	30.0×10^6 psi

Fabrication and Curing

All specimens were cast in the 3/4" plywood forms, shown partially assembled in Figure 6. In addition to the bracing shown, four equally-spaced wooden straps were placed across the top to prevent "bulging" of the sides.

The steel was assembled into a rigid cage with the stirrups being wrapped around the longitudinal steel. To provide adequate stirrup anchorage the free ends were bent to form 135° hooks, as shown in Figure 7. Stirrups were bent

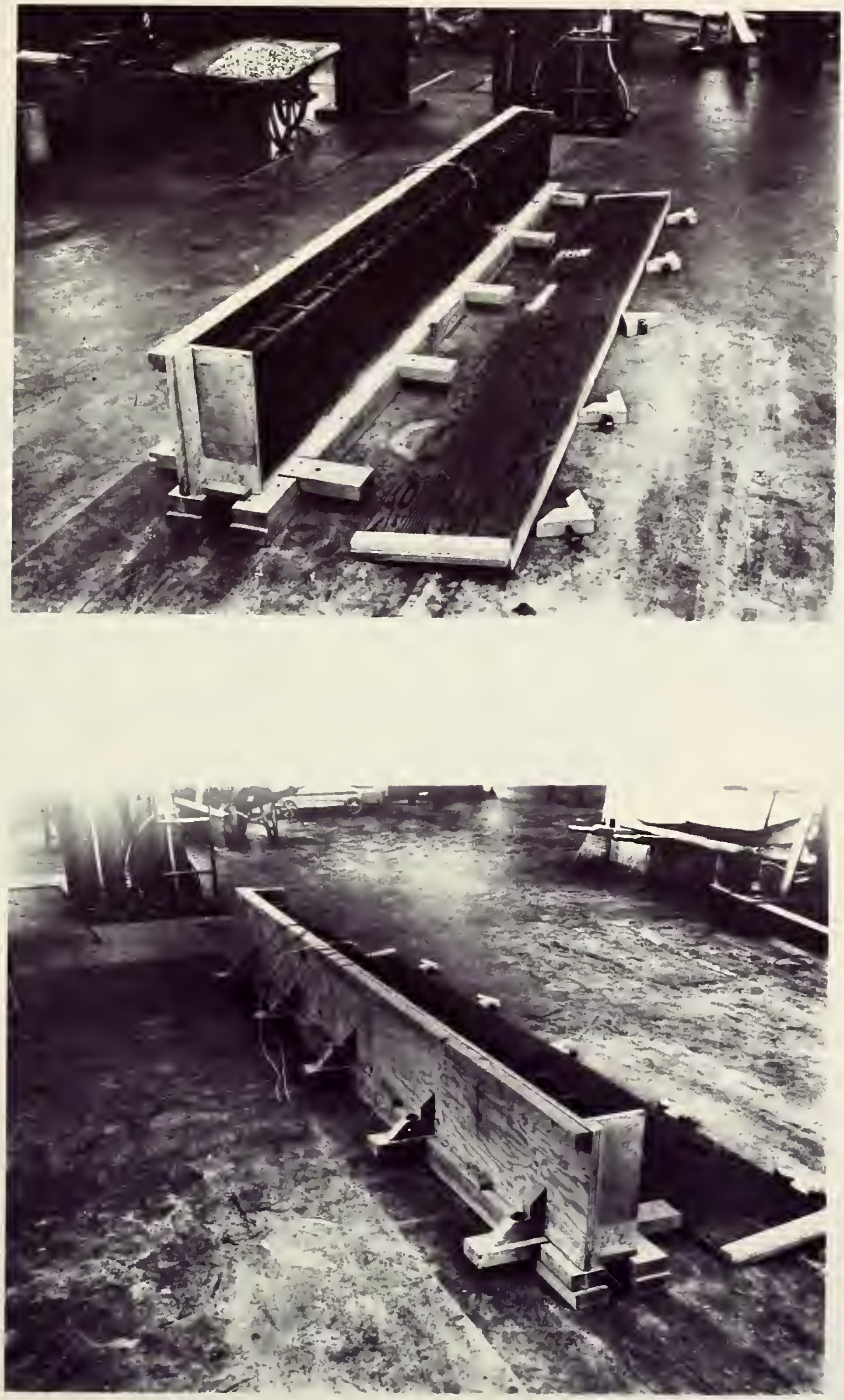

FIGURE 6. VIEW PRIOR TO CASTING

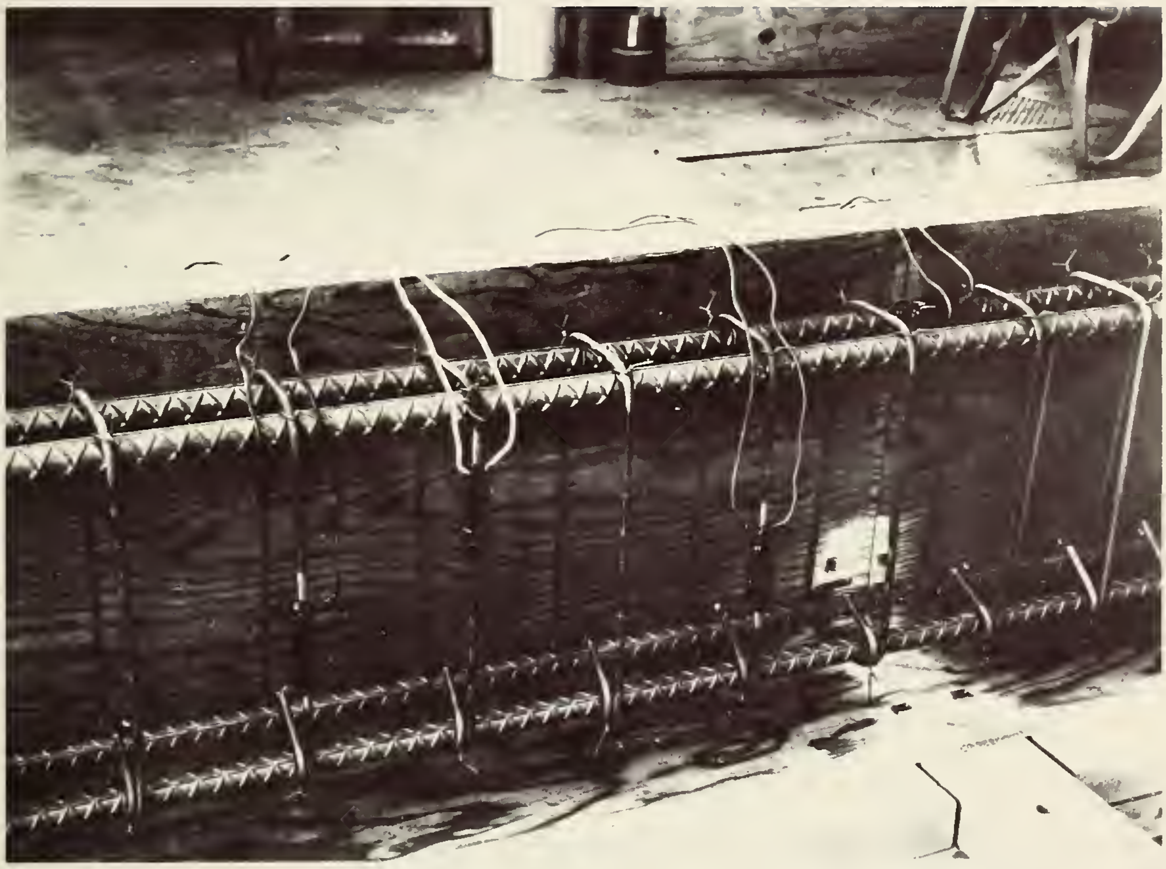

FIGURE 7. REINFORCING CAGE

to maintain a minimum of 1.4" clear between longitudinal bars and 1 1/2" concrete cover on the sides. The assembled reinforcing cage was placed on rigid steel chairs to provide 2" clear cover on the bottom of the specimens. Lateral displacement of the cage during pouring was prevented by wiring it to the chairs and to the forms at the top.

The concrete for each specimen was placed in three equal batches. Two 6" x 12" control cylinders were taken from each batch. Materials for all three batches were weighed prior to mixing, and the total time for placement was approximately 1 1/2 hours. Each batch was thoroughly mixed for 8-10 minutes in a tilting drum mixer. A 3/4" internal vibrator was used during the placing of the concrete in the forms.

The side forms were removed twenty-four hours after casting. The specimens, along with control cylinders, were cured under moist burlap for 5 and 12 days for the 7 and 14-day cures, respectively. One day prior to testing the burlap was removed so that the beam could be prepared for test.

Equipment and Instrumentation

A Baldwin hydraulic testing machine of 600,000 lb. capacity was used in the testing program. A general view of a beam in test position is shown in Figure 8. Figure 9 gives the details of the loading and support apparatus.

Steel strains were measured by Type A-18 SR-4 electric strain gages, mounted prior to casting. These are paperback

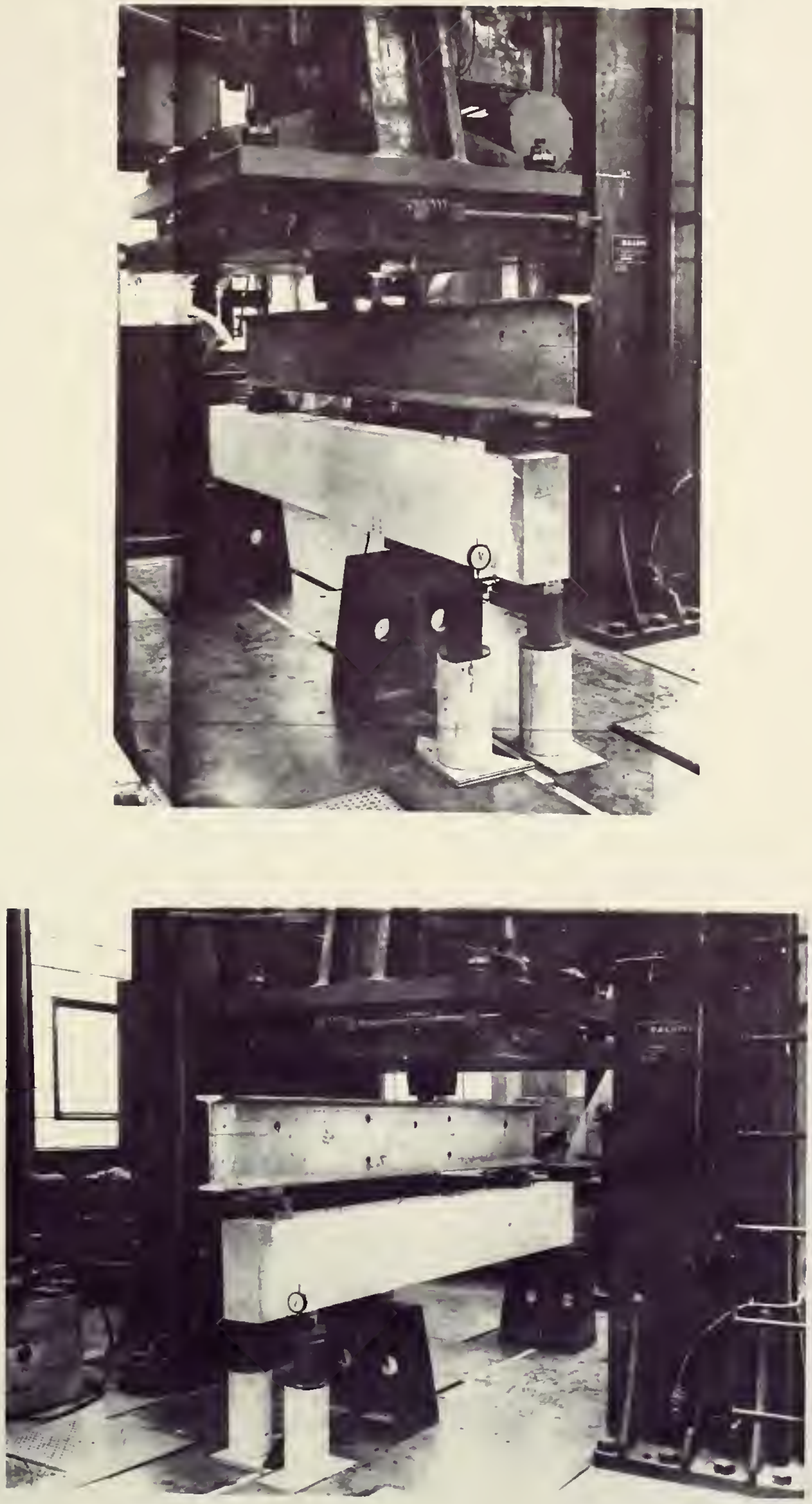

FIGURE 8. BEAM IN TEST POSITION

SERIES	u	v
I	41.9"	22.1"
II	42.2"	29.8"
III	49.2"	40.8"

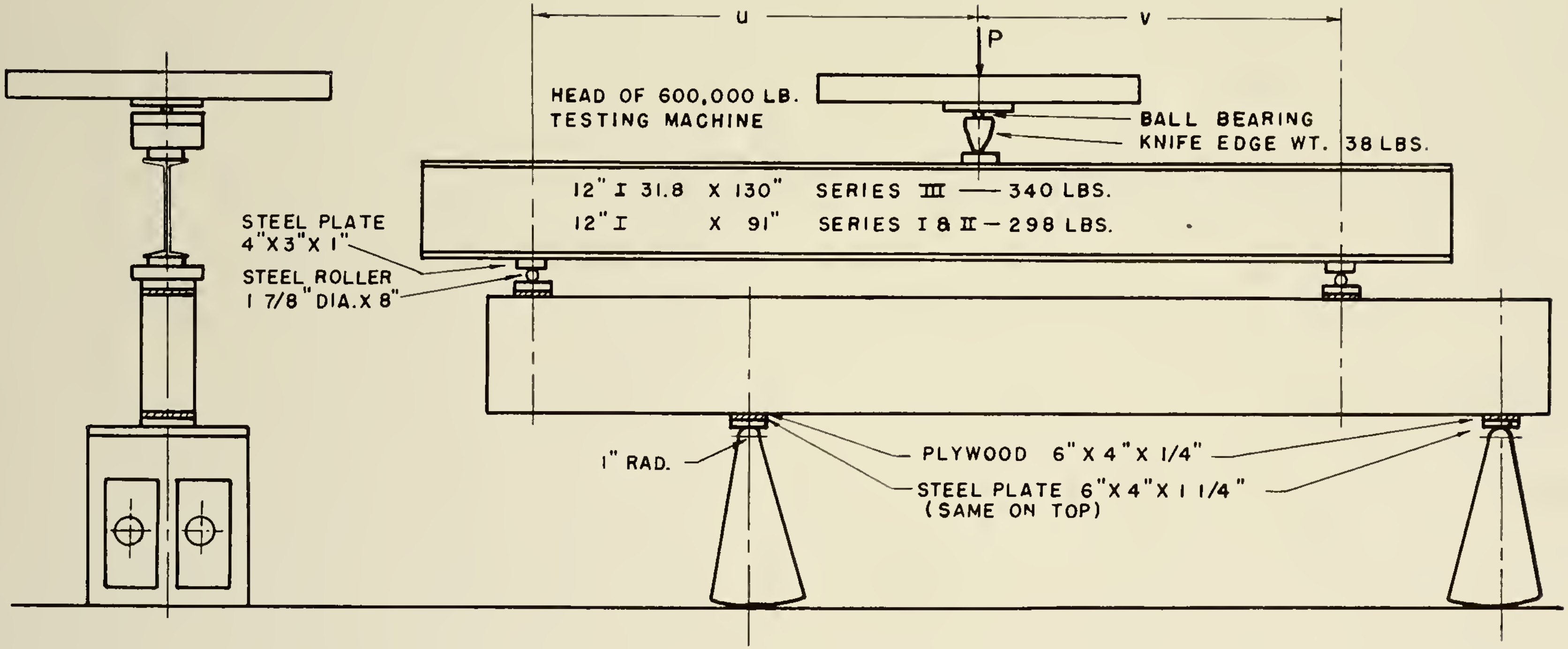

Scale: 1"=20"

FIGURE 9. DETAILS OF TEST SET-UP

gages of 1/8" gage length. The procedures used for mounting and waterproofing are given in Appendix B . Strains were recorded with a Baldwin Model "L" strain indicator.

Generally, strains in the longitudinal reinforcing were measured only at the section of maximum moment. In all but two cases the gages were located at 3 1/2" from the centerline of support x. To obtain adequate waterproofing a length of 2 1/2" to 3" of the reinforcing bar was covered with an asphaltic waterproofing material. Figure 7. It was felt that if gages were placed in the shear span, the loss of bond would significantly affect beam behavior. This effect was strongly indicated in beams IA-4 and IB-1, where two gages were placed at 18" and 24" from the support.

Strain gages were also mounted on stirrups in the critical shear span. Since these gages were placed at the point where the diagonal crack was expected to cross the stirrup, the gage locations are described for each individual beam on the crack pattern sheets.

Surface strains in the concrete compression zone were measured at 3 1/2" from the support with a 2" Whittemore gage. These displacements were read to the nearest .0001 inch. Steel gage points 1/8" thick were embedded in the concrete to receive the Whittemore gage. The vertical positions of these gage points varied somewhat from beam to beam; therefore, the particular locations are also described on the crack pattern sheets.

Deflections under the overhang were read with two .001" Federal dial gages, supported by solid pedestals resting on the floor.

Test Procedure

Load was applied to the beams in increments of one to five kips. In the early stages of loading five kip increments were used. As the diagonal cracks began to form, the increment was gradually reduced.

After the application of each load increment the load was maintained constant, while strain and deflection readings were recorded. All surface cracks were carefully traced, and their penetration at each load was marked. The sides of the beams had previously been painted with Plaster of Paris and gridded to facilitate tracing the crack patterns.

Three control cylinders for each beam were tested in compression and three in split-tension. An 8" extensometer was attached to two of the compression cylinders for modulus of elasticity determination.

TEST RESULTS

Table 5 gives a tabular summary of the pertinent test results for all beams tested. Photographs of the beams after failure are shown in Figures 10 and 11. Strain and deflection measurements for each beam are presented graphically in this section and are given in tabular form in Appendix C. In addition, a brief description of each test is given in an attempt to correlate the recorded measurements with the progression of cracks and with particular observations made during the test.

All loads reported herein are the loads applied by the testing machine. The dead weight of the loading assembly can be obtained from Figure 9.

For beams without web reinforcement the load at formation of the diagonal tension crack was in most cases easily determined. The effects of the crack's penetration into the compression zone were generally immediate. However, for beams with large amounts of web reinforcement the stress redistribution was gradual, and a definite diagonal cracking load was often difficult to determine. For this reason the diagonal cracking load is defined herein as the load at which the critical diagonal crack was observed to cross the

TABLE 5.

SUMMARY OF TEST RESULTS

Beam Designation	Diagonal Cracking Load P_c * (kips)	Ultimate Load P_u * (kips)	Shearing Stress at Diagonal Cracking v_c ** (psi)	Ultimate Shearing Stress v_u ** (psi)	Mode *** of Failure	Remarks
IA-1	30	40.8	173	235	---	
-2	35	49.5	198	280	S.C.	
-3	35	48.0	202	277	S.C.	
-4	32	34.0	181	192	D.T.	
IB-1	30	42.0	158	221	S.C.	
-2	30	58.1	156	302	S.C.	Crushing at interior load point
IIB-1	34	48.0	157	221	S.C.	
-2	36	63.0	167	292	S.C.	
-3	35	67.0	163	312	S.C.	
-4	35	59.0	163	275	D.T.	Bars cut off
-5	25	29.1	116	135	D.T.	Bars cut off
IIIA-1	40	43.0	164	177	D.T.	
-2	42	45.0	171	183	D.T.	
-3	45.9	45.9	185	185	D.T.	
IIIB-1	36	37.1	136	140	D.T.	
-2	36	48.0	134	179	D.T.	
-3	--	71.3	---	263	S.C.-F.T.	Tension steel yielding at $P=58\text{-}60^k$
-4	--	70.0	---	258	S.C.-F.T.	Tension steel yielding at $P = 62^k$
-5	30	59.6	111	221	D.T.	Bars cut off
-6	30	30.0	111	111	D.T.	Bars cut off

* Total applied load. (does not include dead weight of specimen and loading apparatus)

** Average shearing stress, $v = \frac{V}{bd}$, in critical shear span.

*** D.T. - Diagonal Tension; S.C. - Shear-Compression; F.T. - Flexural Tension.

FIGURE 10. BEAMS AFTER TEST - SERIES I AND II

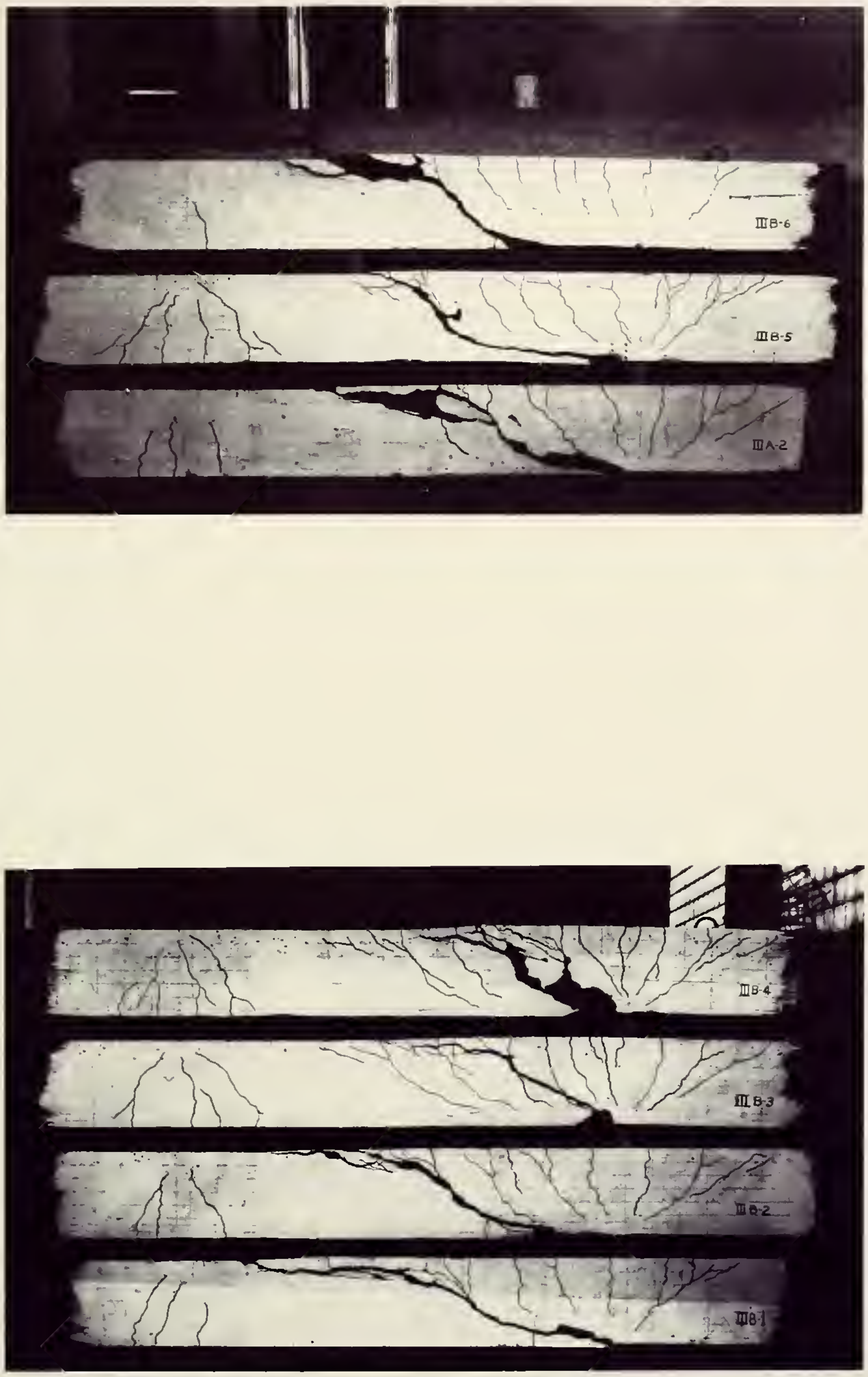

FIGURE 11. BEAMS AFTER TEST - SERIES III

theoretical cracked-section neutral axis. The cracked-section neutral axis for the beams of this investigation ranged from 4.0" to 4.2" from the compression face.

Series I

Beam IB-1 (No Stirrups)

The diagonal crack, an extension of the vertical flexural crack at 11" from the support, was well into the compression region at P = 30^k. However, a significant redistribution of stresses did not occur until a load of 34.8^k was reached. At P = 34.8^k splitting along the tension steel occurred out to the point of inflection. Bond was lost throughout the shear span, as indicated on the load vs. steel strain curve of Figure 12. Note also a significant break in the load vs. deflection curve of Figure 13.

Concrete compressive strains at the extreme fibers reached a maximum of 1025 micro-inches per inch (hereinafter designated MII) at P = 36.4^k and then decreased rapidly with increasing load. See Figure 14. The strain readings at 1" and 2" above the bottom surface were influenced by the deep penetration of the crack and were discontinued after a load of 36^k. However, it is believed that crushing in this region was the primary cause of failure. The appearance of the beam at collapse was similar to that of Beam IIB-1. In IIB-1 a similar loss of strain in the extreme fibers was noted, but

at 1" above the bottom large crushing strains were developed. See Figure 26.

Beam IB-2 (No Stirrups)

The diagonal tension crack developed in the same manner as in IB-1; however, note that it was shifted slightly closer to the support and was slightly higher as it penetrated directly above the support block. At P = 36.9^k splitting cracks were observed out to the point of inflection. As loading was continued, this splitting continued into the positive moment region, and at 39^k had extended to the other load point. Again, a large increase in deflection accompanied this splitting and resulting loss of bond along the tension steel. See Figure 13.

Concrete compressive strains remained practically constant from this point until the last readings were taken at 54^k. At 51^k a diagonal crack formed in the positive moment region. Just prior to failure at 58.1^k a large area of concrete adjacent to the load P_2 appeared to "bulge" out and began spalling off. At collapse, splitting was observed along the bottom steel to the interior support. Evidently failure was primarily due to crushing of the compression zone adjacent to the load, P_2. However, no strain measurements were taken in this region.

Beam 1A-1

(No Stirrups - 2 Layers of Tension Steel)

The initial diagonal tension crack crossed the neutral axis at about 30^k. At 35 to 36^k two flatly inclined cracks began forming out near the inflection point, extending both toward the North support and toward the load point, P_2. The load fell off rapidly at 37.5^k as these cracks began to open noticeably. A maximum load of 40.8^k was sustained, at which time these two cracks split entirely through the beam.

Beam IA-2

(No Stirrups - 2 Layers of Tension Steel)

The diagonal crack was well into the compression zone at 35^k. At 37^k the crack developed rapidly toward the tension steel. The average concrete strain on the bottom decreased slightly from 37 to 38^k and held constant at about 900 MII up to the last reading taken at 42^k. At 44^k several long splitting cracks appeared at intervals along the tension steel directed toward the load point. At the same time, short fine cracks appeared in the compression zone below the end of the diagonal crack. This, plus the appearance of a tension crack on the bottom or the negative moment side of the inflection point, indicates a substantial redistribution following the loss of bond throughout the shear span. Cracking and spalling over the small area below the end of

the crack continued, as the load was increased. The appearance at collapse indicated that failure was by shear-compression much like that evidenced in IIB-1, where large crushing strains were recorded.

Beam 1A-3

(No Stirrups - 2 Layers of Tension Steel)

The behavior of this beam was nearly identical to that of IA-2.

Beam IA-4

(No Stirrups - 2 Layers of Tension Steel)

The diagonal tension crack forming at 32^k was located much farther away from the support than in IA-2 and 3. Development was much more rapid. Failure was quite sudden at $P = 34^k$ and was very much like the failure in the beams of longer shear span.

In this particular beam strain gages were placed out in the shear span (one at 18" and one at 24" from the support.) The presence of these gages may have had an effect on the location of the crack and, in turn, on the ability of the beam to reach a force equilibrium after diagonal cracking.

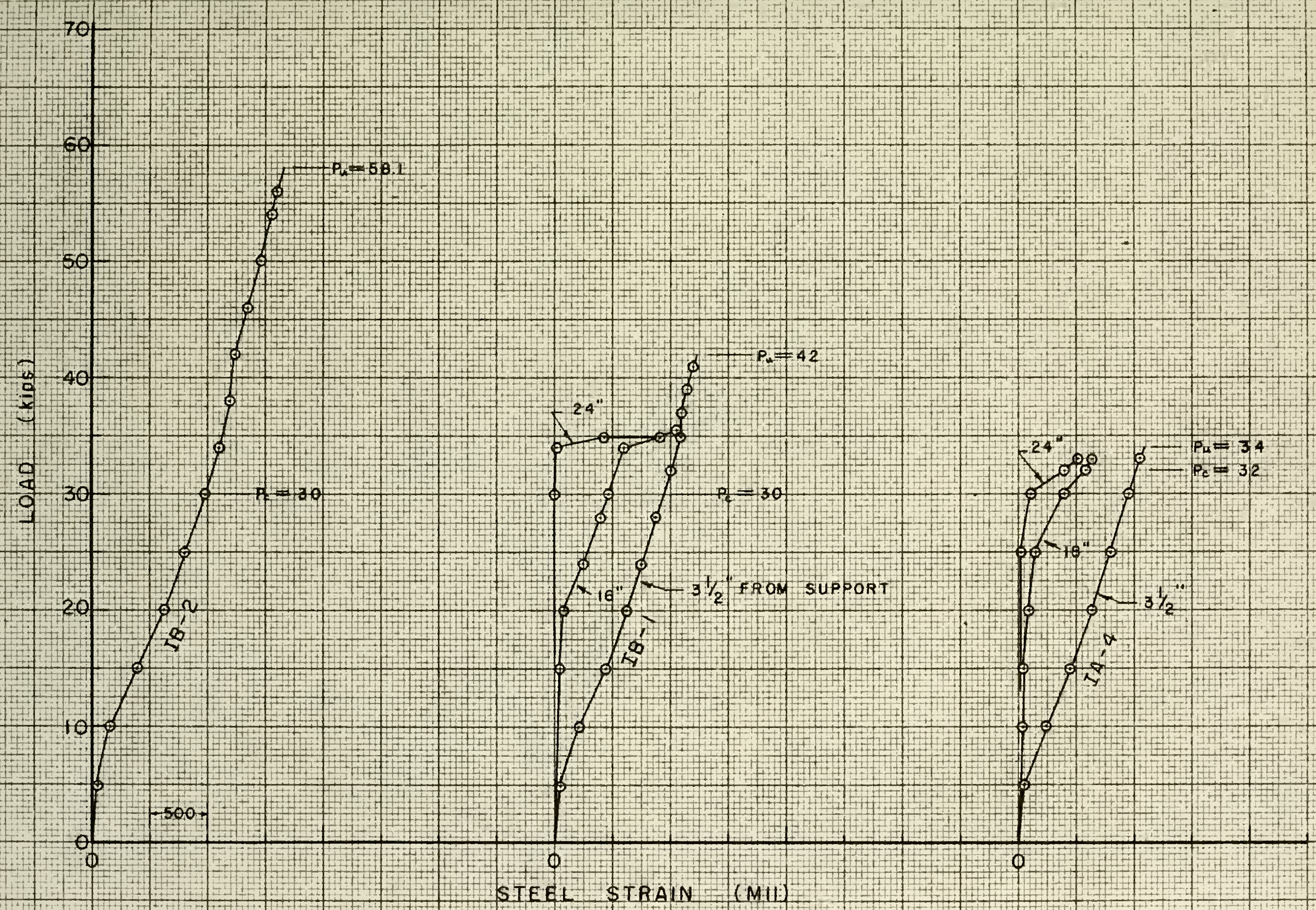

FIGURE 12. LOAD vs. STEEL STRAIN — SERIES I

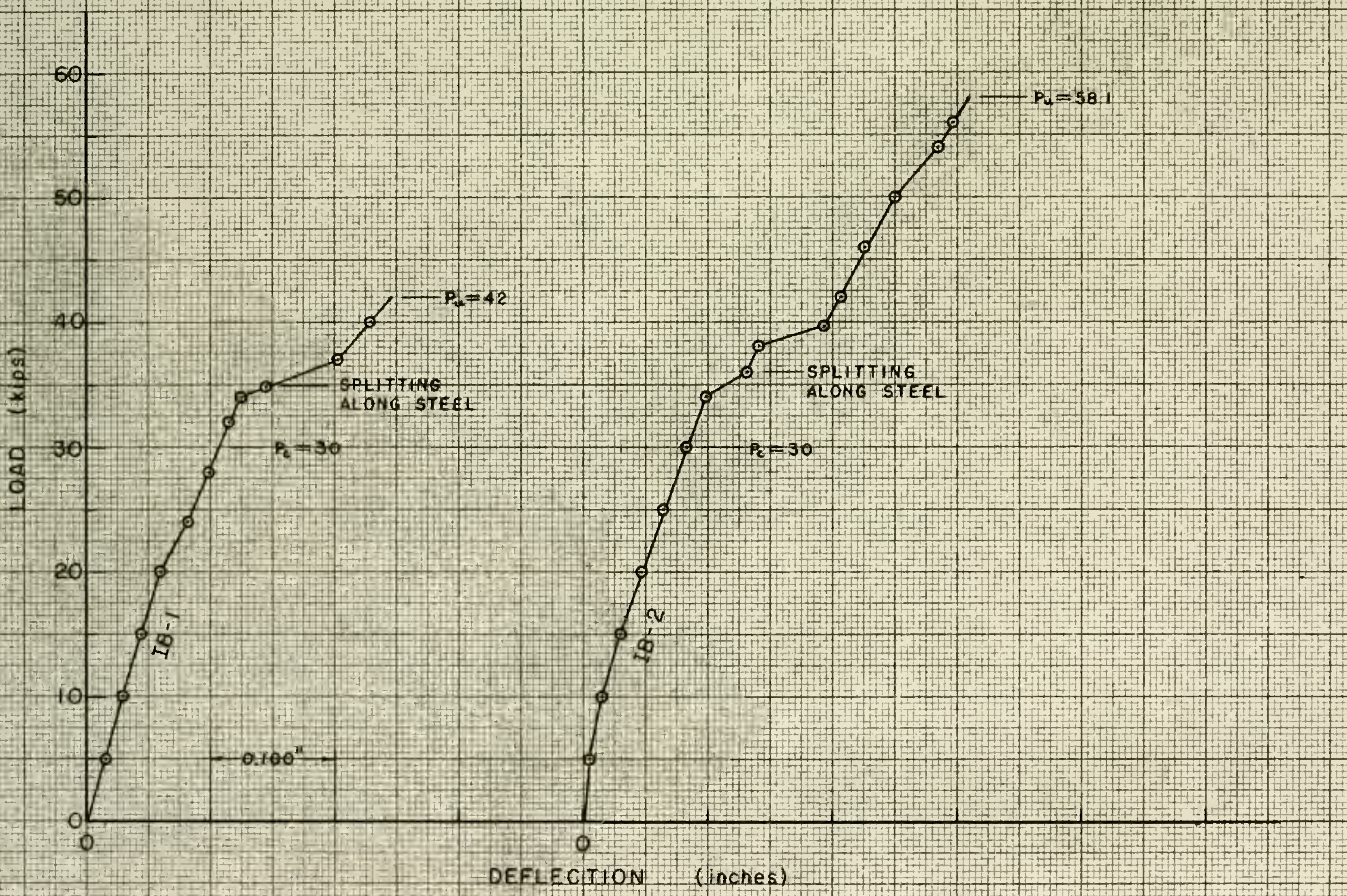

FIGURE 13. LOAD vs. DEFLECTION — SERIES I

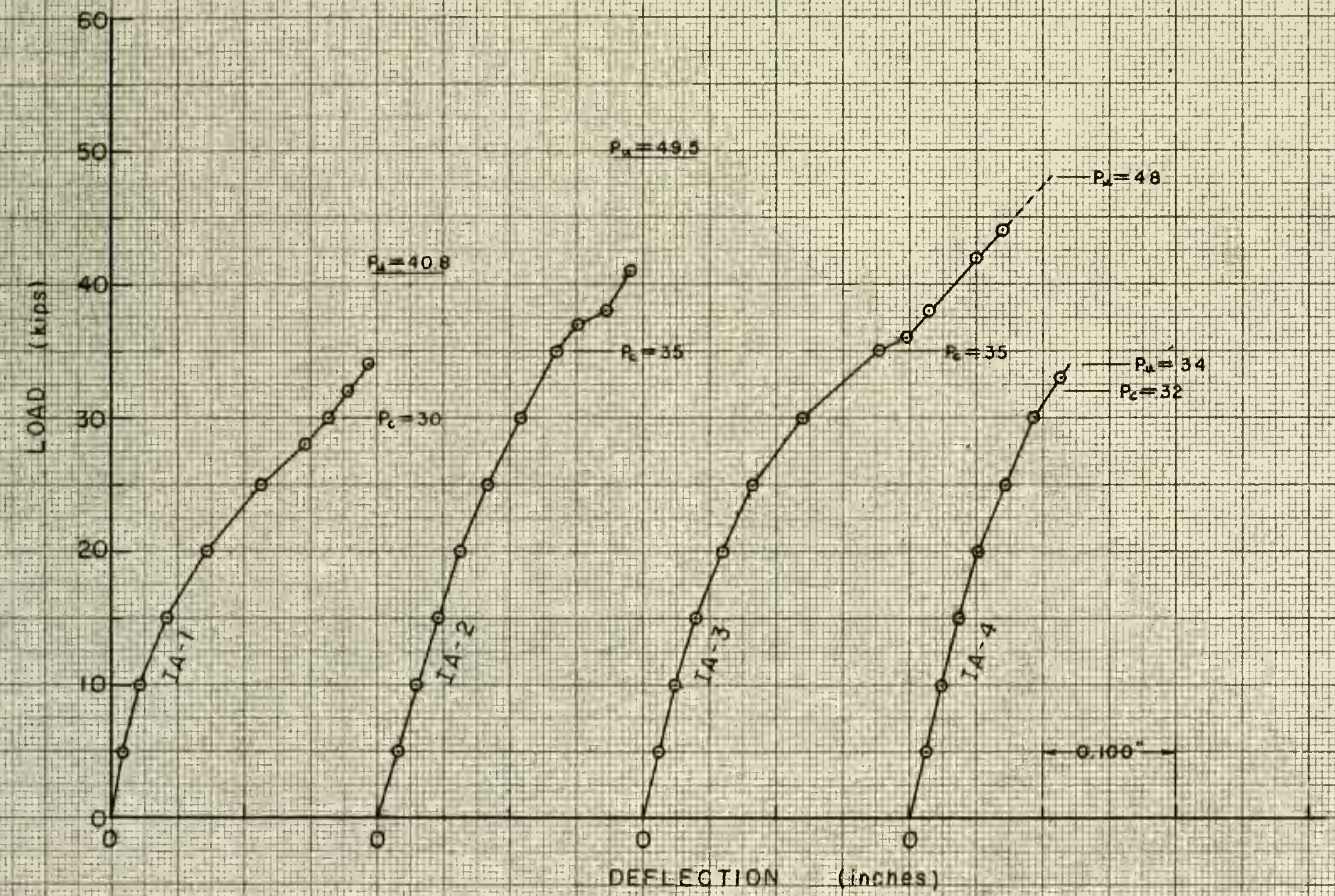

FIGURE 14. LOAD vs. DEFLECTION — SERIES I (cont'd)

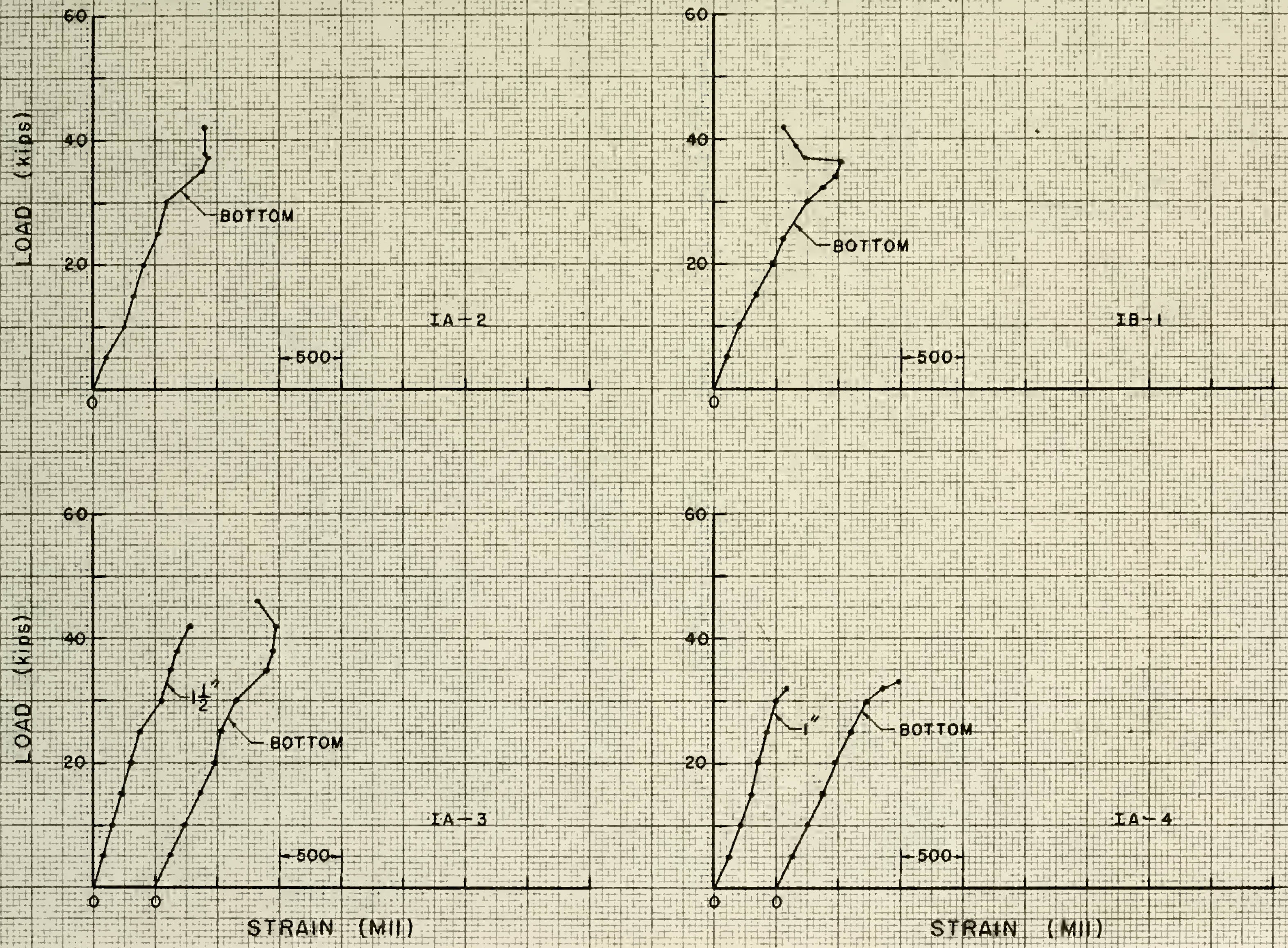

FIGURE 15. LOAD vs. CONCRETE STRAIN — SERIES I

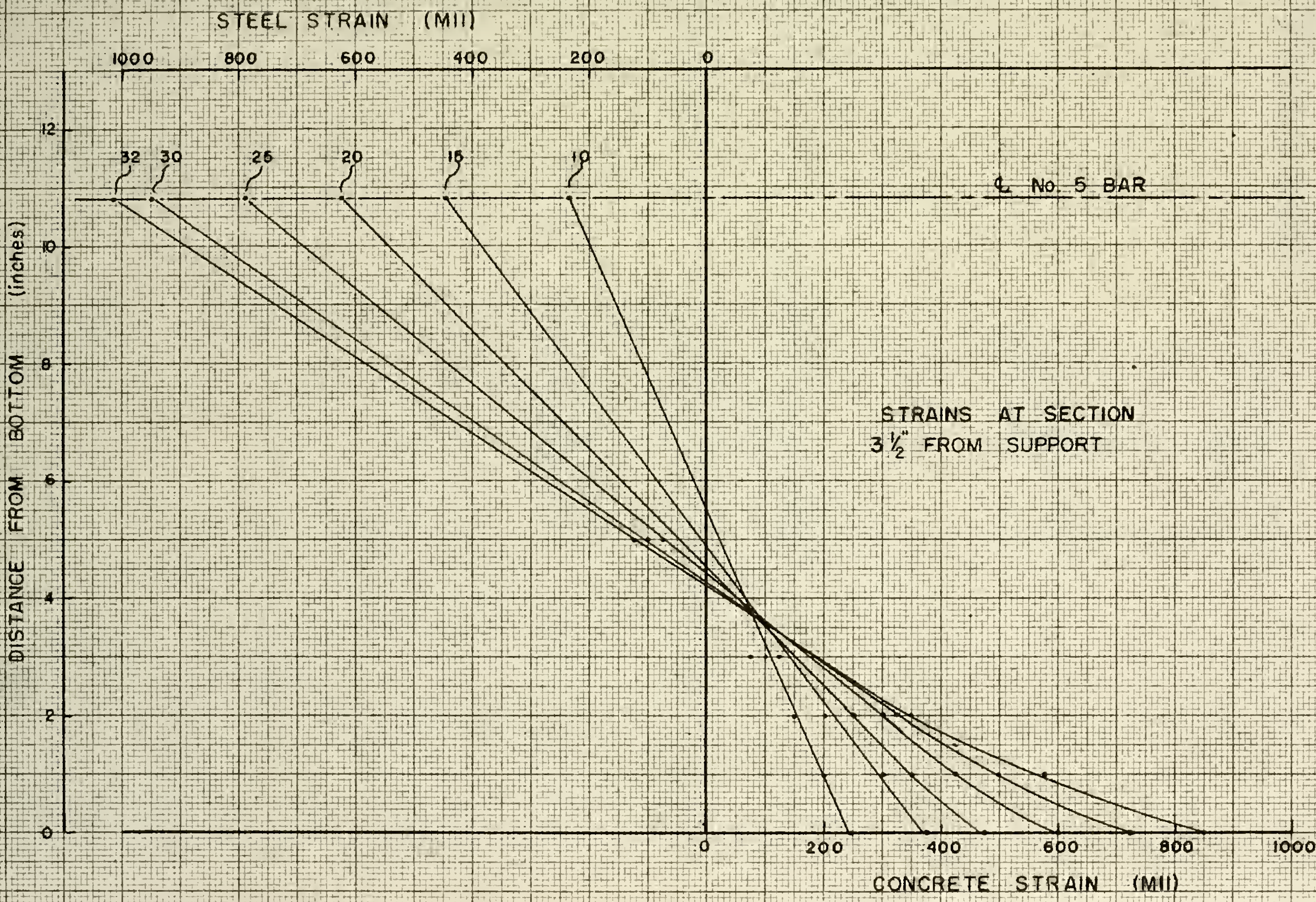

FIGURE 16. STRAIN DISTRIBUTION – BEAM IA-4

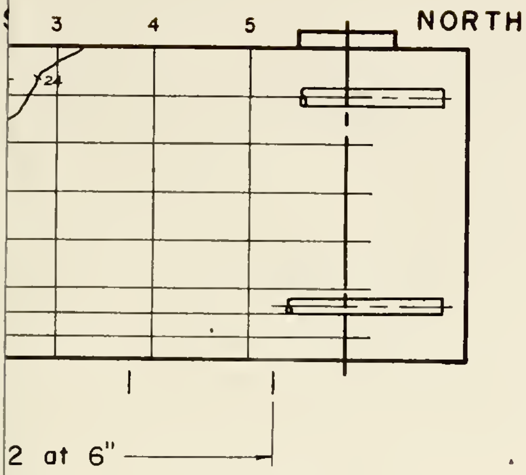
3
4
5
NORTH
24
2 at 6"

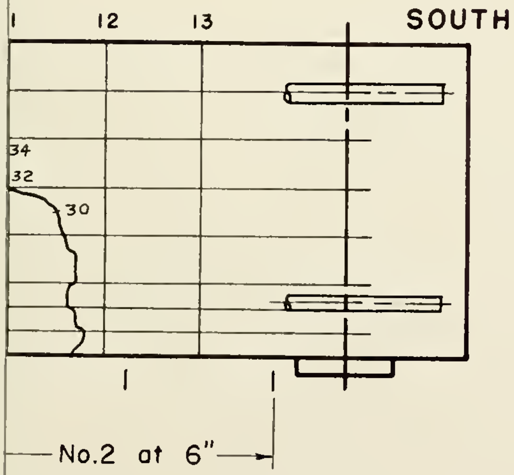
12
13
SOUTH
34
32
30
No.2 at 6"

EAST SIDE

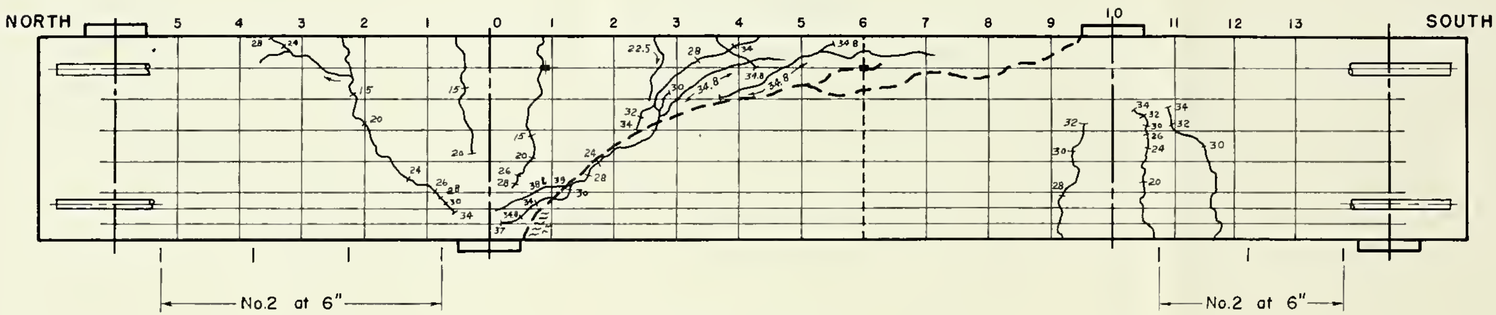

WEST SIDE

SR-4 Gage Locations:
No. 6 Bar — 3 1/2" from support (E)
" " — " " " (W)
" " — 16" " " (E)
" " — 24" " " (W)

Whittemore Gage Locations:
0", 1", 2" from bottom (E & W)

FIGURE 17. BEAM IB-1

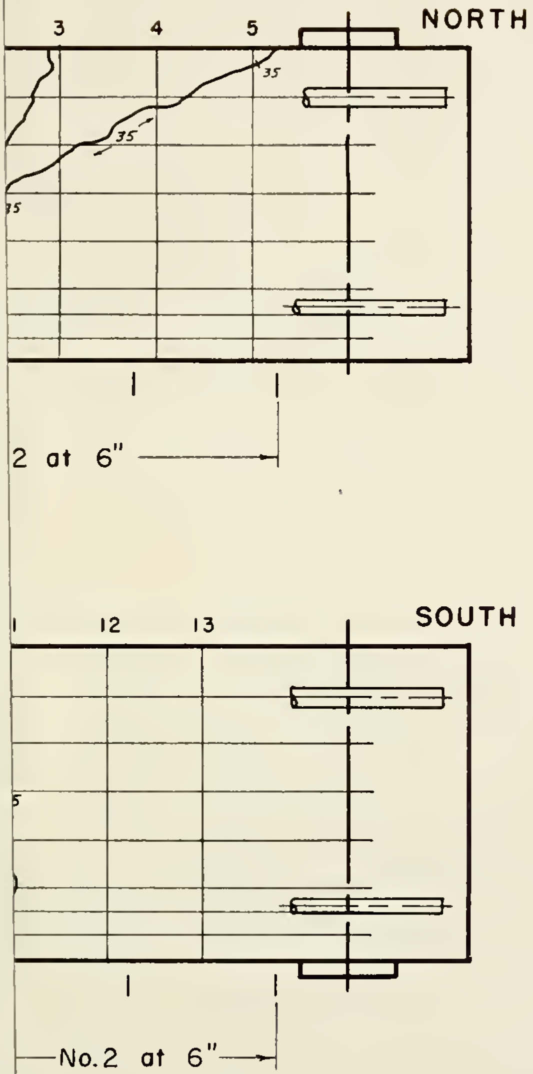
3
4
5
NORTH
35
35
35
2 at 6"
12
13
SOUTH
No. 2 at 6"

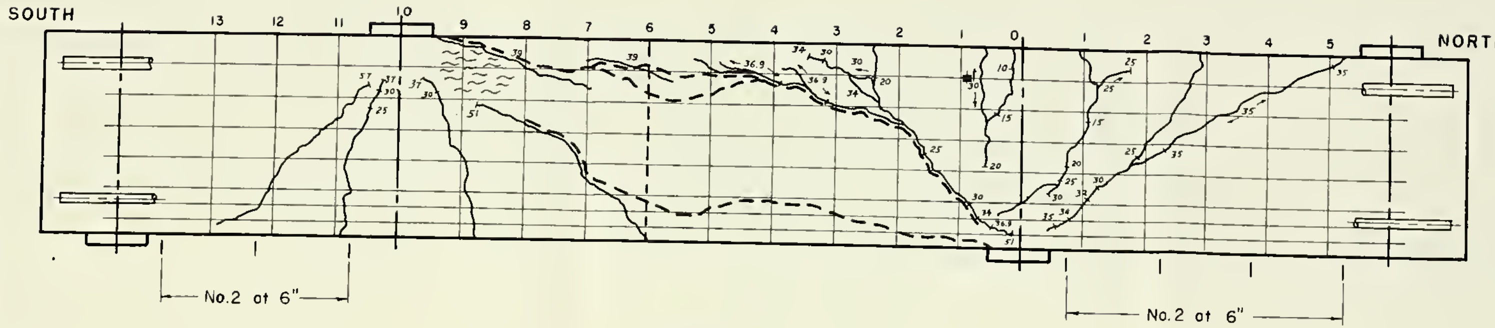

EAST SIDE

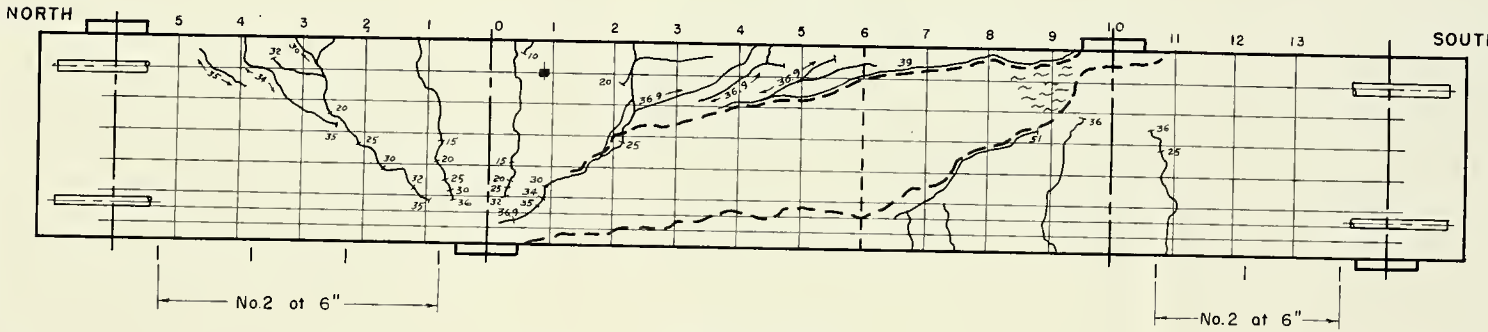

WEST SIDE

SR-4 Gage Locations:

No. 6 Bar — $3\frac{1}{2}''$ from support (E & W)

Whittemore Gage Locations:

0", 1" from bottom (E & W)

FIGURE 1B. BEAM IB-2

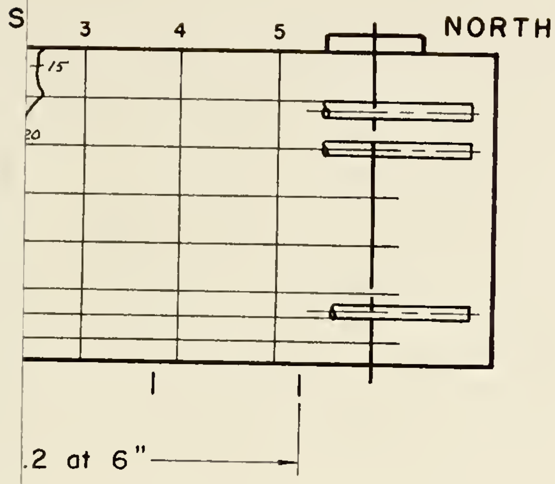

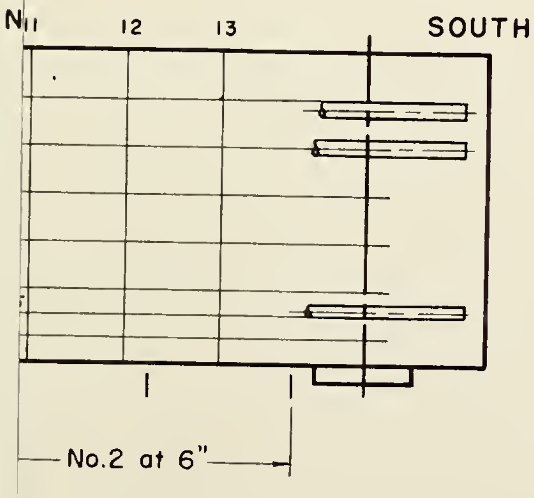

racks prior to failure

racks opening wide at failure

R–4 Strain Gage

Scale: 1"= 8"

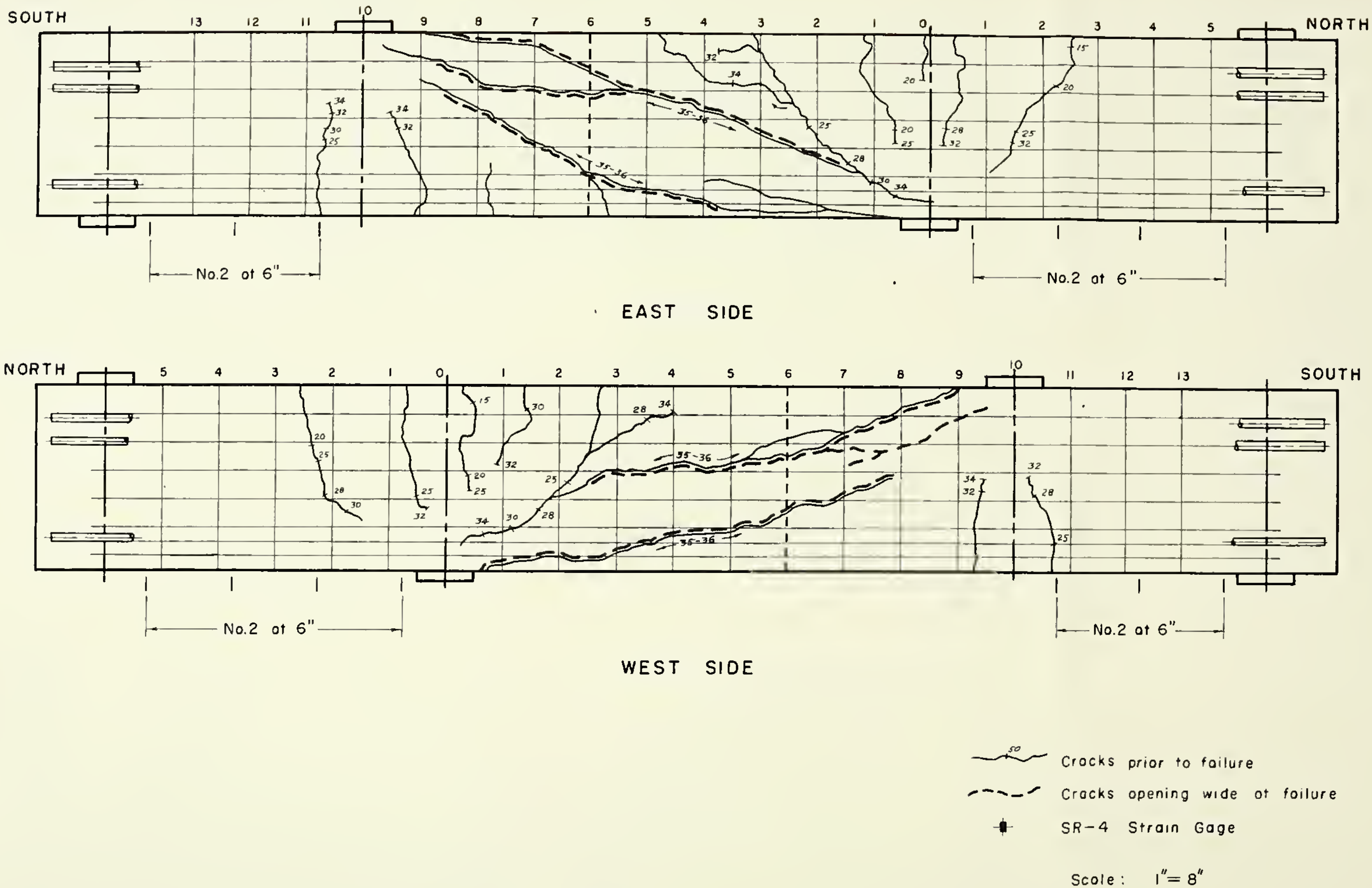

FIGURE 19. BEAM IA-1

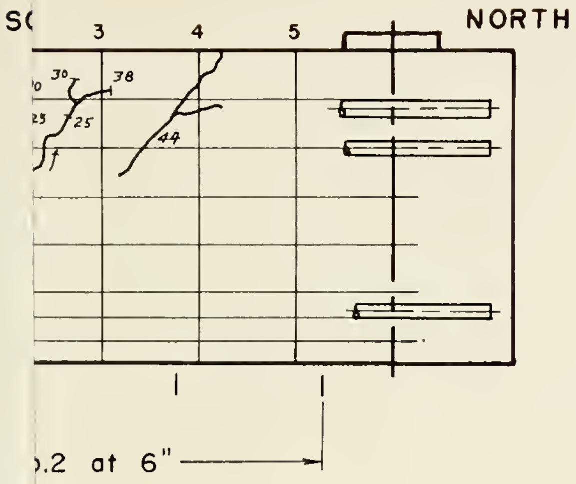
NORTH
3
4
5
30
38
25
44
.2 at 6"

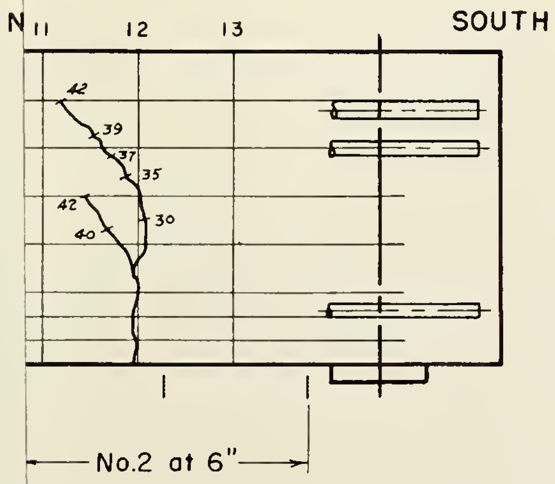
N
11
12
13
SOUTH
42
39
37
35
42
40
30
No.2 at 6"

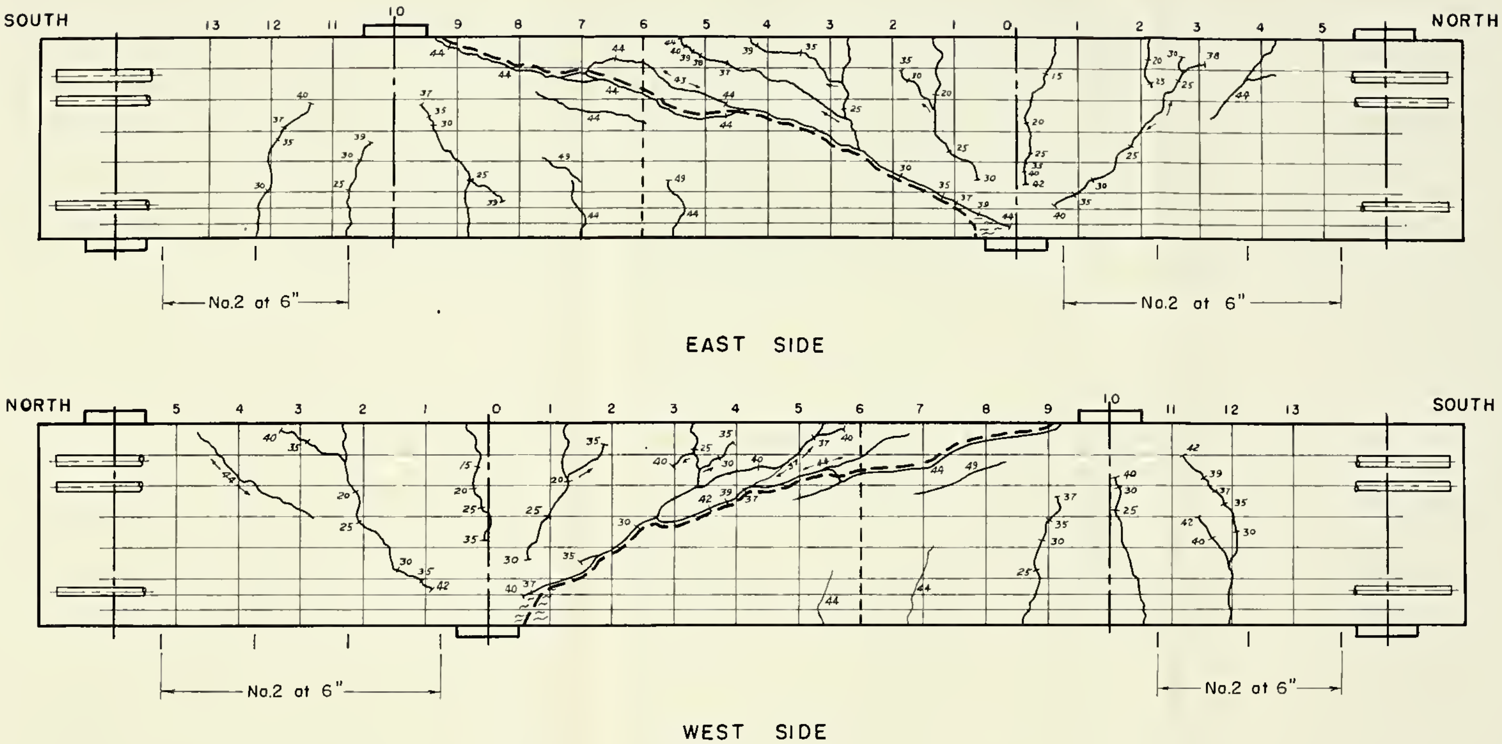

Whittemore Gage Locations:

0", $1\frac{1}{2}$", 3" from support (E & W)

FIGURE 20. BEAM IA-2

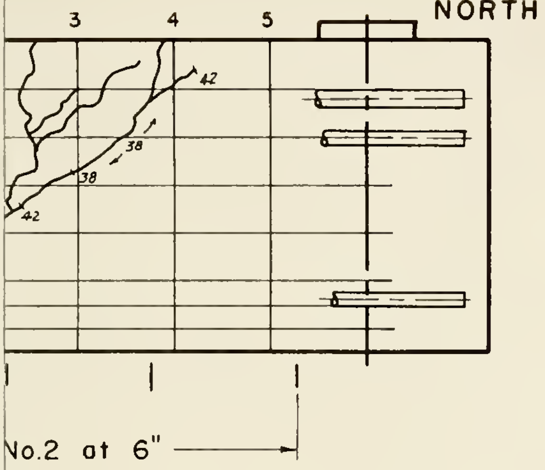
3
4
5
NORTH
42
38
38
42
No.2 at 6"

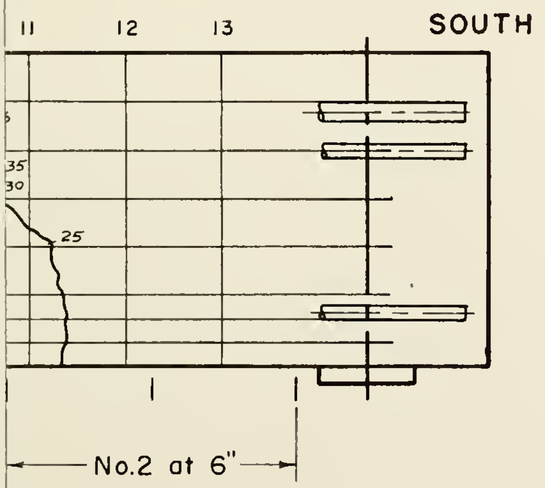
11
12
13
SOUTH
35
30
25
No.2 at 6"

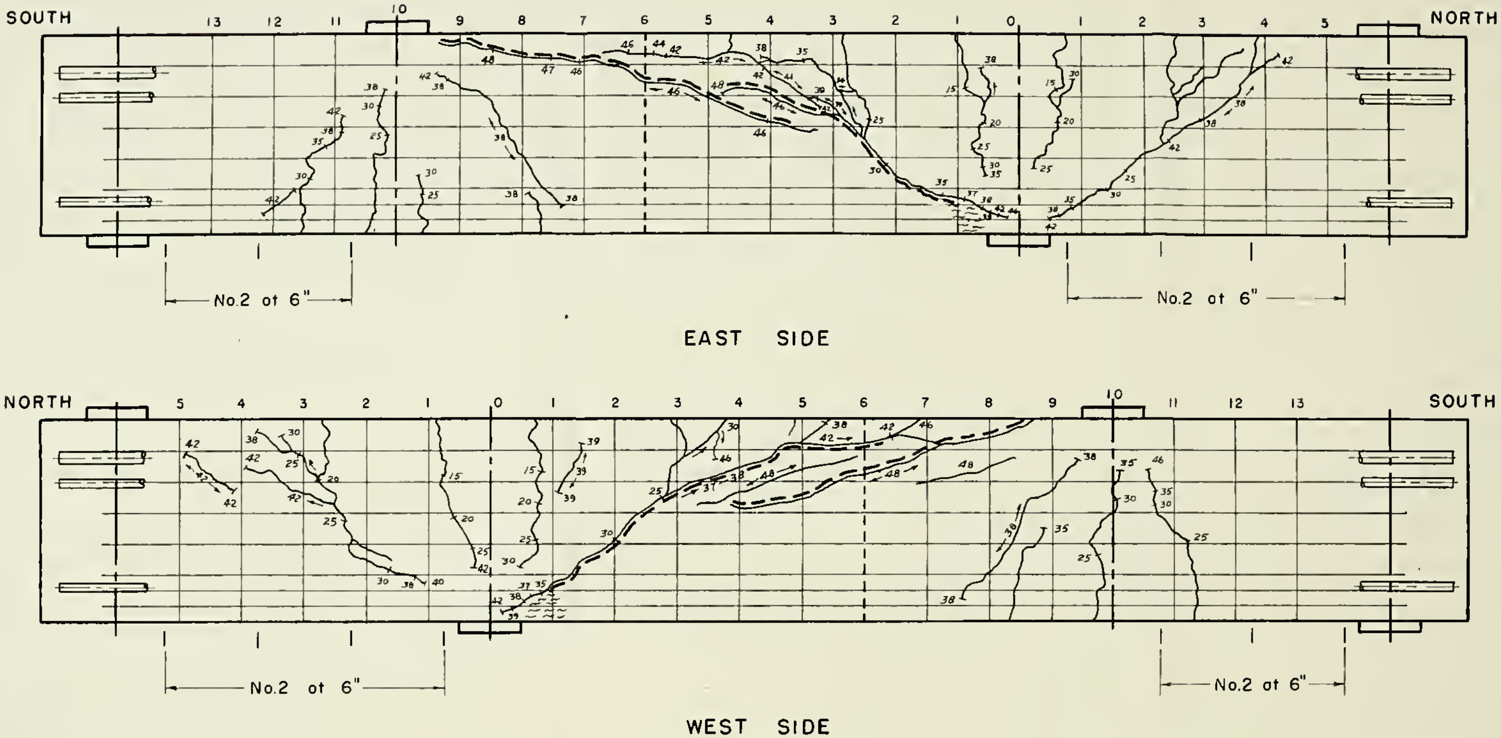

Whittemore Gage Locations:

0", $1\frac{1}{2}$", 3" from bottom (E & W)

FIGURE 21. BEAM IA-3

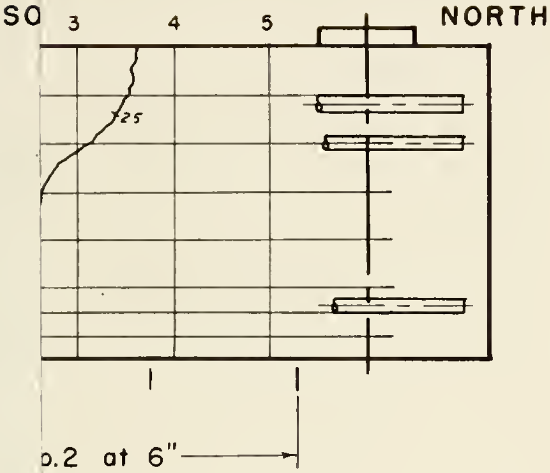
SO
3
4
5
NORTH
25
o.2 at 6"

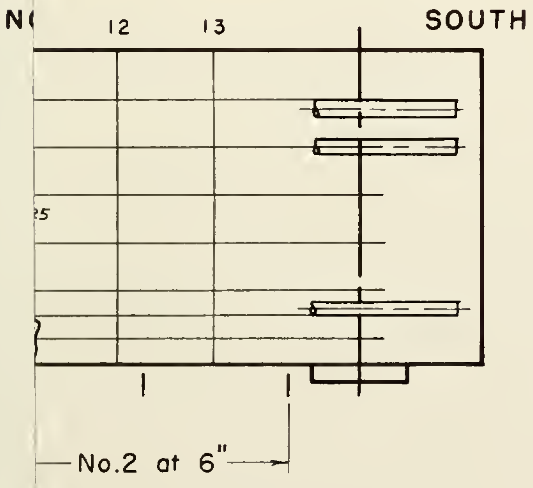
N
12
13
SOUTH
25
No.2 at 6"

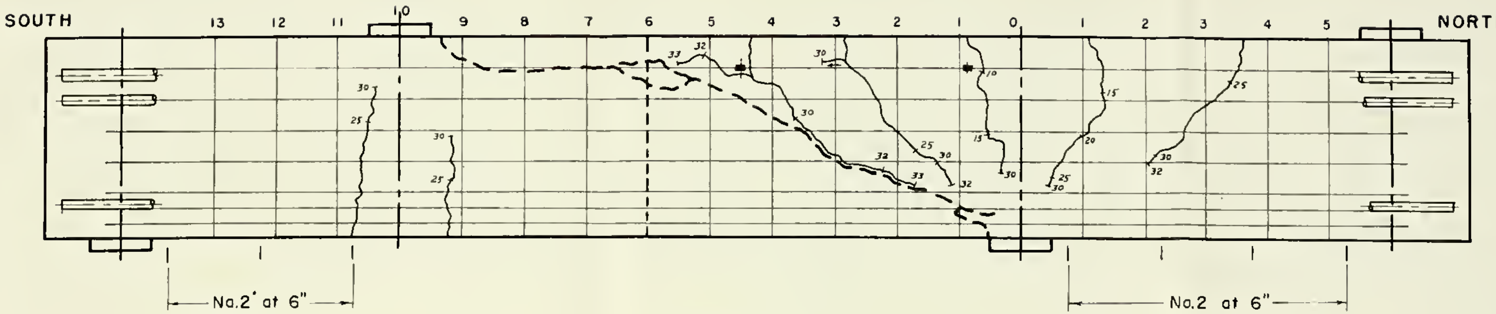

EAST SIDE

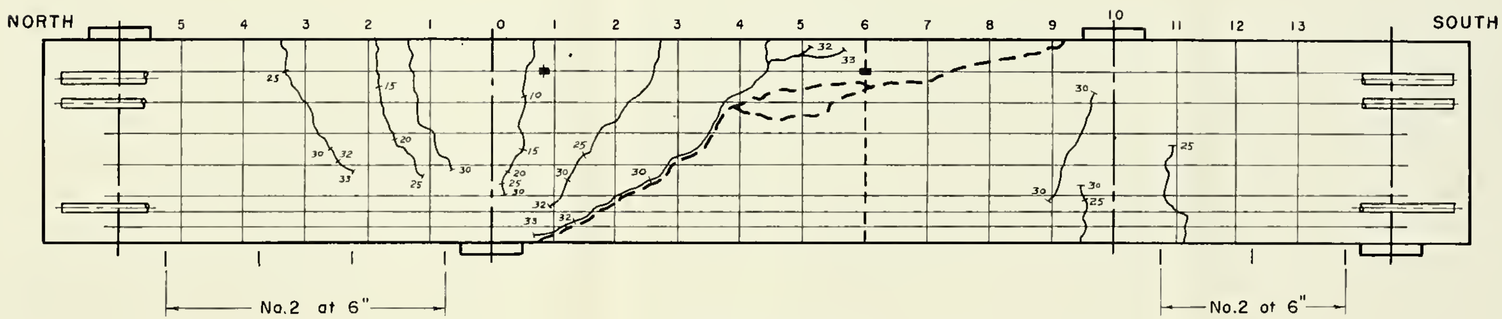

WEST SIDE

SR-4 Gage Locations:

No. 6 Bar	—	$3\frac{1}{2}$"	from	support	(E)
"	" —	"	"	"	(W)
"	" —	18"	"	"	(E)
"	" —	24"	"	"	(W)

Whittemore Gage Locations:

0", 1", 2", 3", 4", 5" from bottom (E & W)

FIGURE 22. BEAM IA-4

Series II

Beam IIB-1 (No Stirrups)

The vertical flexural tension crack (Figure 31), which eventually developed into the critical diagonal tension crack, started at about 12" from the support, bent to a 45° incline near middepth, and headed straight for the support. From $P = 32^k$ to 34^k the diagonal crack penetrated into the compression zone to within 2" of the compressive face, extended back at 45° from middepth to the tension steel, and widened considerably. There was also a noticeable decrease in the stiffness of the beam.

At 39^k short inclined cracks began to appear along the tension steel. At 40^k thissplitting extended through the point of inflection to the other load point. At this point, the load dropped suddenly to 36.5^k, and the splitting cracks, together with the main diagonal crack, opened wide. From this point on, the concrete strains at 1" above the bottom surface increased rapidly. However, those on the bottom surface began dropping off slightly. See Figures 26 and 27.

Figure 27 is a plot of the strains at a vertical section 3 1/2" from the support at various loads. At low loads the distribution was nearly linear. The redistribution of strains following penetration of the diagonal crack into the compression zone is indicated by a shifting of the neutral axis toward the bottom at $P = 30$ and 34^k. At 39^k, the load at

which the splitting cracks appeared along the tension steel, further redistribution occurred, as the point of maximum strain was no longer at the extreme fibers.

Ultimate failure was by crushing of the concrete below the end of the diagonal crack at 48^k. When the load of 48^k was first reached, the strains on the bottom surface remained low, while at 1" above the bottom surface they were of the order of 5000 MII on the East side. However, as the load of 48^k was sustained, crushing gradually spread out and collapse followed.

Beam IIB-2

(Low Percentage of Stirrups - 6" Spacing)

Two diagonal cracks developed in this beam (Figure 32), each of which was located approximately equidistant on either side of the critical diagonal tension crack in IIB-1. The diagonal crack which ultimately became critical penetrated into the compression zone and extended back to the tension steel at the load, $P = 36^k$. The penetration of both cracks farther into the compression zone was clearly not as rapid as that of beam IIB-1 without stirrups. Note the large increases in strain in all three stirrups crossed by the crack (Figure 24). Stirrup (b) reached yield strain at the load 36^k. In addition, there was a significant break in the deflection curve. (Figure 25).

As soon as the critical diagonal crack began penetrating the compression zone, the concrete strains increased noticeably. Two other instrumented stirrups, crossed by the crack, were yielding at 42^k and 44^k. By 46^k the crack was down to within one inch of the compressive face. Also at 46^k splitting cracks along the tension steel began to appear. Although this splitting was considerably delayed by the presence of stirrups, it still extended to the other load point by $P = 55^k$.

As in IIB-1, the concrete strains at 1/2" above the bottom began picking up relative to the strains at the extreme fibers, as soon as this splitting occurred. (See Figure 28.) At the ultimate load of 63^k concrete strains of 3100 MII were recorded at the 1/2" gage line and crushing over the lower 1 1/2" to 2" soon followed.

Note also from Figure 28 that the point of zero strain remained nearly stationary from $P = 44^k$ to failure.

Beam IIB-3

(High Percentage of Stirrups - 3 1/2" Spacing)

Two diagonal cracks developed (Figure 33), located in the same approximate position as in Beam IIB-2. The critical crack crossed the neutral axis at 35^k, but further increase in load (40^k - 50^k) was required to extend it back to the tension steel.

Stirrup (c) was the first to yield at 50^k. The other two stirrups with gages yielded at 56^k and 66^k. (See Figure 24). Splitting along the longitudinal steel was still not prevented with the increased amount of stirrups, but was considerably delayed and did not extend into the positive moment region until near ultimate load.

At 66^k the tension steel began to yield. (Figure 23). Concrete strains were also increasing rapidly at this load (Figure 26), and crushing over the lower 1/2" was apparent after 66^k had been sustained for some time. (See Table 19 in Appendix C.) Collapse followed at 67^k.

The effect of the amount of web reinforcement on the redistribution of strains following diagonal cracking can be seen by comparing Figures 28 and 29. Redistribution in IIB-3 did not occur to any great extent until all stirrups were yielding at 66^k. Note also from Figure 29 that the high concentration of strain above the extreme fibers -- as noted in beams IIB-1 and IIB-2 -- was not evident in beam IIB-3. Evidently the maintainance of bond along the tension steel did not allow the arching action.

The effect of the increased percentage of web reinforcement is also indicated by the load vs. deflection curves of Figure 25. In beams IIB-1 and IIB-2 substantial increases in deflection accompanied the formation of the diagonal tension crack. The two beams gradually lost stiffness as the load was increased. The closely spaced stirrups of

beam IIB-3, however, maintained a more nearly linear load deflection curve.

Beam IIB-4

(3 1/2" Stirrup Spacing-Longitudinal Steel Cut-Off)

Four closely spaced diagonal cracks (Figure 34) crossed into the compression region at about the same load of 35^k. The two farthest from the support eventually opened wide at failure. One of these cracks was definitely associated with the steel cut-off and had penetrated to within 1/2" of the compressive face at 50^k.

Both stirrups with gages yielded at 57^k - 58^k. A diagonal tension type failure followed at 59^k with both cracks opening wide and splitting entirely through the beam. Concrete strains remained low adjacent to the support.

Although the mode of failure of this beam was quite different from its companion beam with extended steel (IIB-3), the load-strain behavior was nearly the same prior to failure. See Figures 23, 26, 29, and 30. The load vs. deflection curves of Figure 25, however, indicate a difference in stiffness following formation of the diagonal crack.

Beam IIB-5

(No Stirrups - Longitudinal Steel Cut-Off)

The diagonal crack (Figure 35) formed at 25^k along the

same path as IIB-1. At 29.1^k the crack was within 1/2" of the bottom and splitting occurred along the steel to the cut-off. The load fell suddenly to 25.3^k. Load was again increased to 27^k at which time both top bars split out and the beam fell in two pieces.

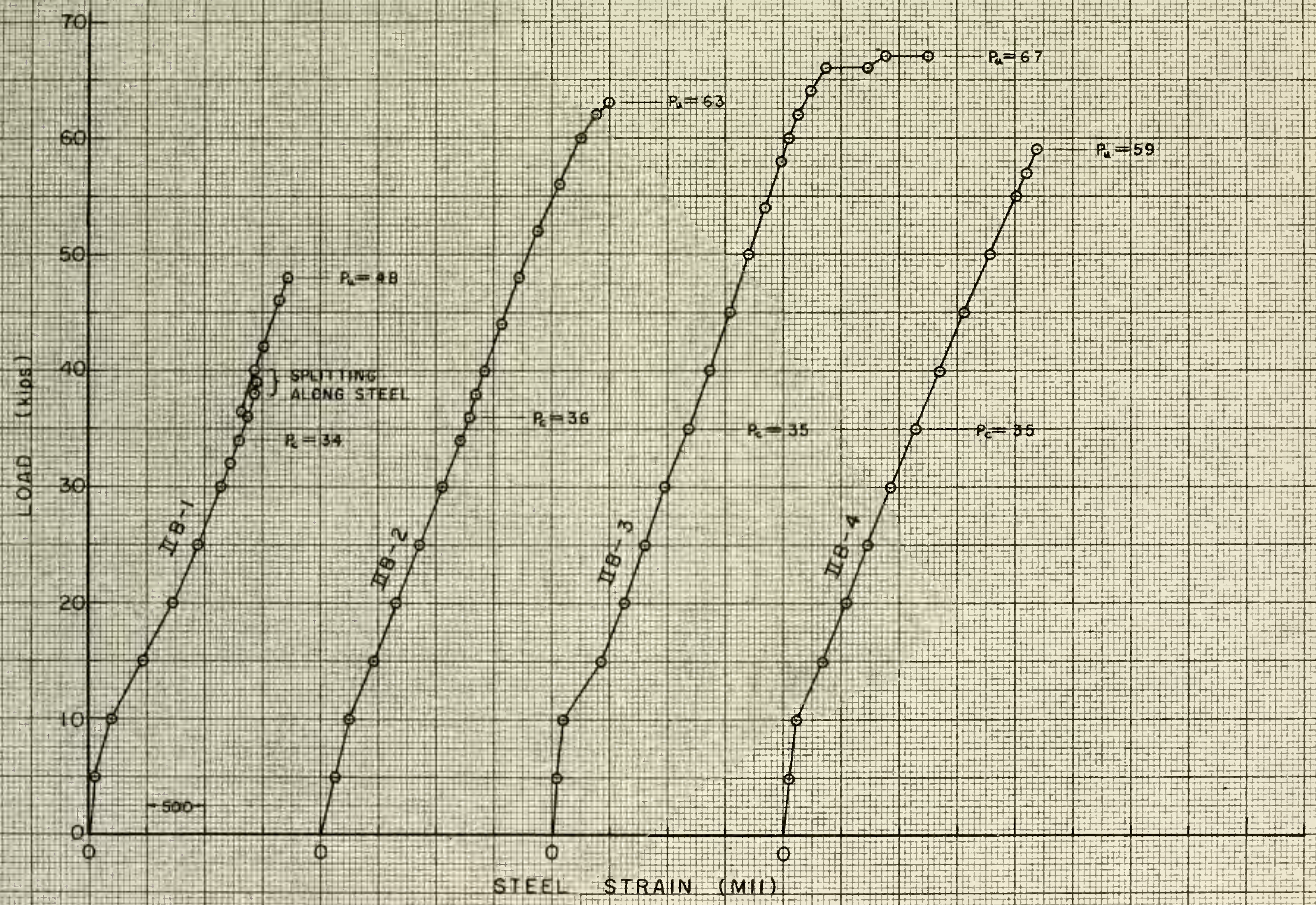

FIGURE 23. LOAD vs. STEEL STRAIN — SERIES II

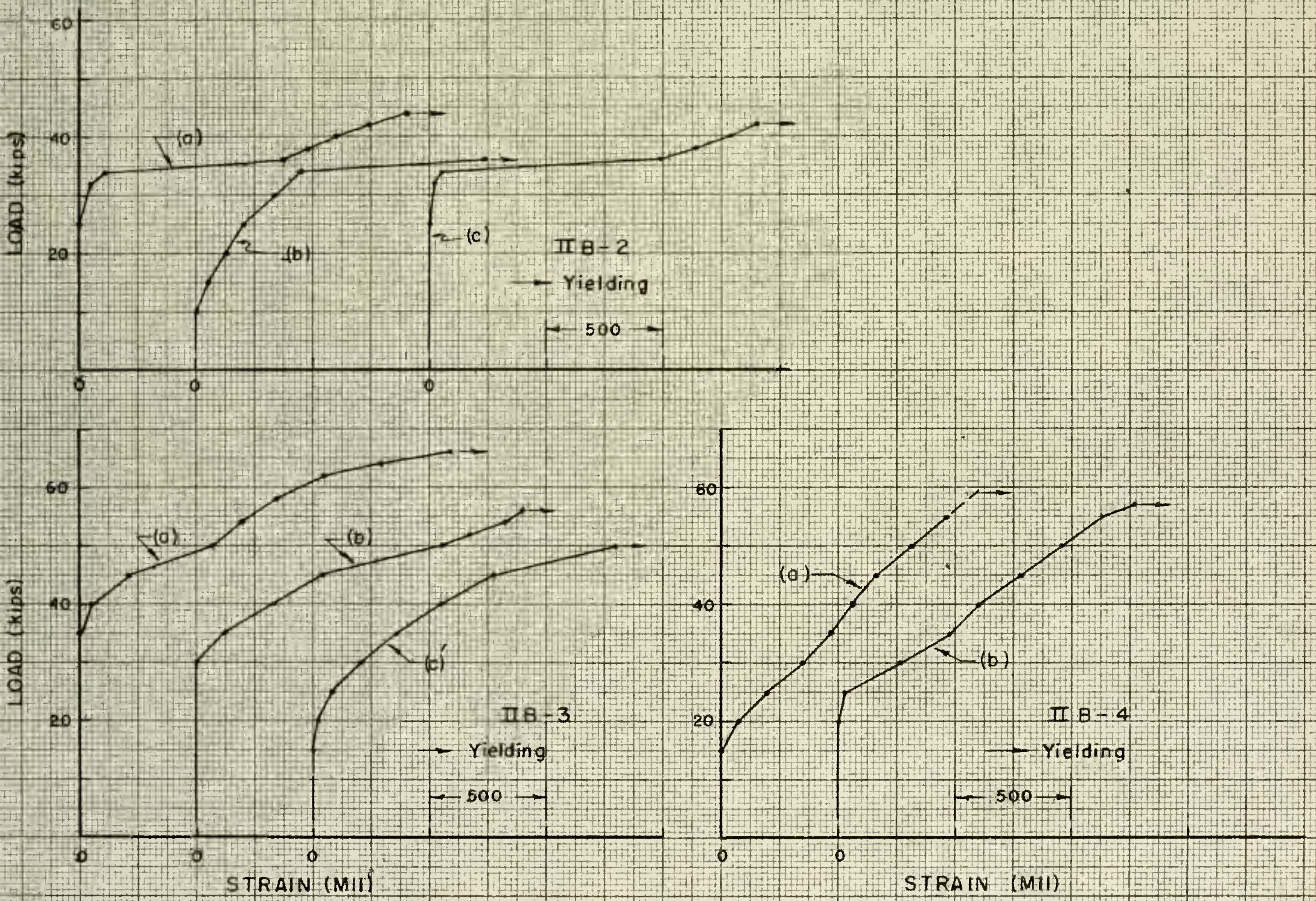

FIGURE 24. LOAD vs. STIRRUP STRAIN — SERIES II

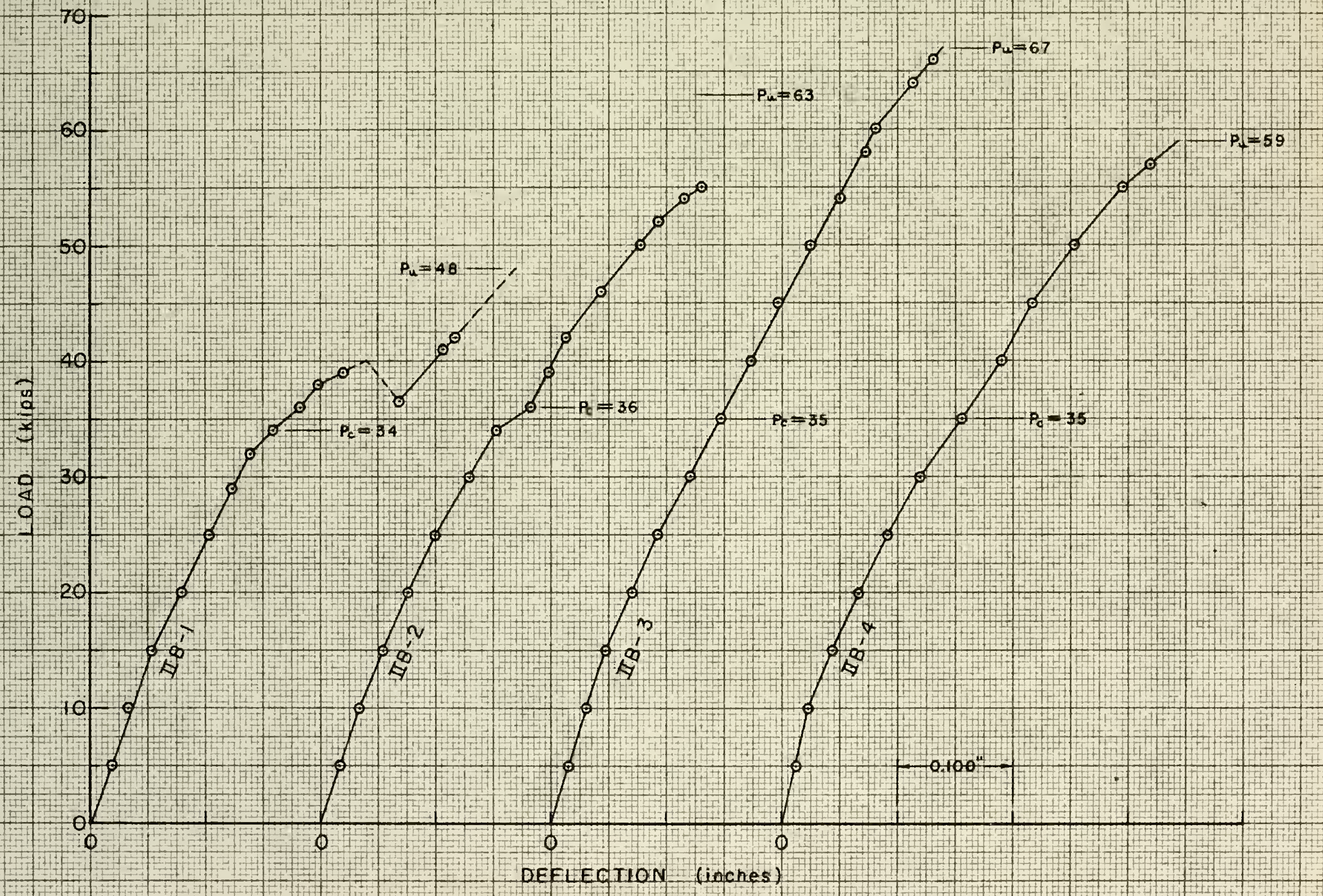

FIGURE 25. LOAD vs. DEFLECTION — SERIES Ⅱ

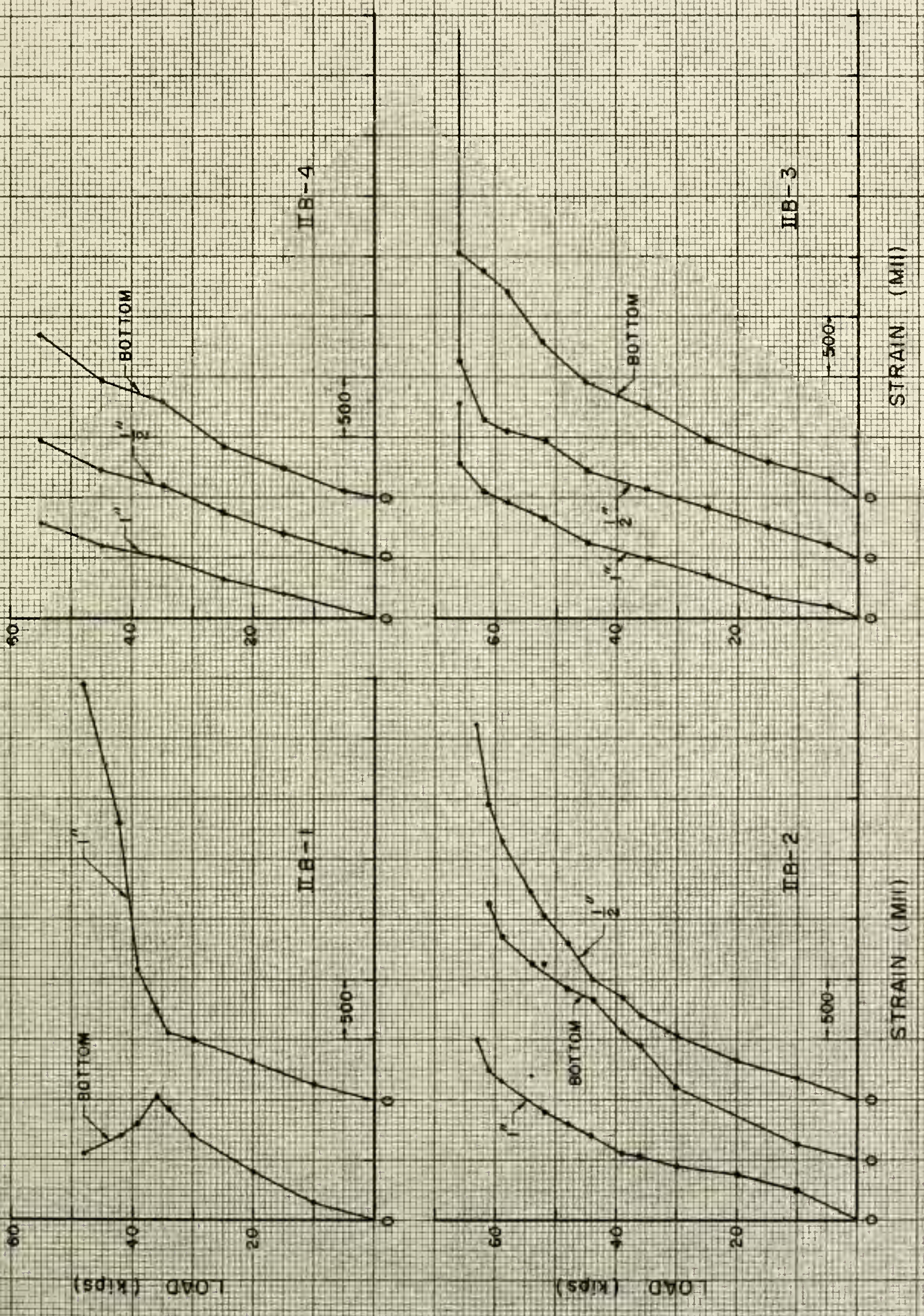

FIGURE 26. LOAD vs. CONCRETE STRAIN — SERIES II

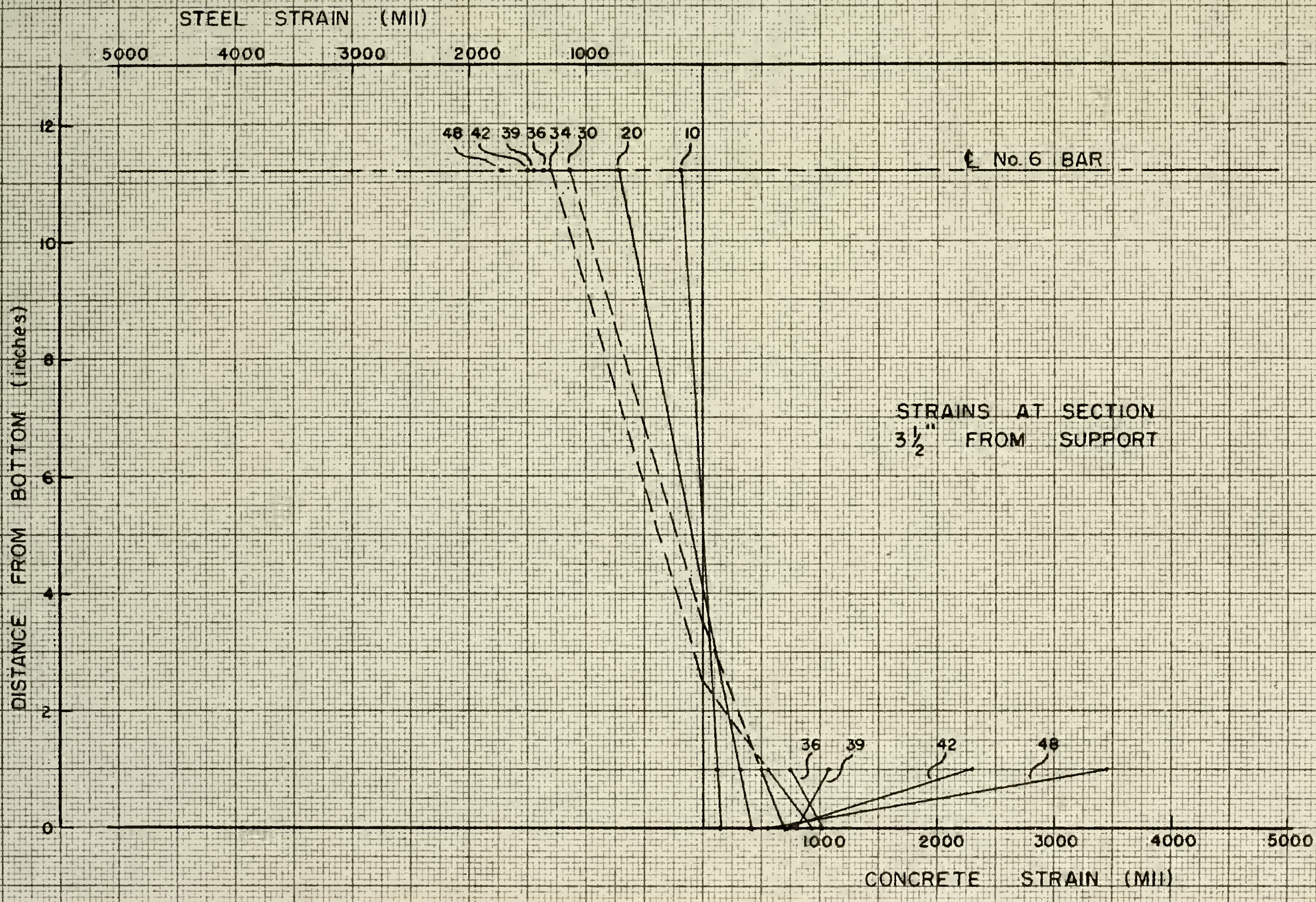

FIGURE 27. STRAIN DISTRIBUTION — BEAM II B-I

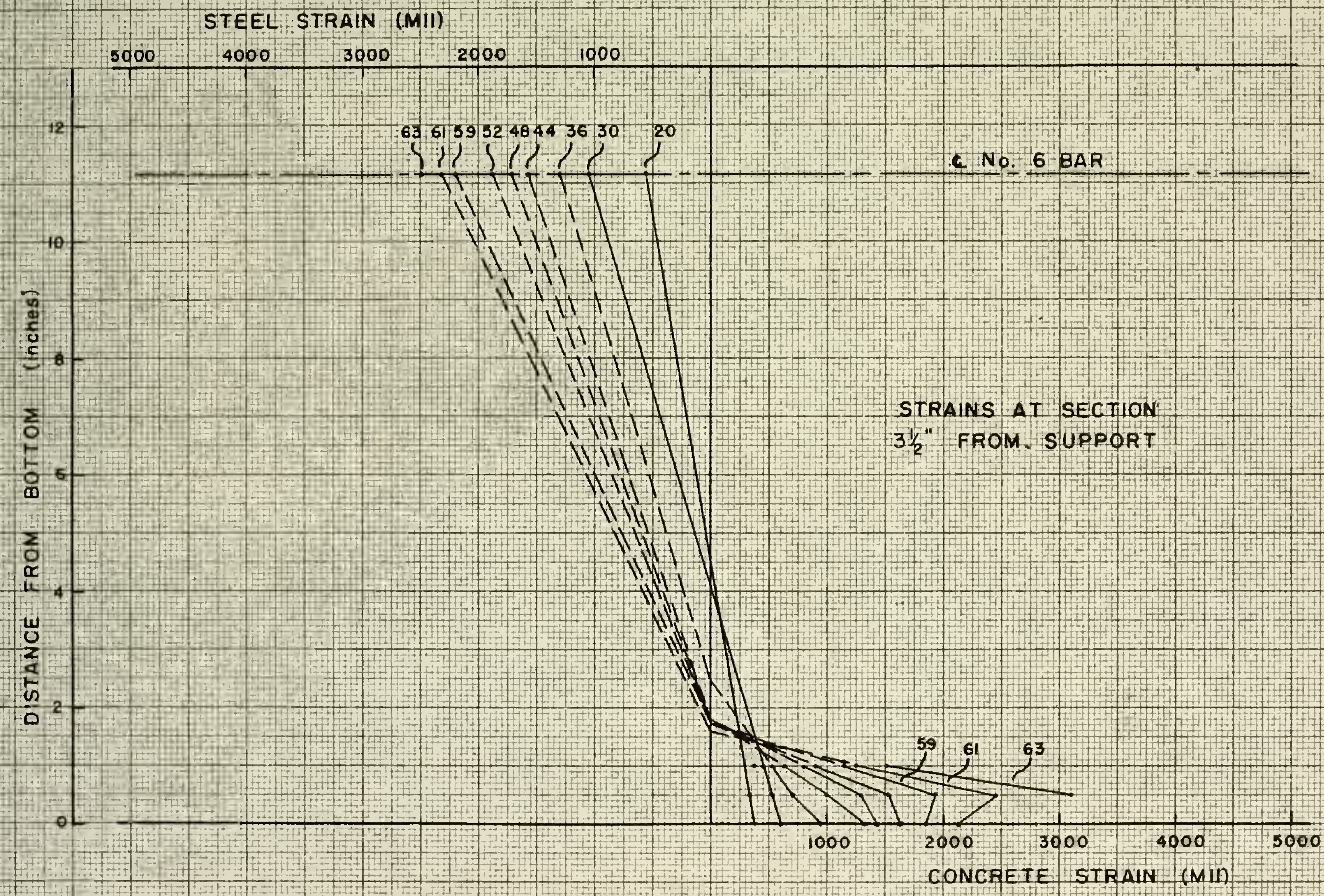

FIGURE 28. STRAIN DISTRIBUTION — BEAM IIB-2

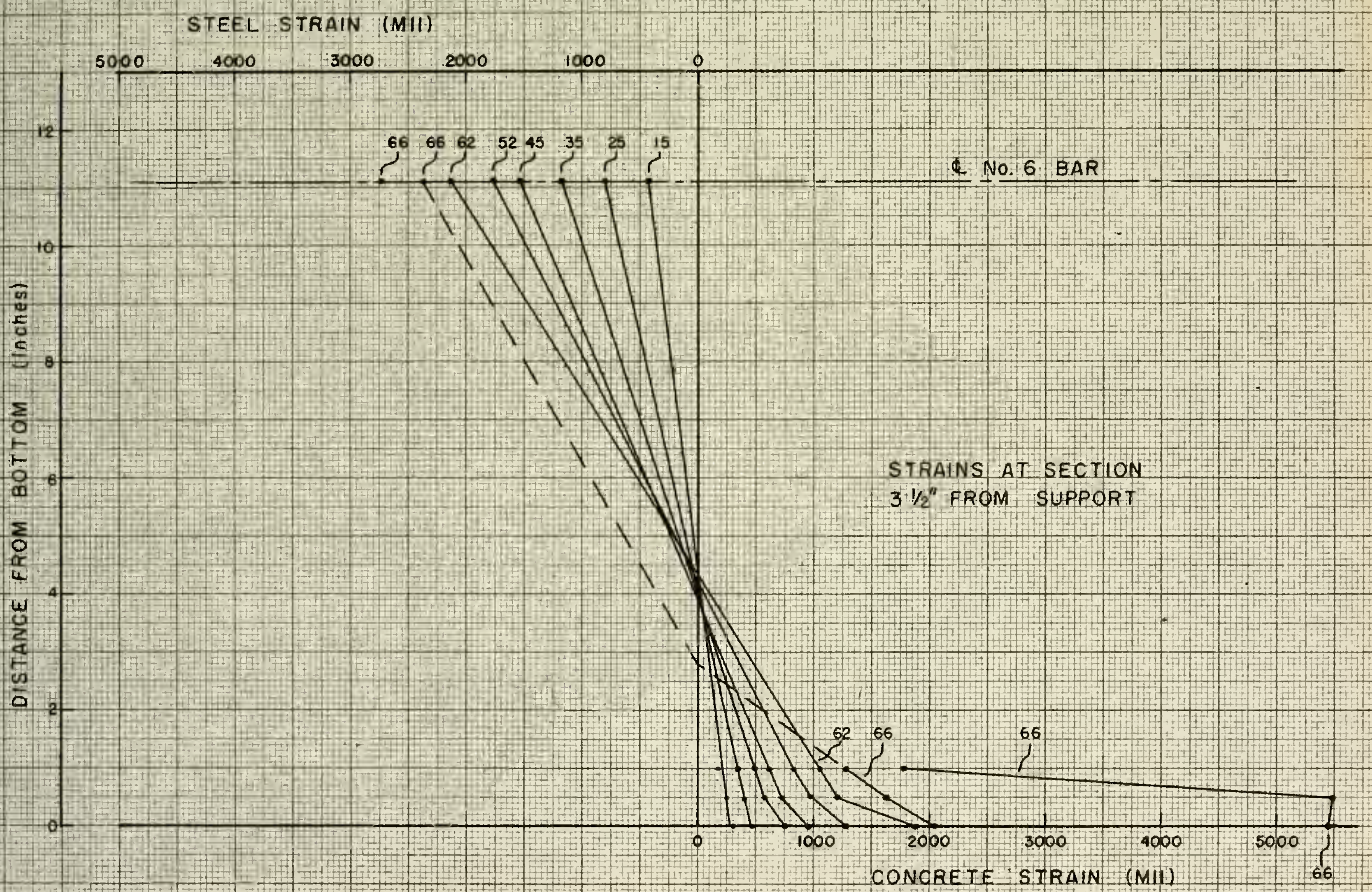

FIGURE 29. STRAIN DISTRIBUTION — BEAM IIB-3

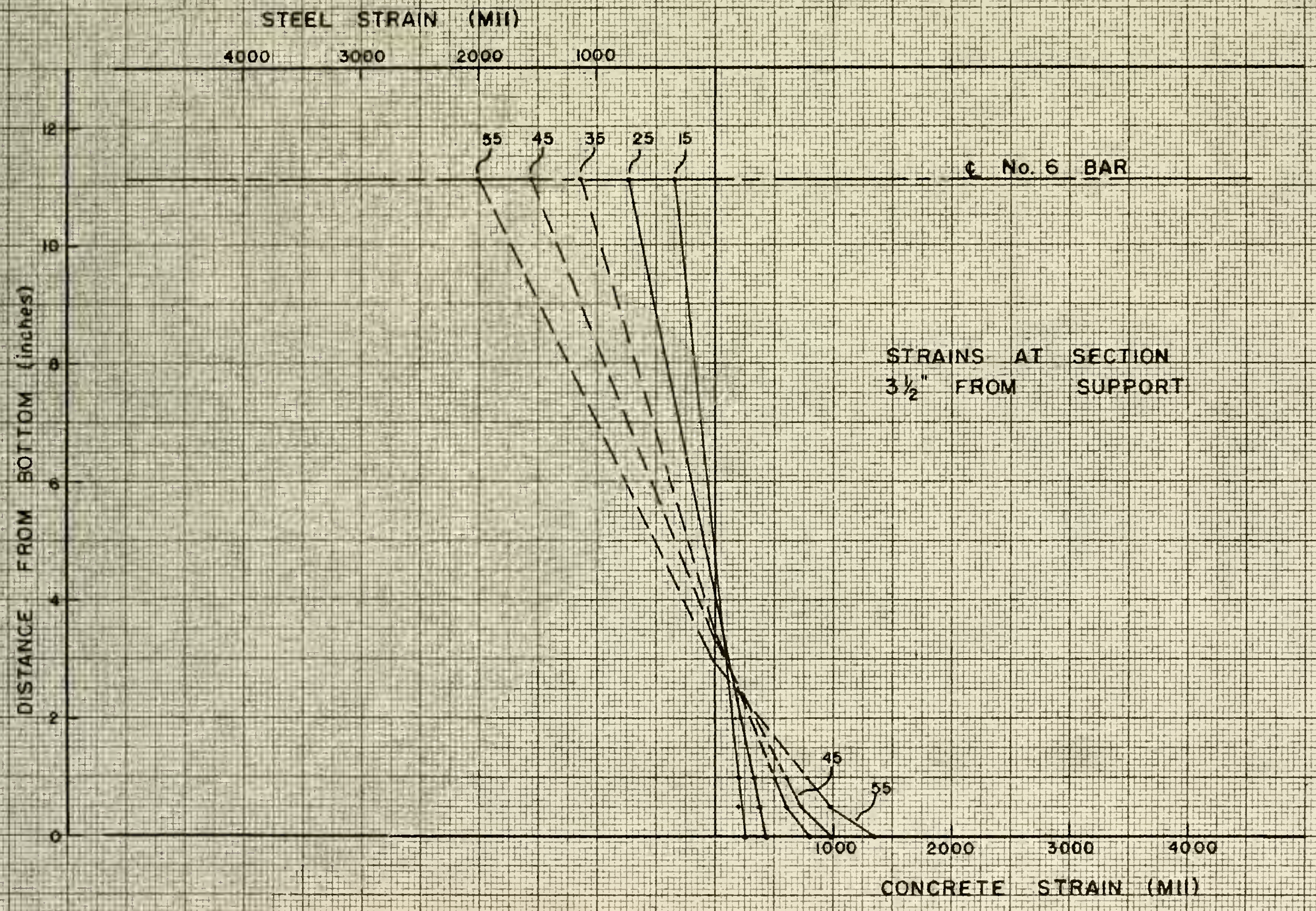

FIGURE 30. STRAIN DISTRIBUTION — BEAM II B-4

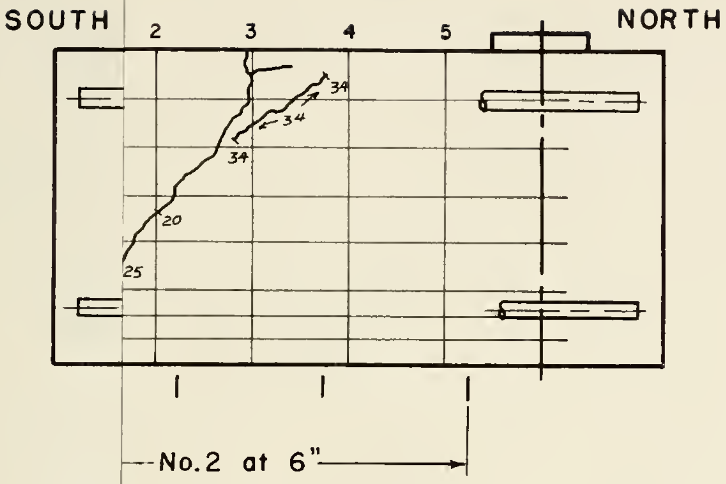

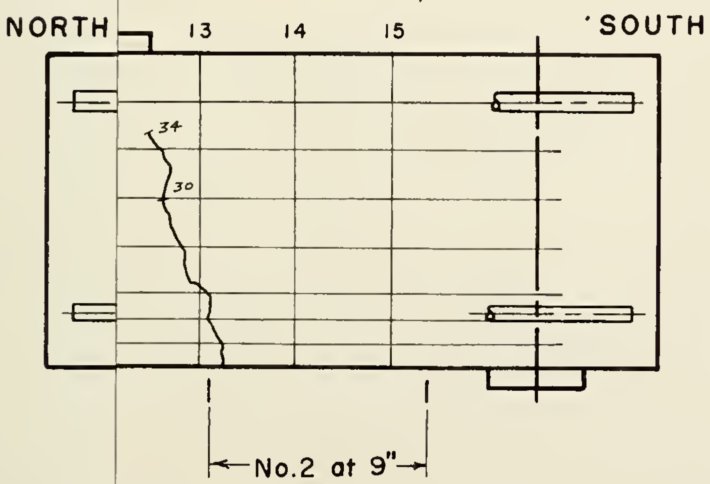

Cracks prior to failure

Cracks opening wide at failure

SR – 4 Strain Gage

Scale: 1" = 8"

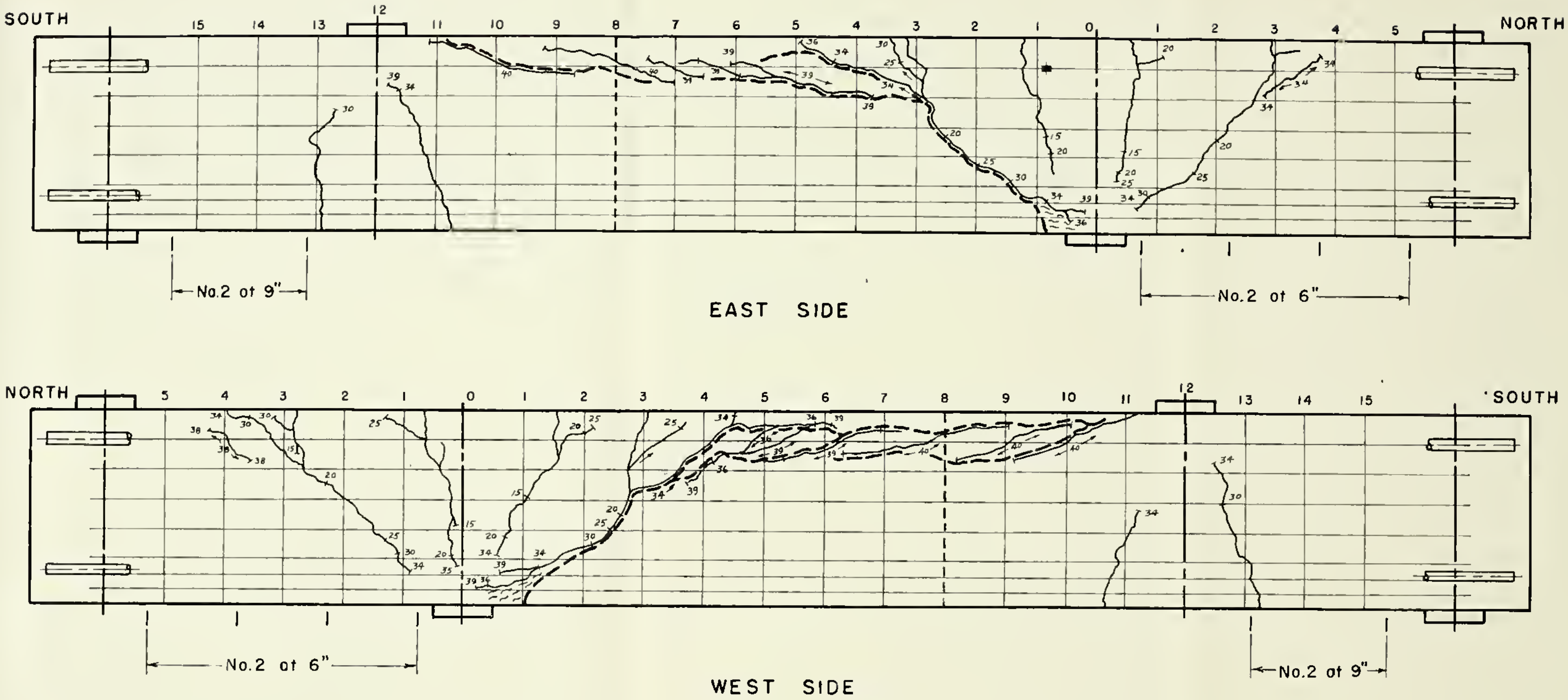

SR-4 Gage Locations:

No. 6 Bar — $3\frac{1}{2}$" from support (E)

Whittemore Gage Locations:

0", 1", 2", from bottom (E & W)

Cracks prior to failure

Cracks opening wide at failure

SR-4 Strain Gage

Scale: 1" = 8"

FIGURE 31. BEAM IIB-1

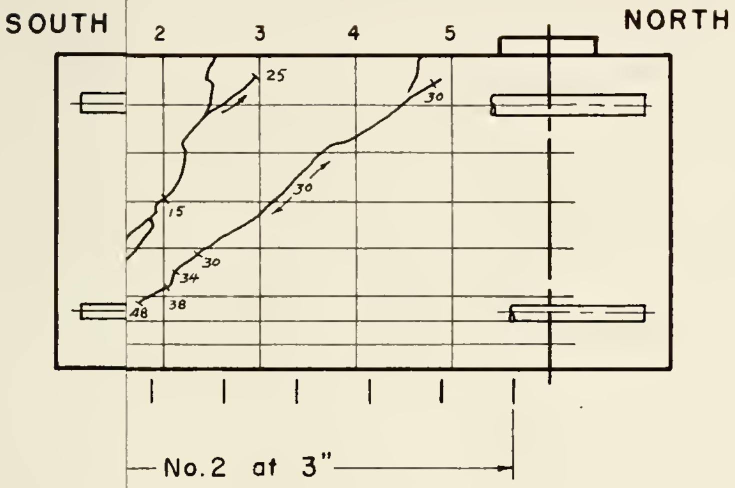
SOUTH
NORTH
2
3
4
5
25
30
30
15
30
34
38
48
No.2 at 3"

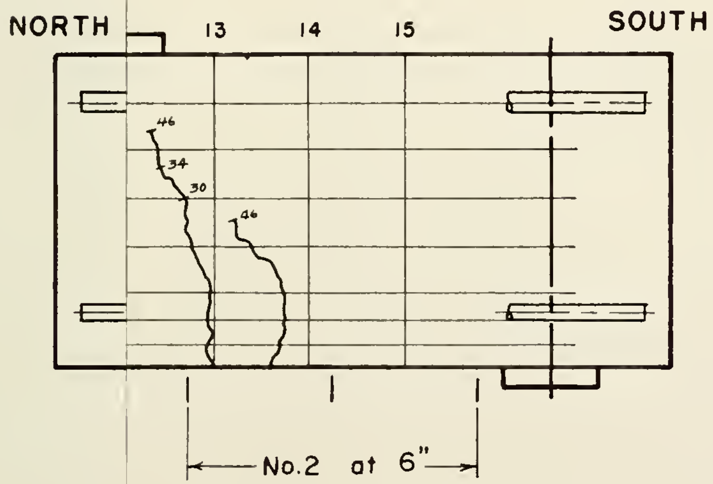
NORTH
SOUTH
13
14
15
46
34
30
46
No.2 at 6"

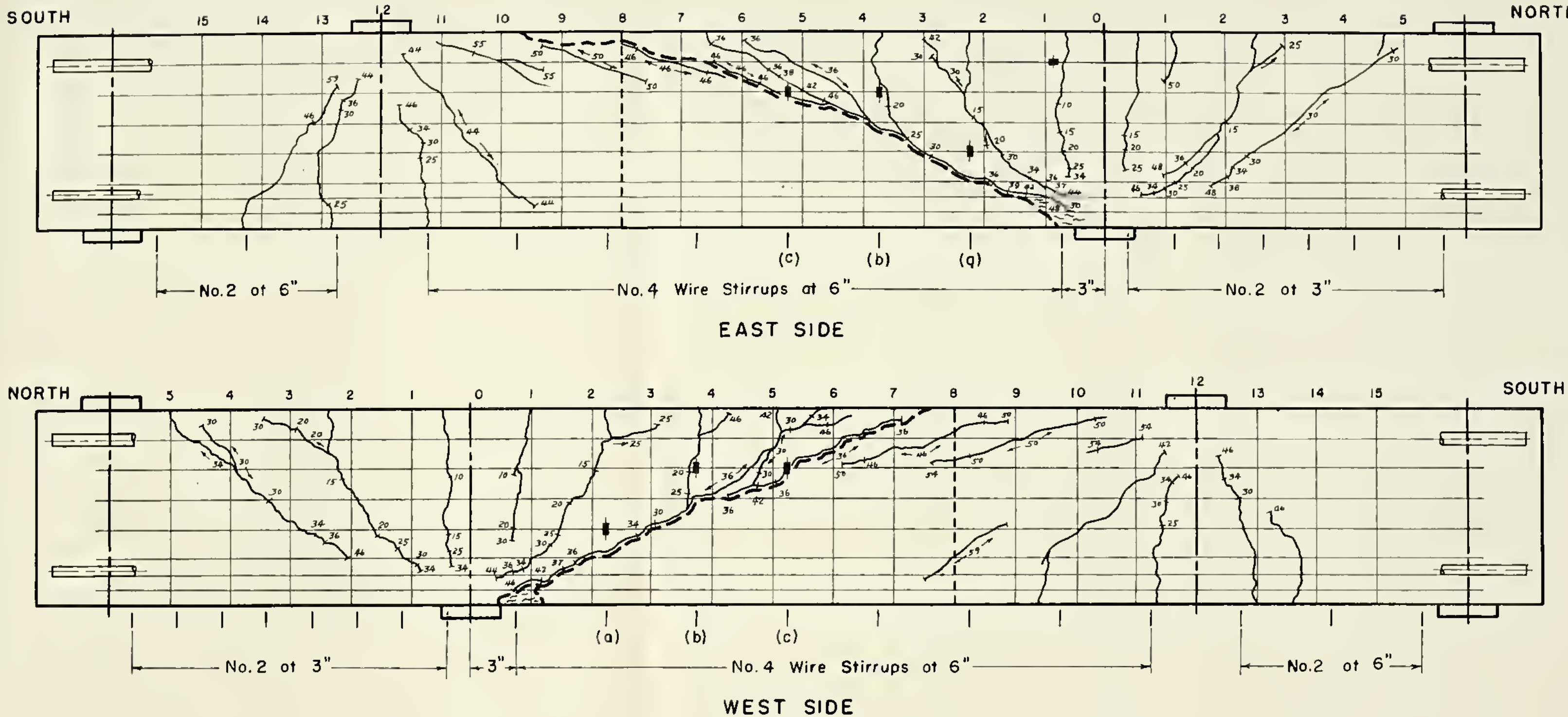

SR-4 Gage Locations:

No. 6 Bar — 3 1/2" from support (E)
Stirrup (a) — 5" " bottom (W)
" (b) — 9" " " "
" (c) — " " " "

Whittemore Gage Locations:

0", 1/2", 1", 2" from bottom (E & W)

FIGURE 32. BEAM IIB-2

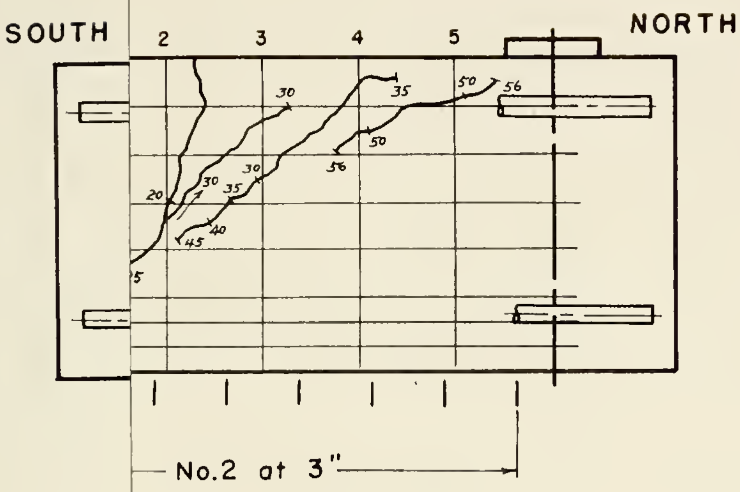
SOUTH
NORTH
2
3
4
5
No.2 at 3"

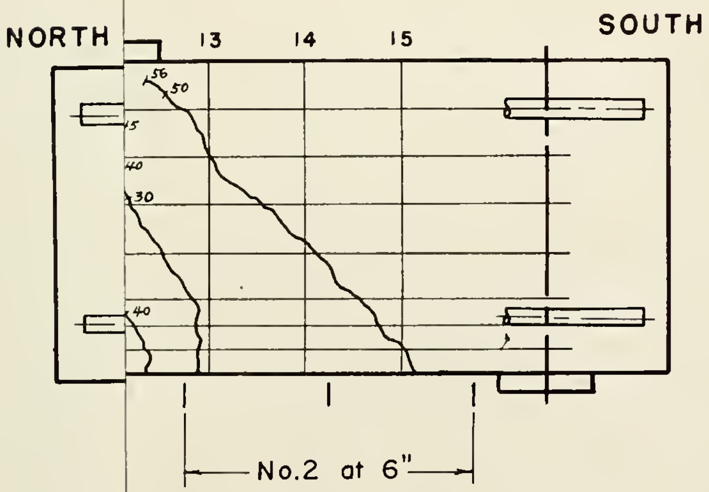
NORTH
SOUTH
13
14
15
No.2 at 6"

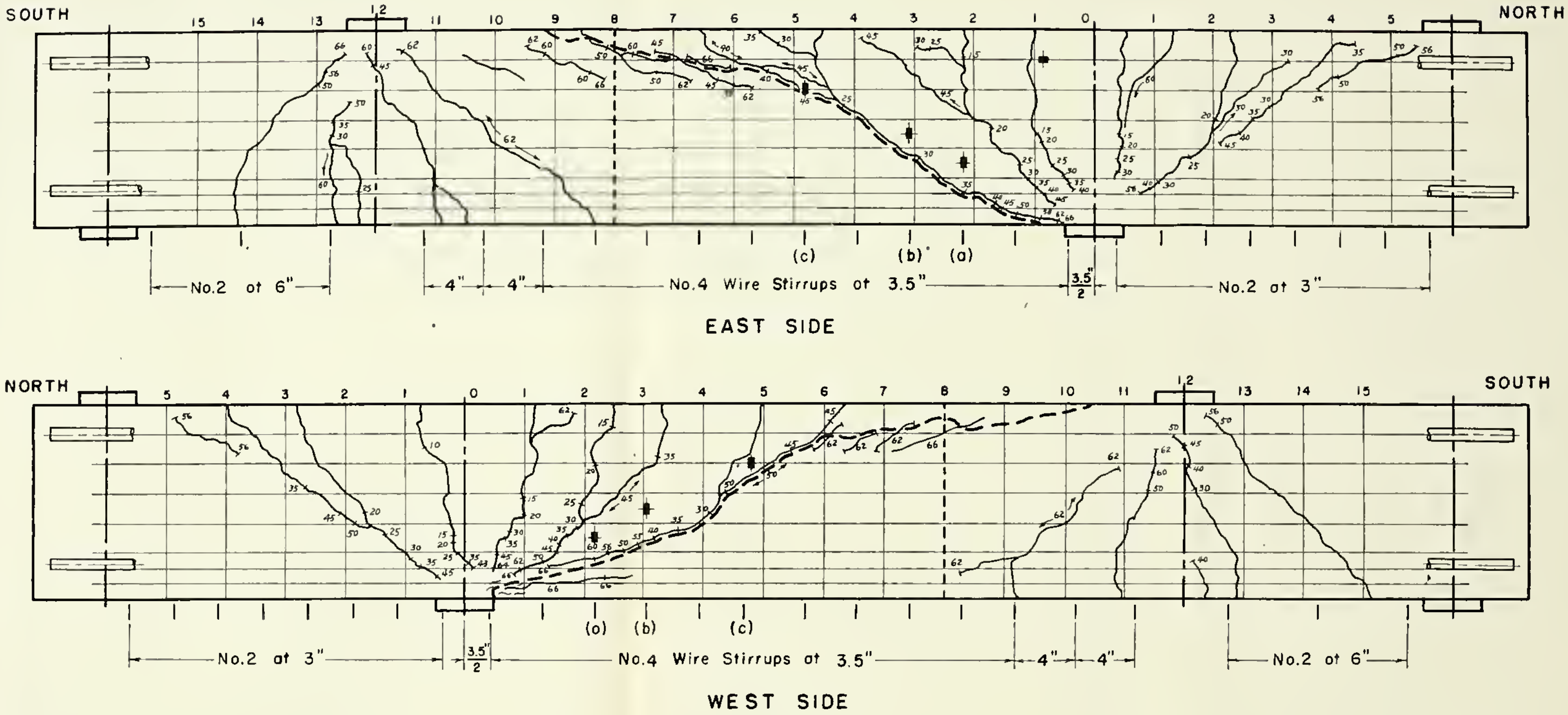

SR-4 Gage Locations:

No. 6 Bar — 3 1/2"	from	support	(E)
Stirrup (a) — 4"	"	bottom	(W)
" (b) — 6"	"	"	"
" (c) — 9"	"	"	"

Whittemore Gage Locations:

0", 1/2", 1", 2" from bottom (E & W)

FIGURE 33. BEAM IIB-3

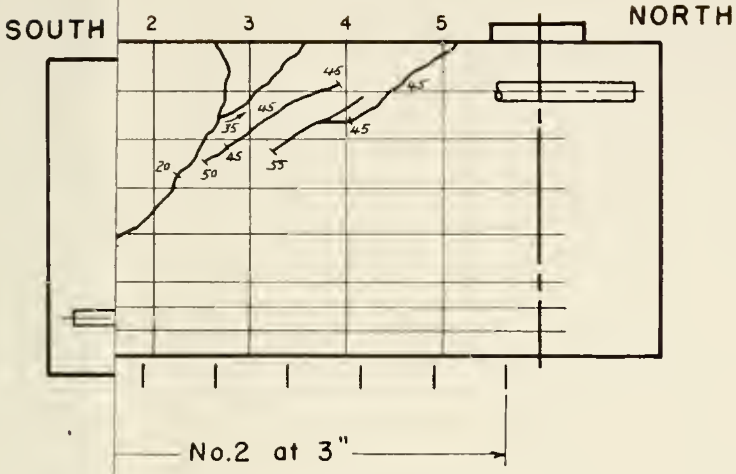
SOUTH
2
3
4
5
NORTH
45
45
45
35
45
45
20
50
55
No.2 at 3"

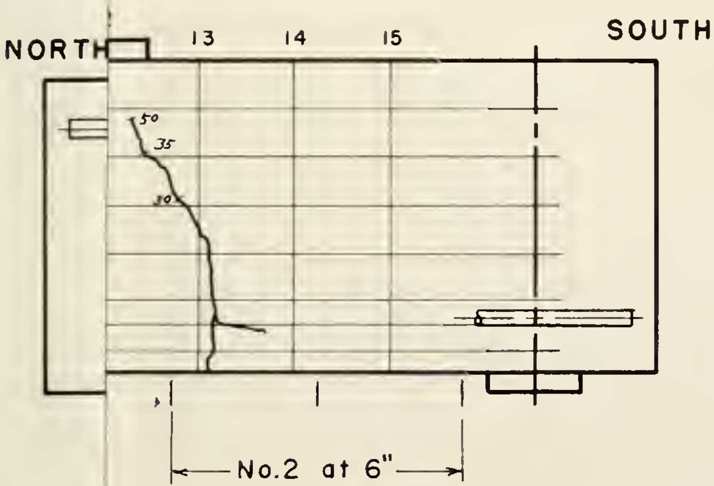
NORTH
13
14
15
SOUTH
50
35
30
No.2 at 6"

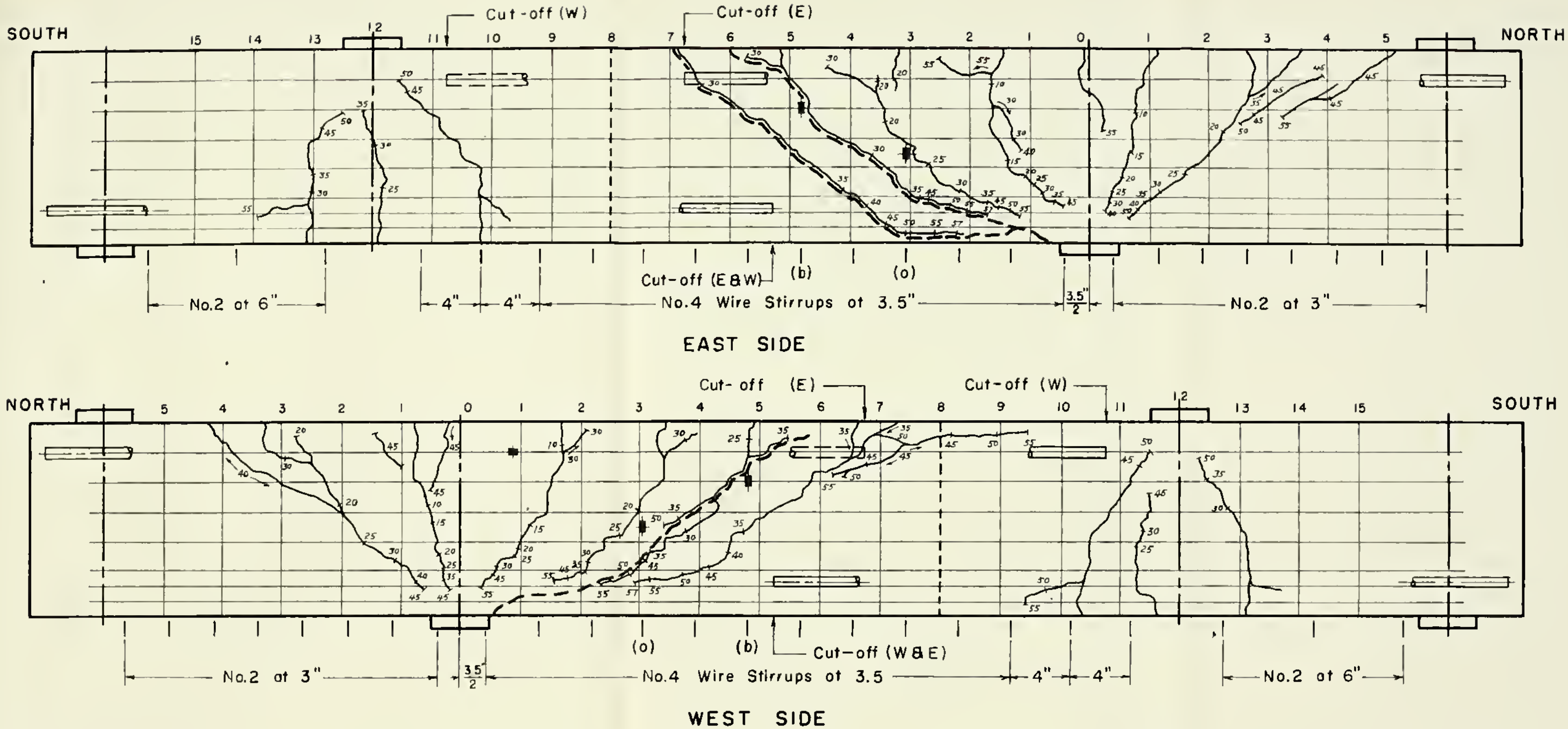

SR-4 Gage Locations:

No.6 Bar — 3 1/2" from support (W)
Stirrup (a) — 6" " bottom (E)
" (b) — 9" " " (W)

Whittemore Gage Locations:

0", 1/2", 1", 2" from bottom (E & W)

FIGURE 34. BEAM IIB-4

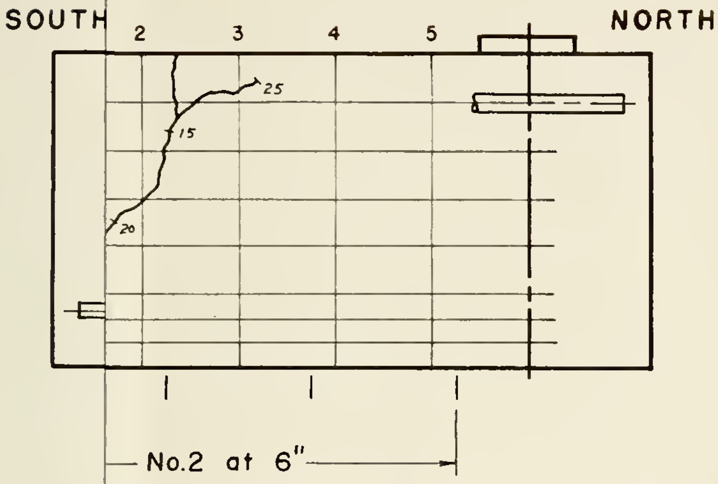
SOUTH
2
3
4
5
NORTH
25
15
20
No.2 at 6"

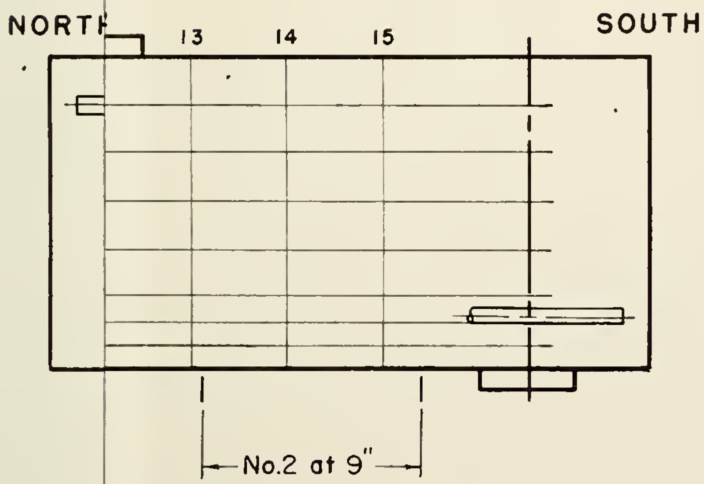
NORTH
13
14
15
SOUTH
No.2 at 9"

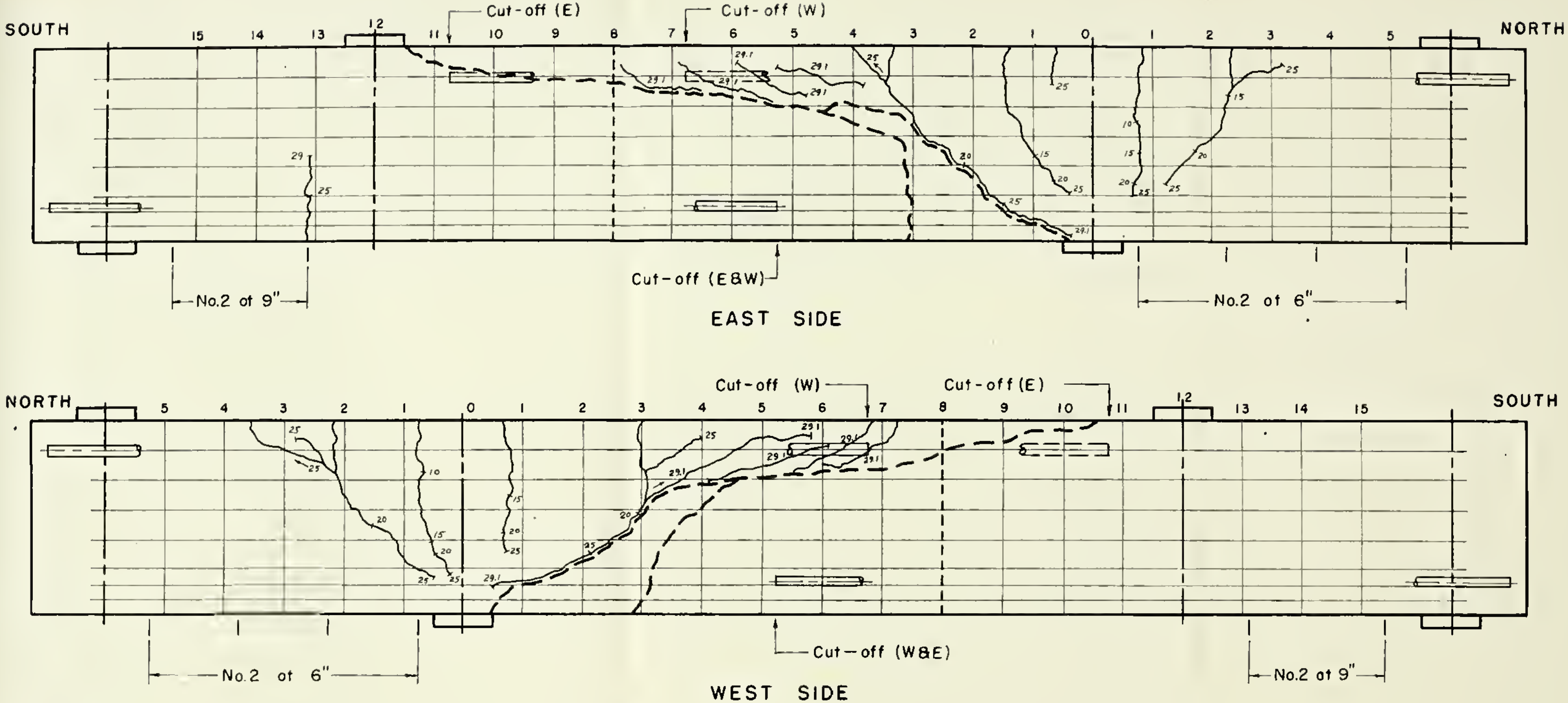

FIGURE 35. BEAM IIB-5

Series III

Beam IIIB-1 (No Stirrups)

Up to the load $P = 36^k$ the flexural cracks had penetrated no farther than the depth to the cracked section neutral axis (4.1" from the compressive face). See Figure 45. At 36^k a distinct inclined crack penetrated deep into the compression zone (to within 1 1/2" of the compressive face on the west side) and extended back towards the tension steel, including the top of the existing flexural crack. At 37^k a very sudden diagonal tension type failure occurred. The load of 37^k was sustained with little change at first. Complete separation then took place almost instantaneously with no appreciable widening or extension of the diagonal crack.

This was a most undesirable type of failure, occurring with very little warning. There was no noticeable loss in stiffness when the diagonal crack formed at 36^k (See Figure 39). Prior to collapse there was no indication of impending failure, since the critical crack was only hairline in nature.

Beam IIIB-2

(Low Percentage of Stirrups - 8" Spacing)

Behavior of this beam at low loads was essentially identical with that of Beam IIIB-1. The critical diagonal crack formed at the same load, $P = 36^k$ (See Figure 46);

however, its penetration was not quite as deep as in IIIB-1. Formation of the critical crack occurred after the load of 36^k had been sustained for some time. Note the large increases in the strain of stirrups (b) and (c) (Figure 38) and the increased deflection (Figure 39) after the diagonal crack had formed.

On the east side the diagonal crack was an extension of the existing flexural tension crack; whereas on the west side it was separate and crossed the flexural crack.

Following the formation of the critical diagonal crack, the stirrups effectively maintained beam action, as seen by only a slight decrease in stiffness and by the linear load-steel strain curve (See Figure 36). Stirrup (c) began yielding at $P = 46^k$. As soon as this occurred, stirrup (b) began picking up strain rapidly. At 48^k stirrup (b) yielded, the load fell off to 44.5^k, and the diagonal crack split entirely through the beam. No further increase in load could be sustained. Stirrup (a) was not affected by the critical diagonal crack..

Failure was essentially the diagonal tension type failure as in Beam IIIB-1, occurring after the stirrups crossed by the crack had yielded.

In this particular test the load was removed after a load of 23.4^k had been applied. The beam was then reloaded continuously to failure. Figures 36 and 39 show the difference in behavior between the uncracked section (initial loading)

and the fully cracked section (reloading. The convergence of the initial and reload curves beyond the load of 23.4^k indicate that the behavior at the diagonal cracking load ($P_c = 36^k$) was not appreciably affected by this procedure.

Beam IIIB-3

(High Percentage of Stirrups - 5 1/2" Spacing)

In Beam IIIB-3 the stirrup spacing in the shear span was set at 5 1/2" compared to 8" for Beam IIIB-2 (Figure 47). The increased amount of stirrups restrained the rapid, if not instantaneous, formation of the long diagonal tension crack. Three inclined cracks formed, each penetrating gradually into the compression zone at different loads. Stirrup strains began increasing as a crack crossed them, but not nearly as rapidly as in Beam IIIB-2.

The two stirrups with gages (a) and (b), along with the longitudinal steel, reached yield strains at 58^k to 60^k. At these loads the diagonal tension crack closest to the support extended toward the tension steel at a very flat slope. This crack later opened considerably at failure.

As soon as the tension steel had begun to yield (58^k), widening of the flexural cracks directly over the support was apparent, and a flexural failure seemed imminent. In addition, the concrete strains increased rapidly with an increase in load. Concrete strain on the east side picked up much more rapidly than that on the west side. At 63^k

crushing was visible on the east side over the lower 1/2". As load was further increased this crushing spread gradually across the bottom to the west side. Ultimate failure was by crushing of the concrete in the lower 1 1/2" to 2" at the sections adjacent to the support.

However, indications were that the diagonal crack also had a large effect. At ultimate load the diagonal crack was the only one to open widely. In addition, it has been shown that the distribution of strain over the section remains linear in a flexural failure. For this beam there was a definite concentration of compressive strain over the lower 1" and an indication that the distribution was not continuous, but broken at about 2" above the bottom face, Figure 42. Hence, the mode of failure for this beam would best be described as a combination shear-compression and flexural tension.

Comparison of the load versus deflection curve (Figure 39) of this beam with that of Beam IIIB-2 shows the greater ductility of a beam failing in flexure. Approaching failure in Beam IIIB-3 was marked by a considerable increase in deflection. The shear failure of Beam IIIB-2, however, was much more brittle in nature -- giving very little warning of impending failure.

Beam IIIB-4

(High Percentage of Stirrups - 4; Spacing)

The crack development of Beam IIIB-4, Figure 48, was gradual due to the high percentage of web reinforcement.

Three diagonal cracks began penetrating the compression zone on the east side at a load of 35^k - 40^k. The cracks on the west side penetrated less rapidly probably due to the strain gage placement on the east legs of the stirrups.

Stirrup (b) began picking up strain rapidly at 35^k and was the first to yield at 54^k. Stirrups (c) and (d), farther out from the support (See Figure 47), yielded at loads of 70^k and 64^k, respectively. These stirrups, however, were not crossed by the critical diagonal crack, which was again shifted closer to the support as in Beam IIIB-3.

Yield strain in the longitudinal steel was reached at a load of 62^k, as compared to a yield load of 58^k in Beam IIIB-3. Although the steel strain increased considerably as the load of 62^k was maintained constant (Figure 37), the concrete compressive strains remained relatively low, and equilibrium was restored.

At a load of 68^k the strains in both the tension steel and the concrete compression zone were increasing rapidly with no increase in load. (See Figures 37 and 41). A maximum concrete strain of 3200 MII was recorded as this load was first reached. Signs of crushing became visible over the lower 1/2" as the load of 68^k was sustained. However, equilibrium was again restored, and more load was applied. The beam collapsed at 70^k as the concrete over the lower 1 1/2" to 2" was crushed.

Failure was essentially flexural in nature. However, there was again a concentration of compressive strain over

the lower 1/2" adjacent to the support and an indication that the distribution of strain across the section was not linear. As in Beam IIIB-3 the diagonal crack opened widely at failure. However, the increased percentage of web steel restrained the penetration of the diagonal crack, as compared to Beam IIIB-3. This can be seen in Figure 41 by comparing the compressive strains of the two beams at comparable loads.

Beam IIIB-5

(4" Stirrup Spacing - Longitudinal Steel Cut-Off)

The behavior of Beam IIIB-5 (Figure 49) at low loads was identical with that of the first four beams of this series. At $P = 30^k$ a long, steeply inclined crack formed suddenly, crossing the tension steel at the cut-off point. The crack was so steep that essentially only one stirrup was crossed. The strain in this stirrup (c) increased from 0 to 400 MII immediately.

As load was increased, the crack penetrated at a flat slope to within 1" of the compressive face at the yield load of stirrup (c), $P = 50^k$. A diagonal tension type failure occurred at 59.6^k, when this crack split entirely through the beam.

Beam IIIB-6

(No Stirrups - Longitudinal Steel Cut-Off)

The formation of the diagonal crack and complete failure occurred simultaneously at 30^k. (See Figure 50). The diagonal tension crack was an extension into the compression zone of a flexural crack which was initiated at the cut-off point of the top steel in the tension region. While the mode of failure was the same as its companion Beam IIIB-1 with steel extended throughout the full length of the beam, the strength was greatly reduced. The load at diagonal cracking was reduced from 36^k to 30^k and ultimate load from 37^k to 30^k.

Beams IIIA-1, 2, and 3

(No Stirrups - 2 Layers of Tension Steel)

Behavior of these three beams was nearly identical to that of Beam IIIB-1, (Figures 51, 52, and 53), except that they were significantly stronger. Each beam in this series failed suddenly in diagonal tension. Beam IIIA-3 failed simultaneously with the formation of the diagonal tension crack. The other two beams sustained slightly more load than that at which the diagonal crack penetrated the compression zone. Collapse of each beam was quite sudden with no appreciable widening of the diagonal crack prior to ultimate load.

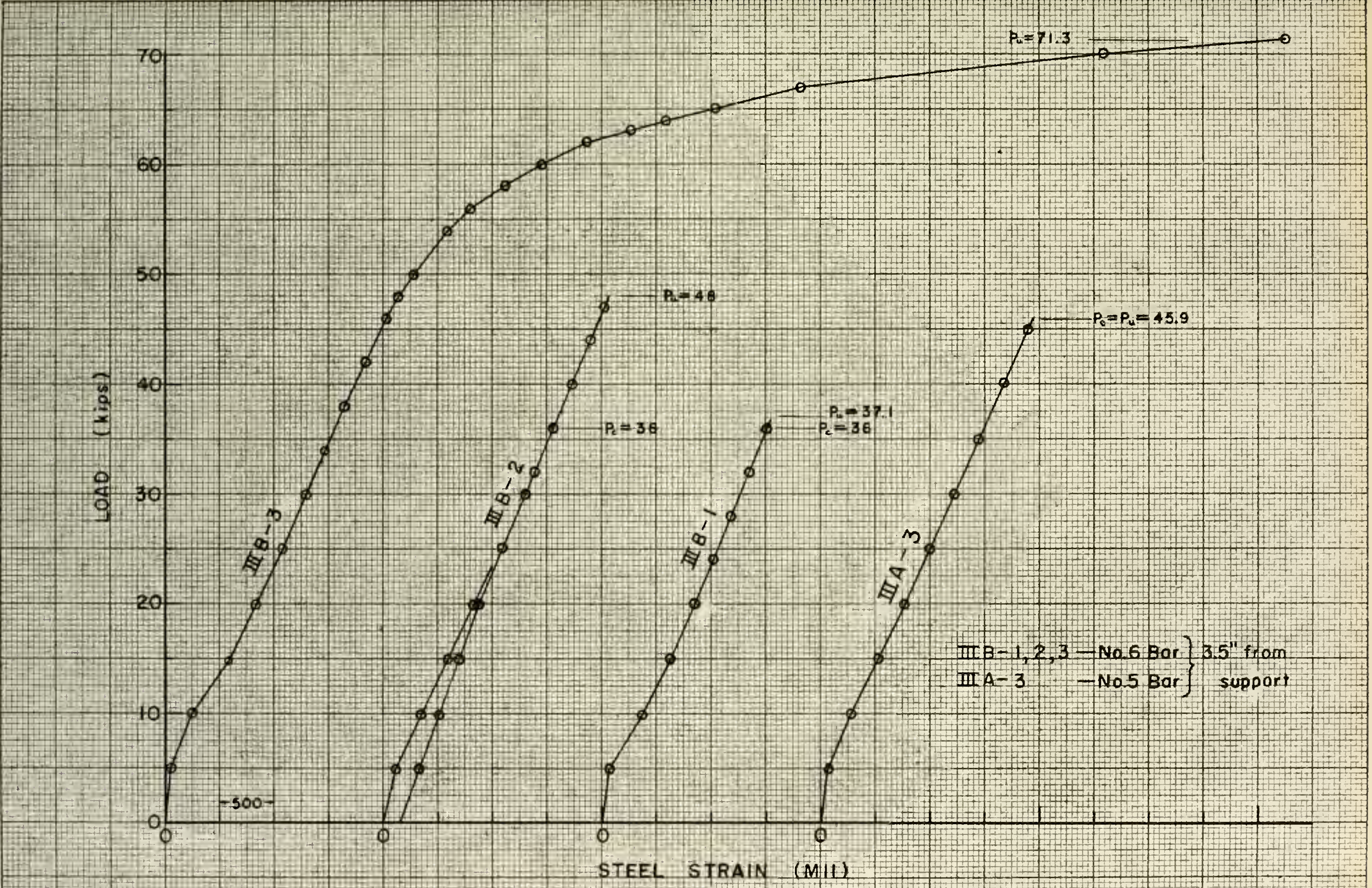

FIGURE 36. LOAD vs. STEEL STRAIN — SERIES III

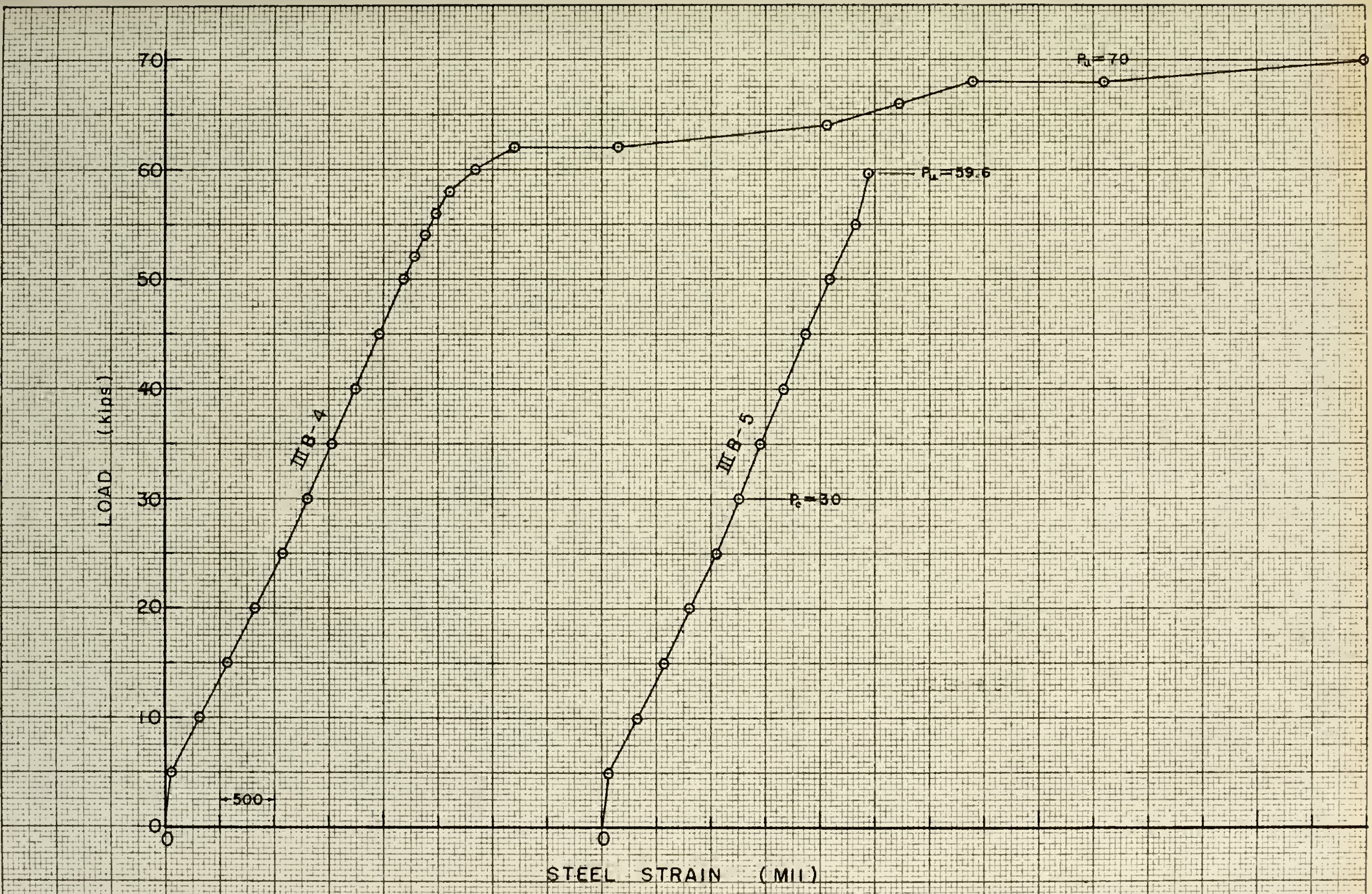

FIGURE 37. LOAD vs. STEEL STRAIN — SERIES III (cont'd)

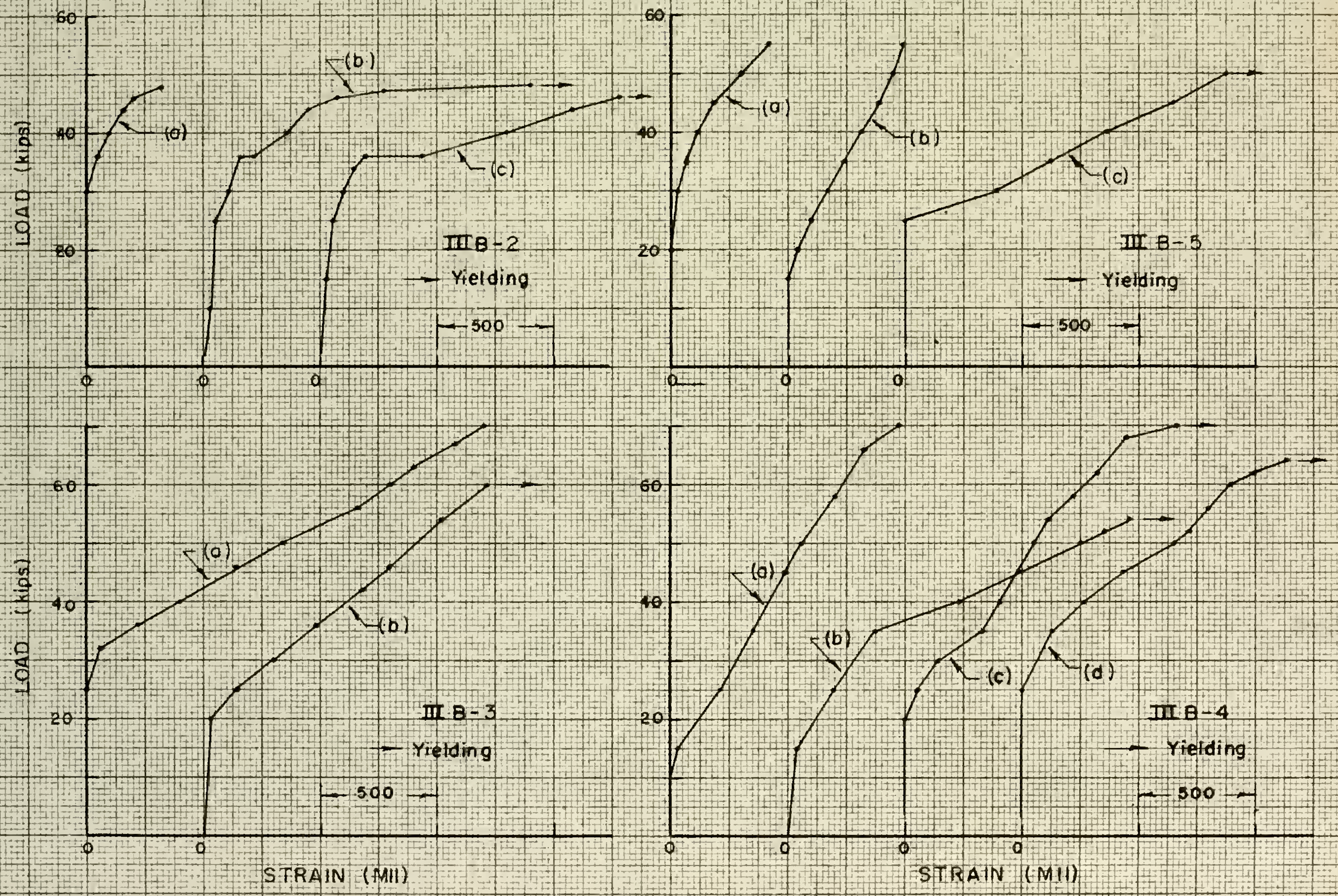

FIGURE 38. LOAD vs. STIRRUP STRAIN — SERIES III

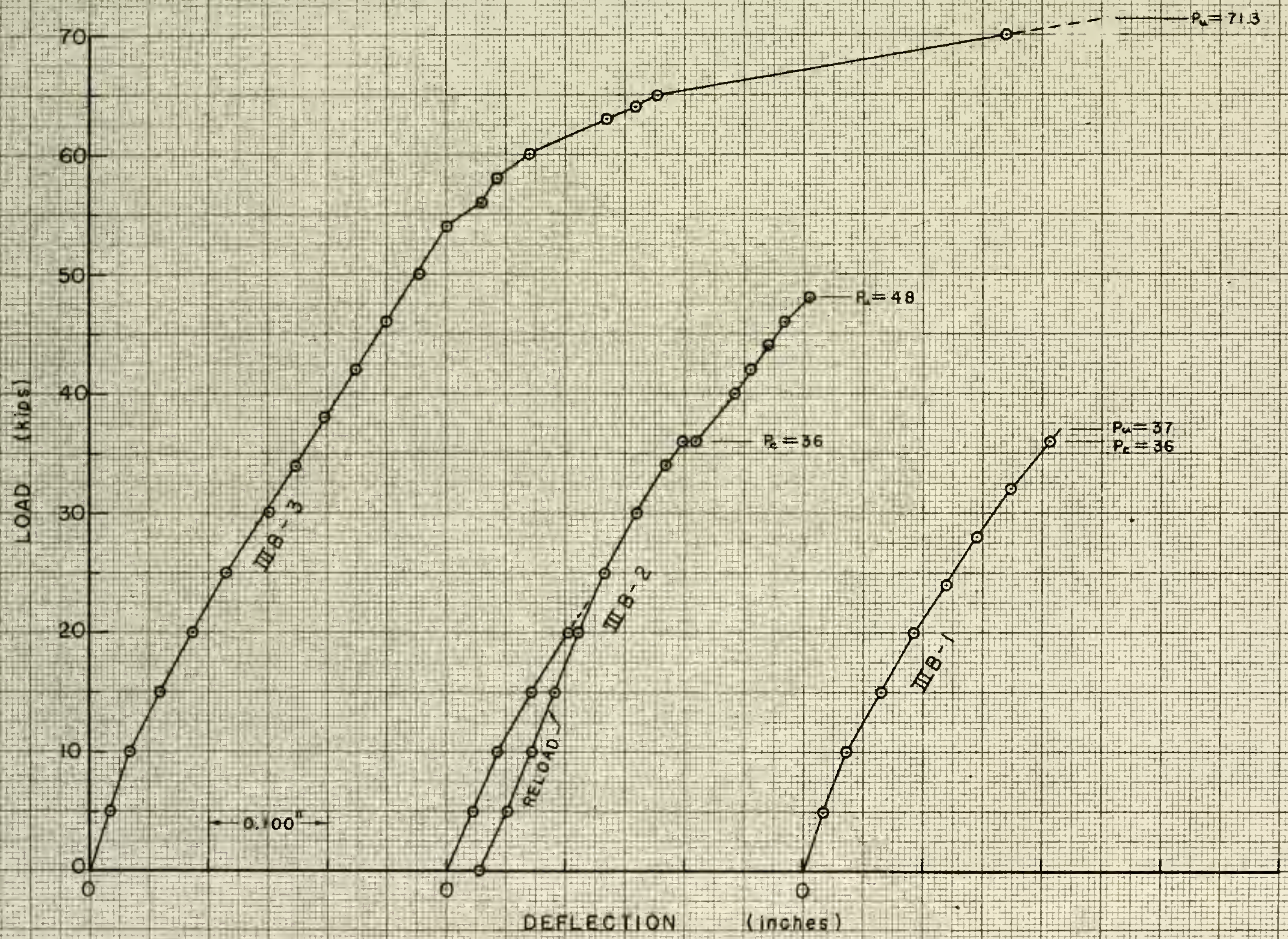

FIGURE 39. LOAD vs. DEFLECTION — SERIES III

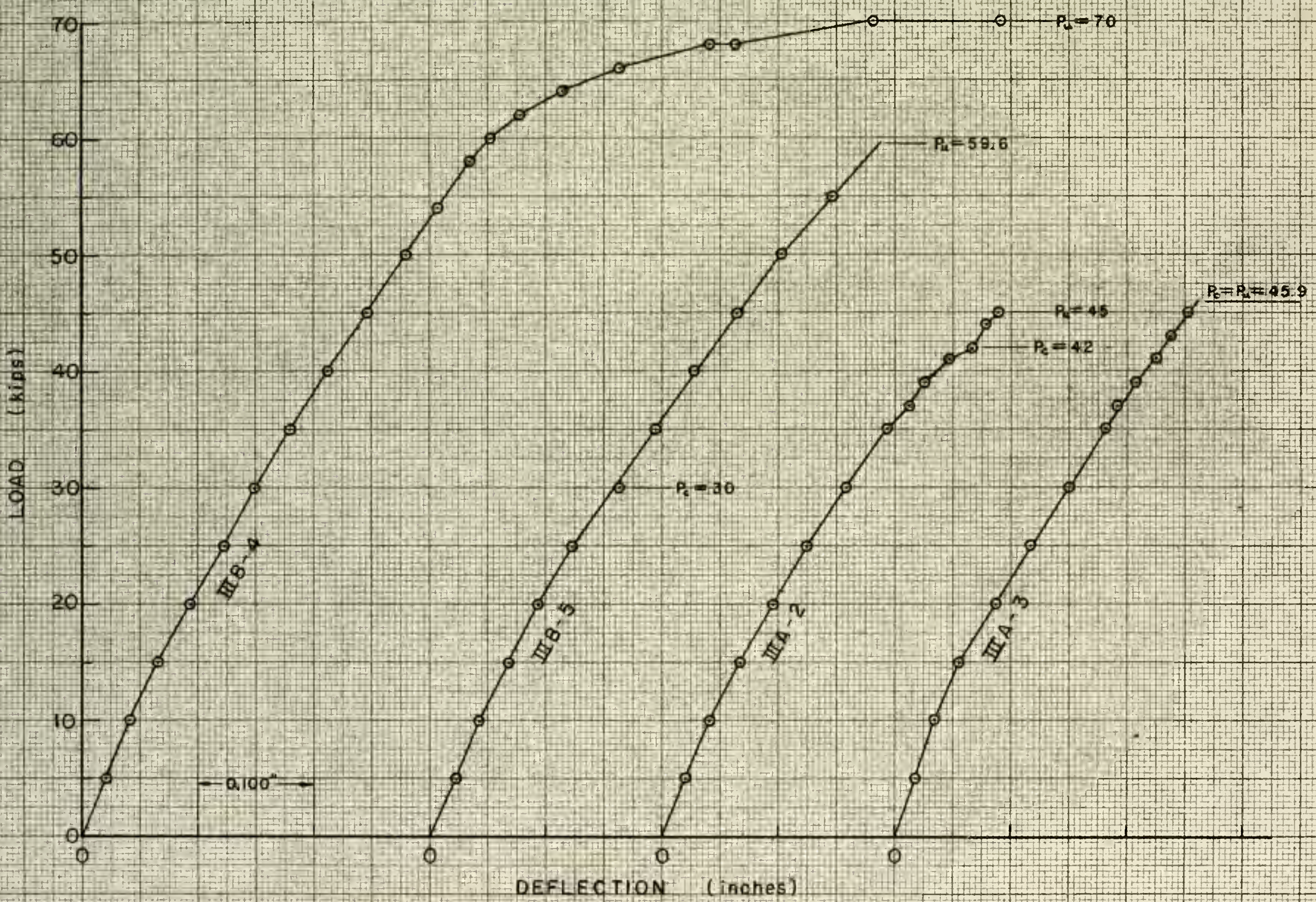

FIGURE 40. LOAD vs. DEFLECTION — SERIES III (cont'd)

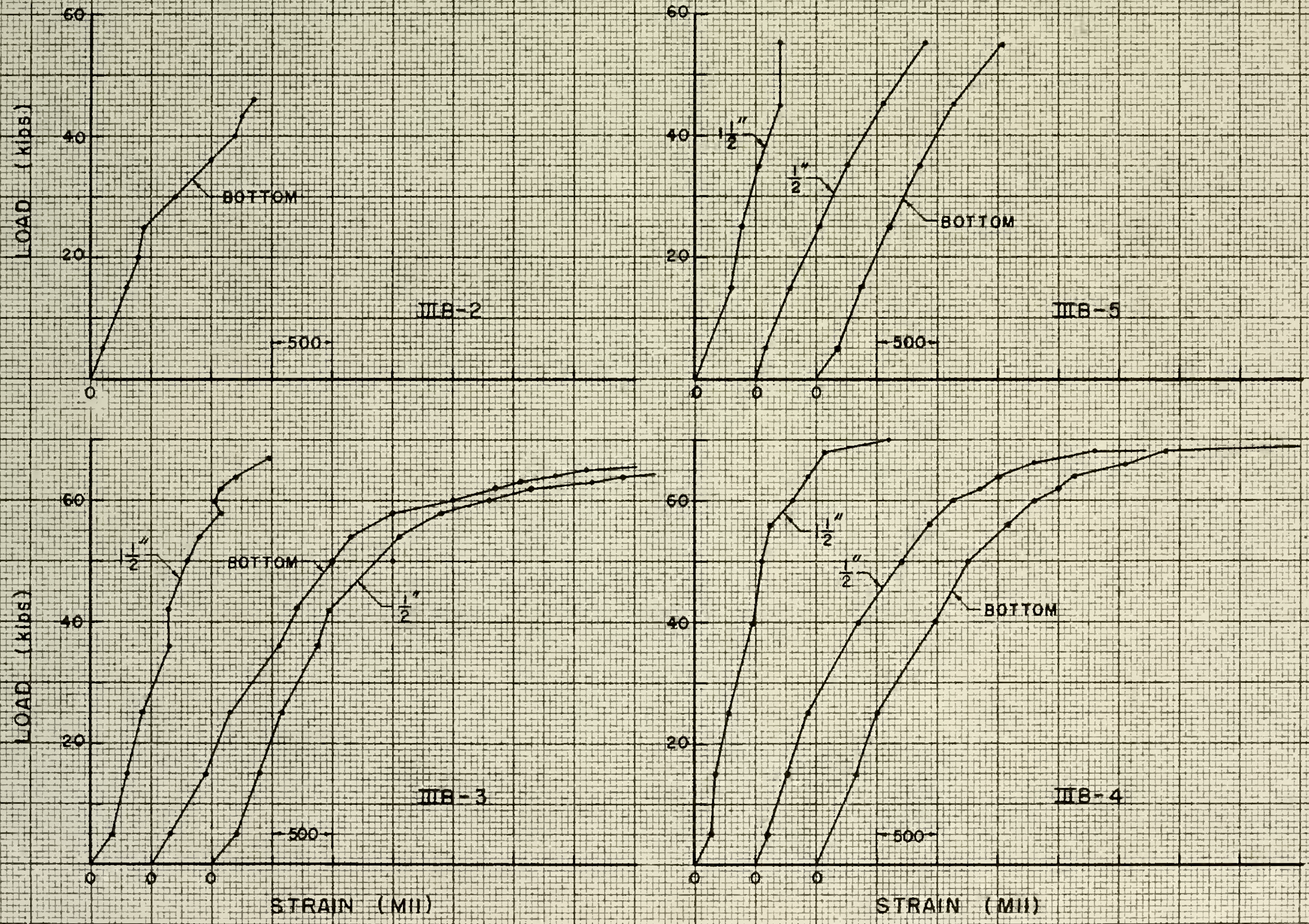

FIGURE 41. LOAD vs. CONCRETE STRAIN — SERIES III

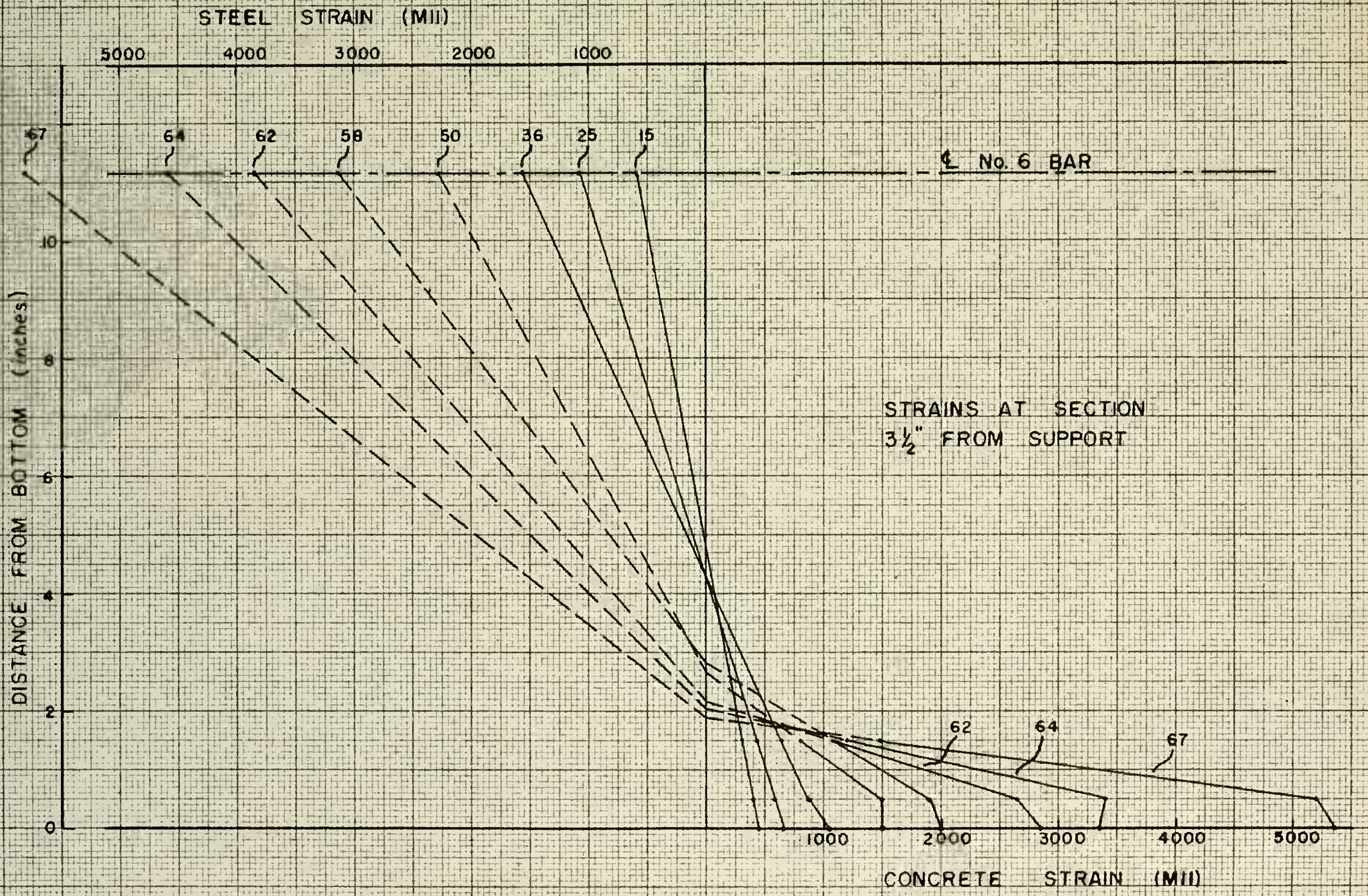

FIGURE 42. STRAIN DISTRIBUTION — BEAM III B-3

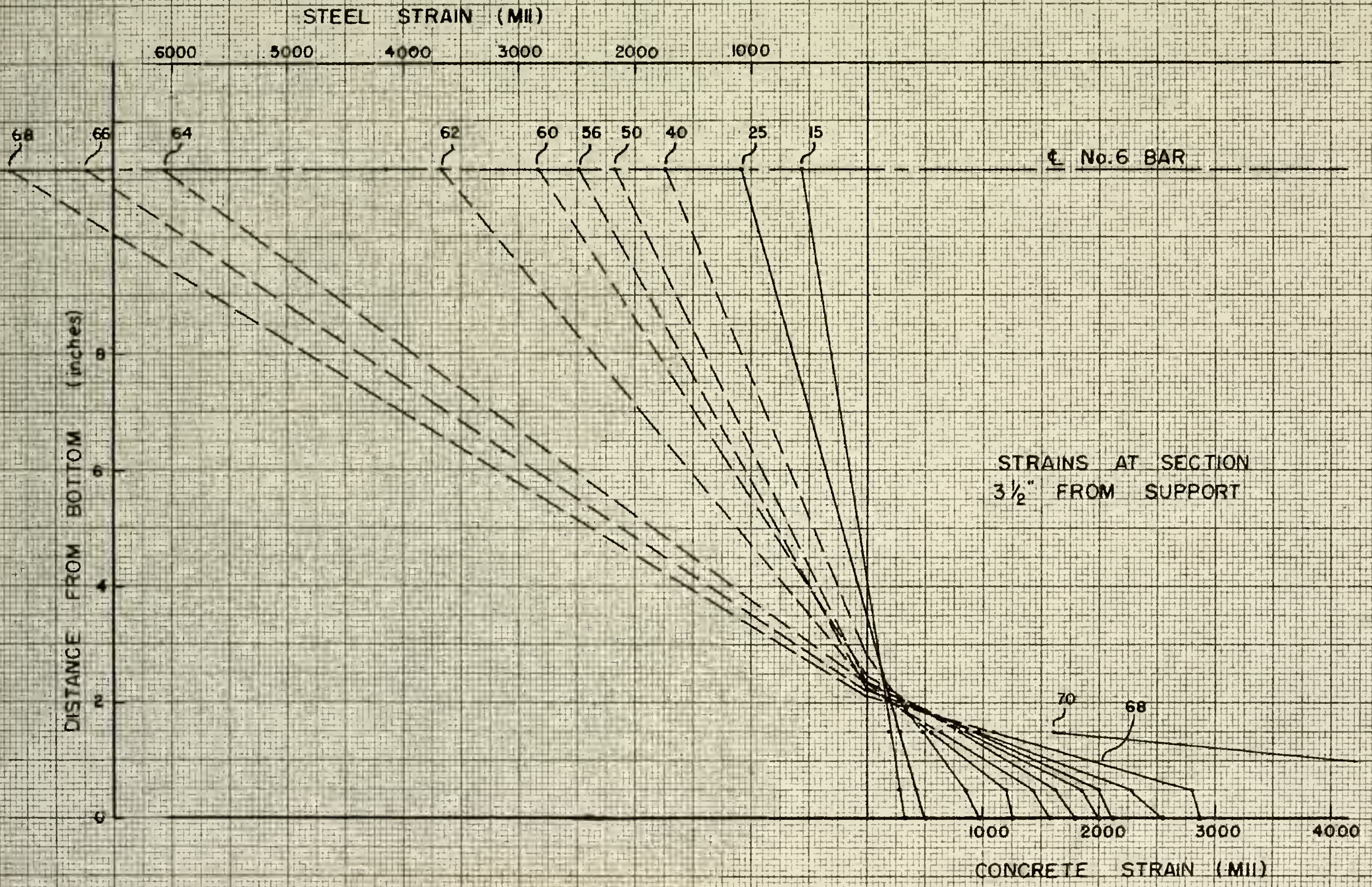

FIGURE 43. STRAIN DISTRIBUTION — BEAM III B-4

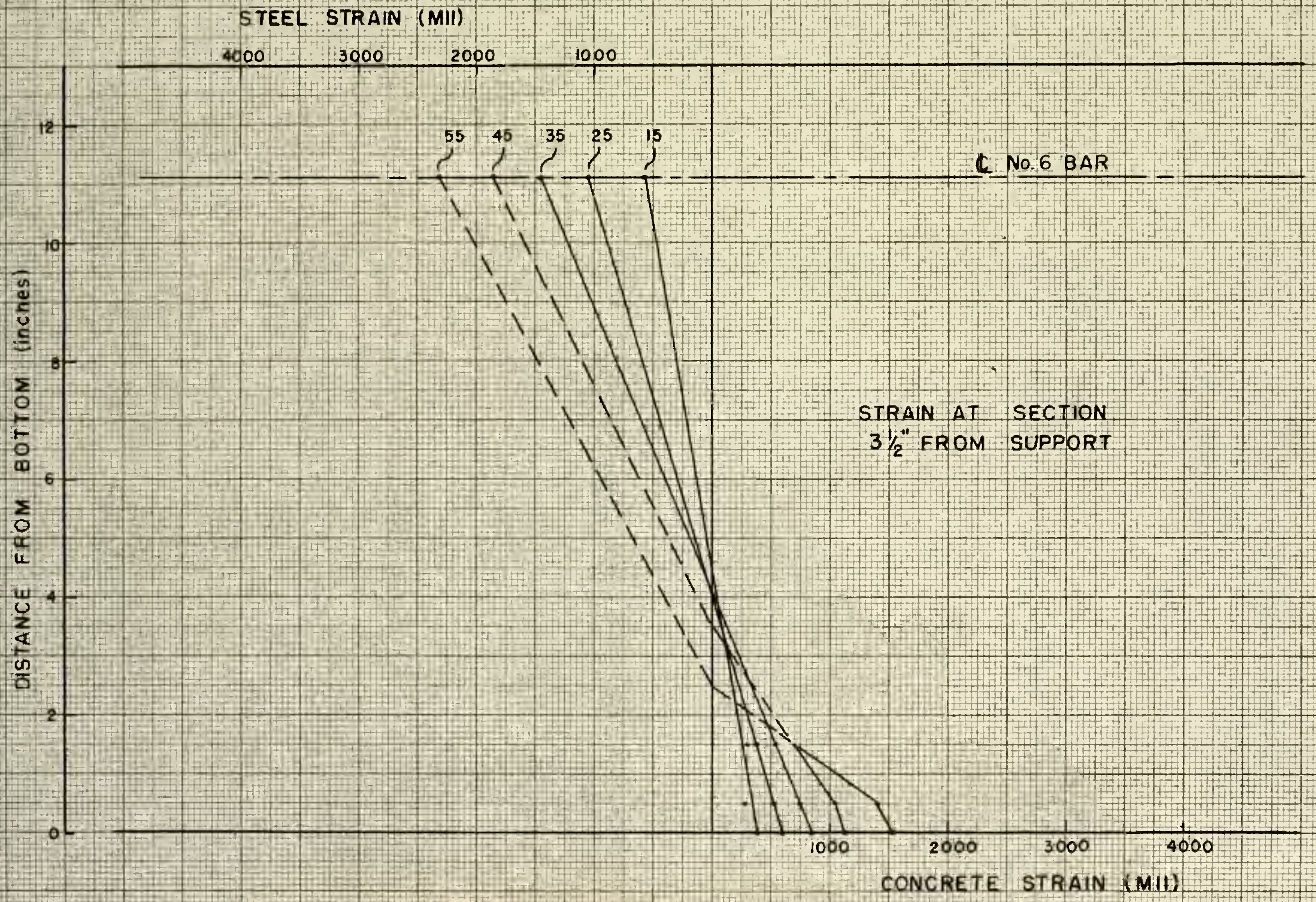

FIGURE 44. STRAIN DISTRIBUTION — BEAM III B - 5

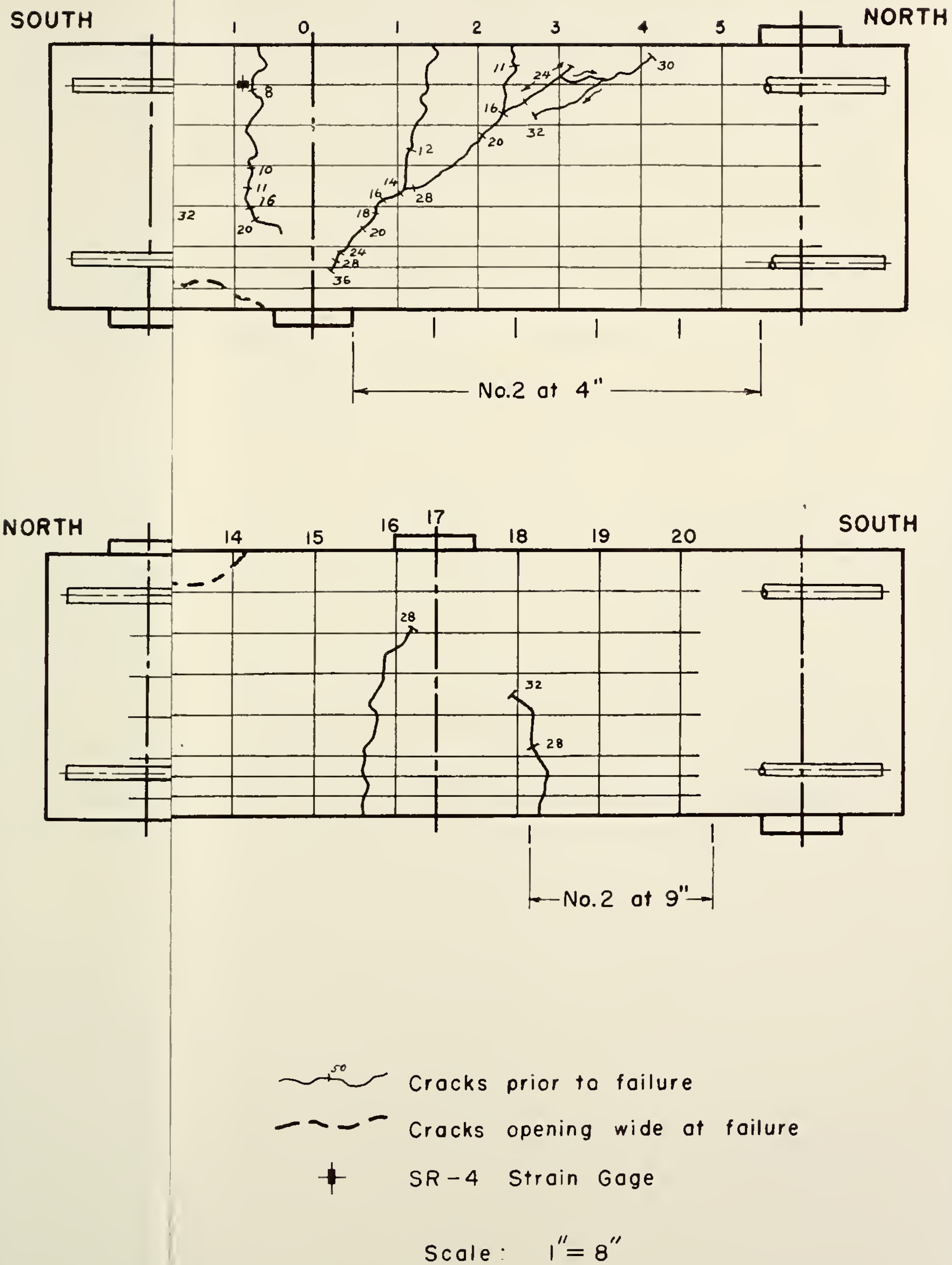
SOUTH
NORTH
No.2 at 4"
NORTH
SOUTH
No.2 at 9"
Cracks prior to failure
Cracks opening wide at failure
SR-4 Strain Gage
Scale: 1" = 8"

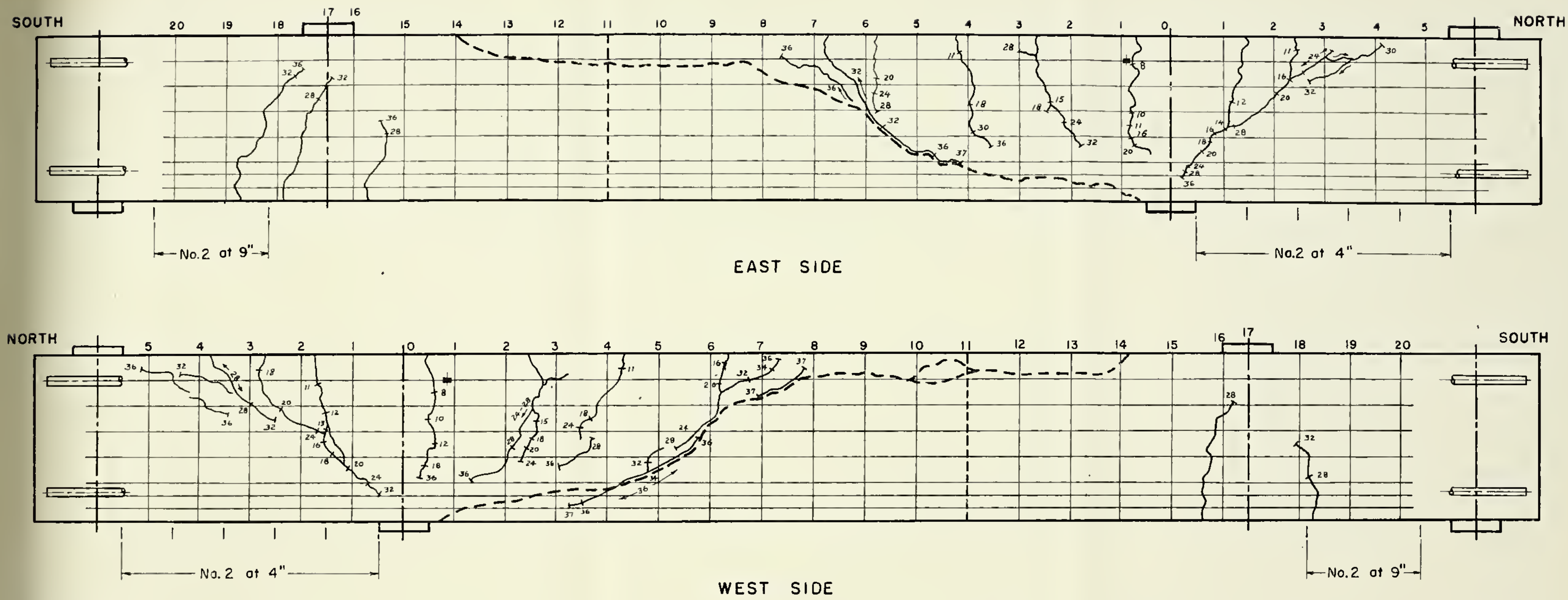

SR-4 Gage Locations:

No.6 Bars — $3\frac{1}{2}''$ from support (E & W)

Cracks prior to failure

Cracks opening wide at failure

SR-4 Strain Gage

Scale · $1'' = 8''$

FIGURE 45. BEAM III B-1

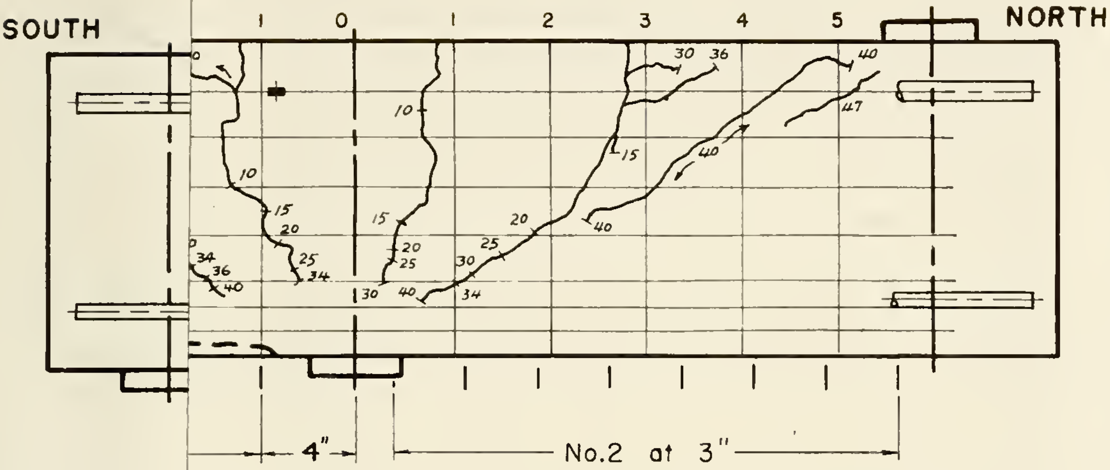
SOUTH
NORTH
4"
No.2 at 3"

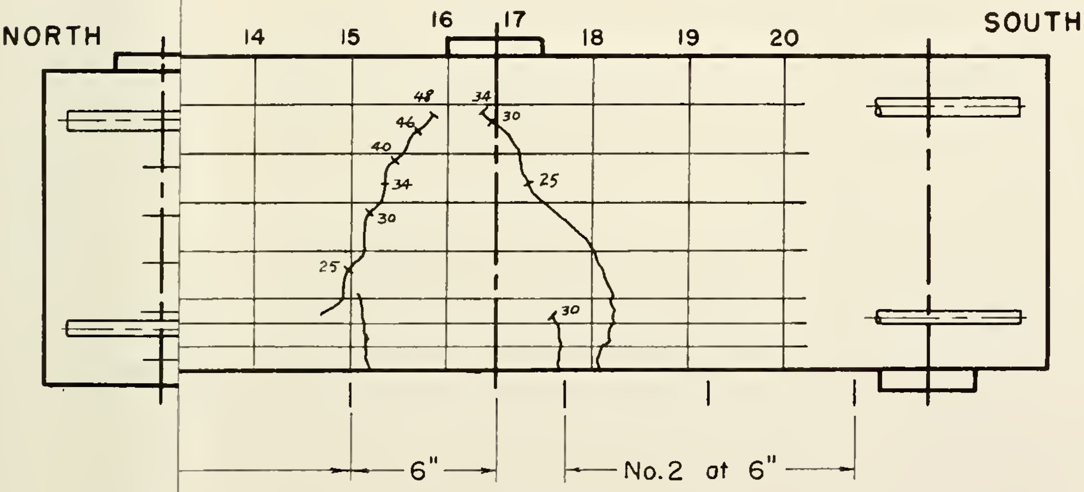
NORTH
SOUTH
6"
No.2 at 6"

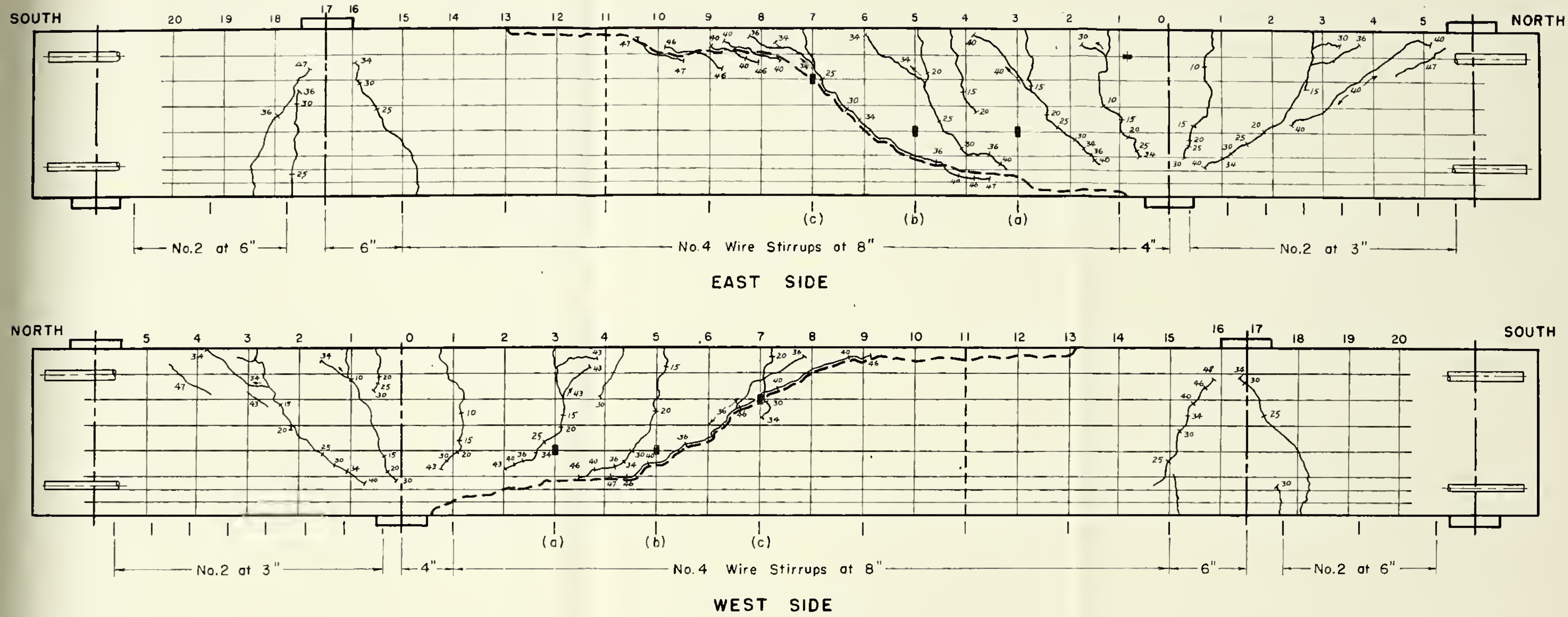

SR-4 Gage Locations:

No.6 Bar — 3 1/2" from support (E)
Stirrup (a) — 5" " bottom (W)
" (b) — 5" " " "
" (c) — 9" " " "

Whittemore Gage Locations:

Bottom only

FIGURE 46. BEAM IIIB-2

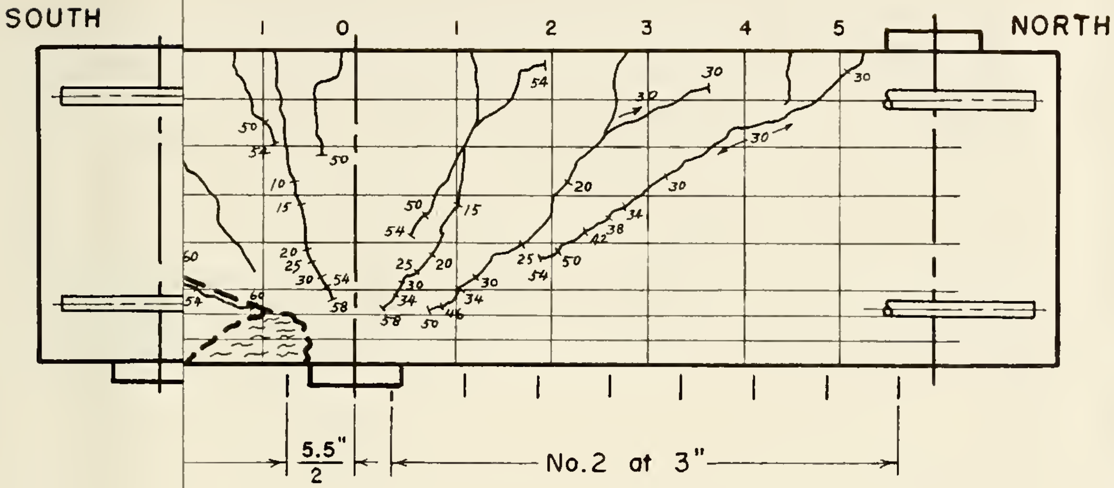
SOUTH
NORTH
1 0 1 2 3 4 5
5.5"/2
No.2 at 3"

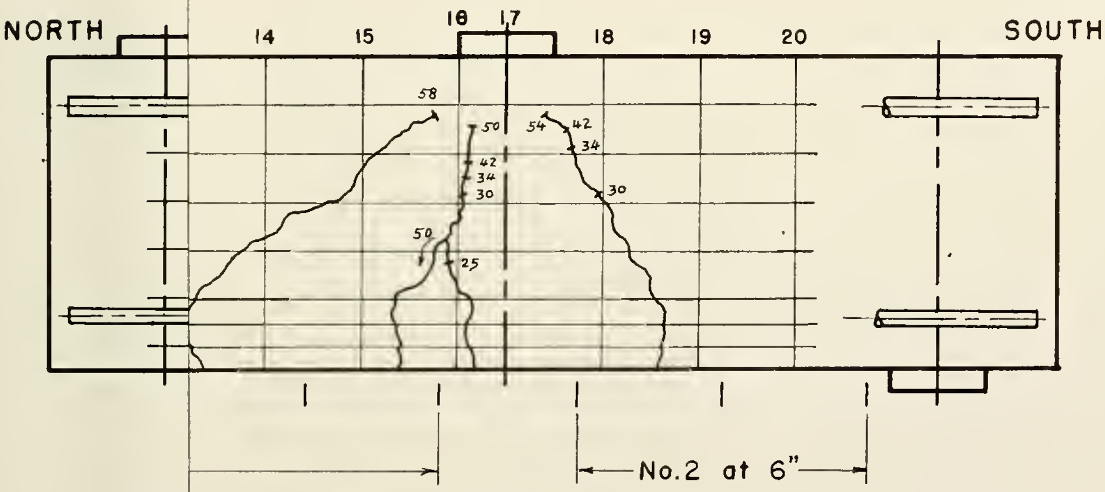
NORTH
SOUTH
14 15 16 17 18 19 20
No.2 at 6"

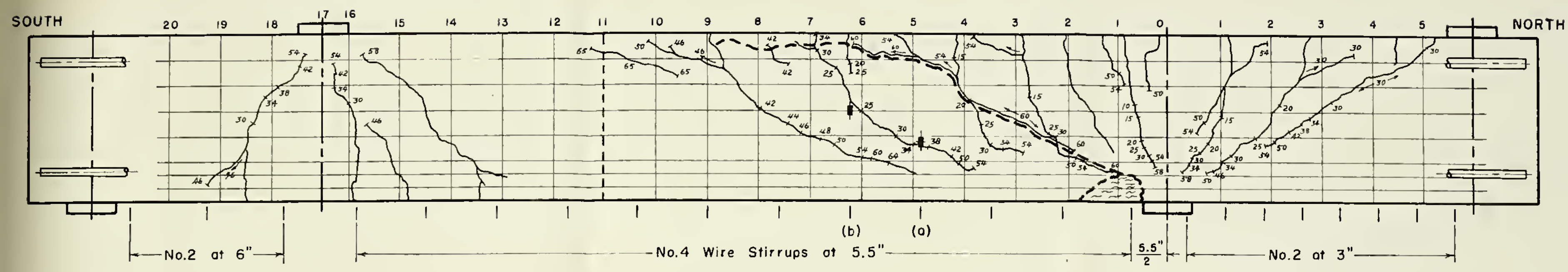

EAST SIDE

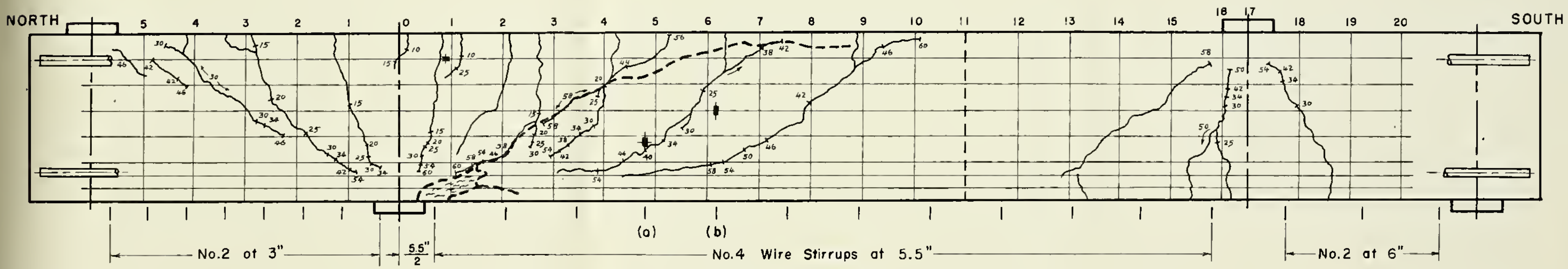

WEST SIDE

SR-4 Goge Locations:

No. 6 Bor — 3 1/2" from support (W)
Stirrup (a) — 4 1/2" from bottom (E)
" (b) — 7" " " (E)

Whittemore Goge Locations:

0", 1/2", 1 1/2" from bottom (E & W)

FIGURE 47. BEAM IIIB-3

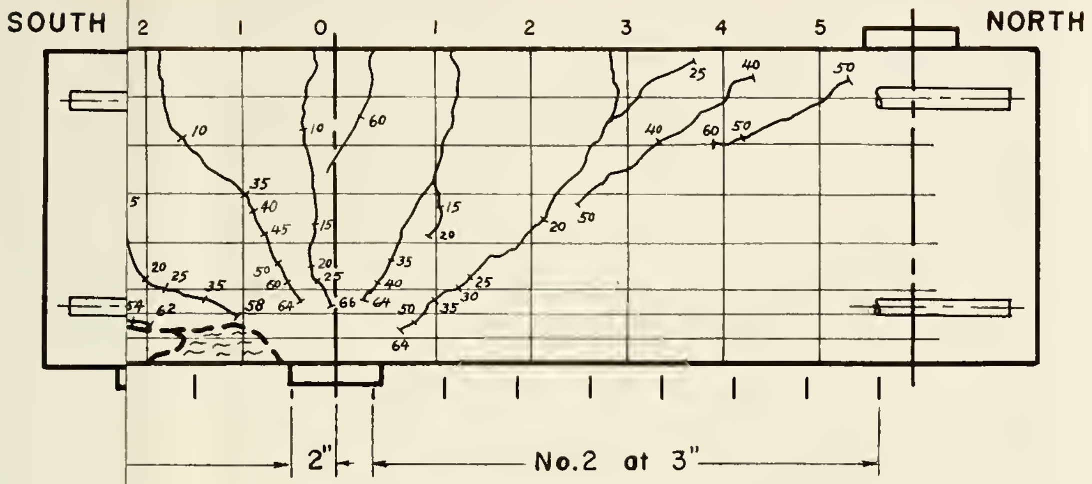
SOUTH
NORTH
2
1
0
1
2
3
4
5
2"
No.2 at 3"

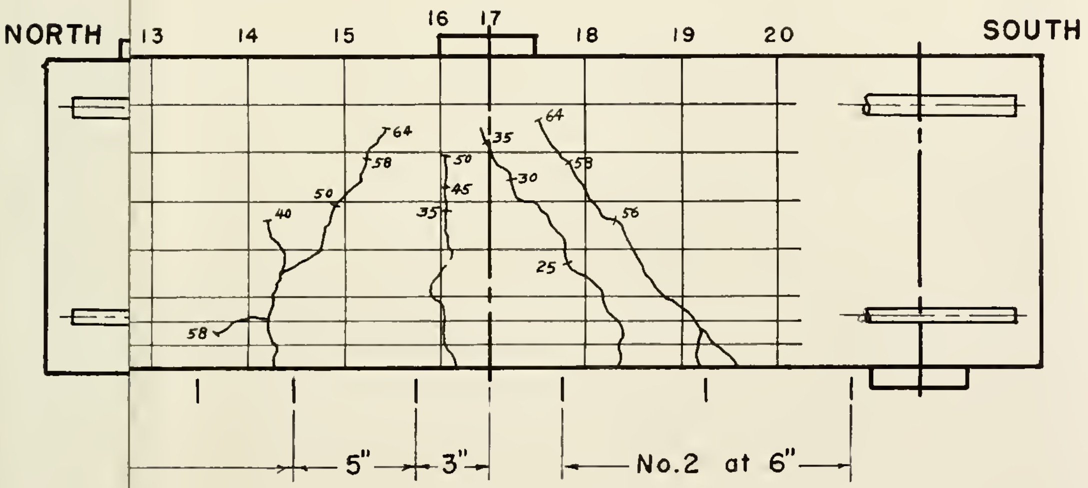
NORTH
SOUTH
13
14
15
16
17
18
19
20
5"
3"
No.2 at 6"

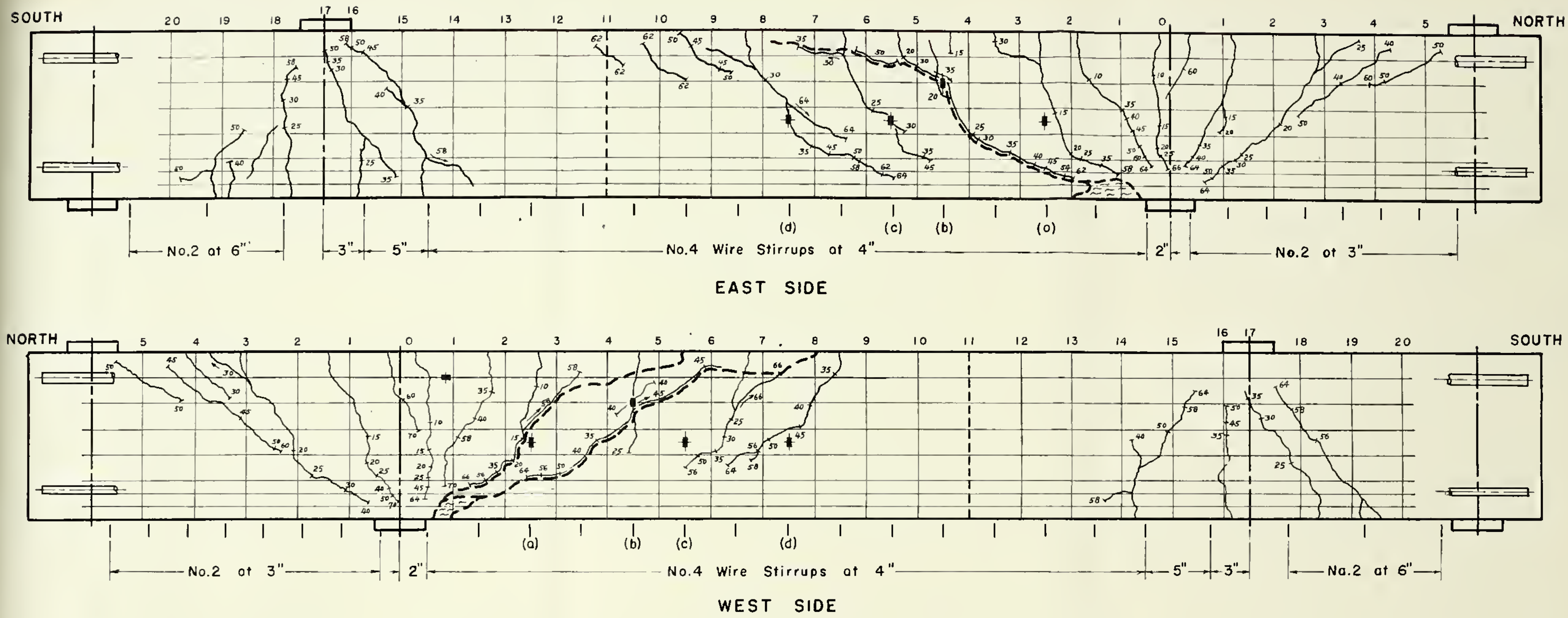

SR-4 Gage Locations:

No. 6 Bar — 3 1/2" from support (W)
Stirrup (o) — 6" from bottom (E)
" (b) — 9" " " "
" (c) — 6" " " "
" (d) — 6" " " "

Whittemore Gage Locations:

0", 1/2", 1 1/2", 2 1/2" from bottom (E & W)

FIGURE 48. BEAM IIIB-4

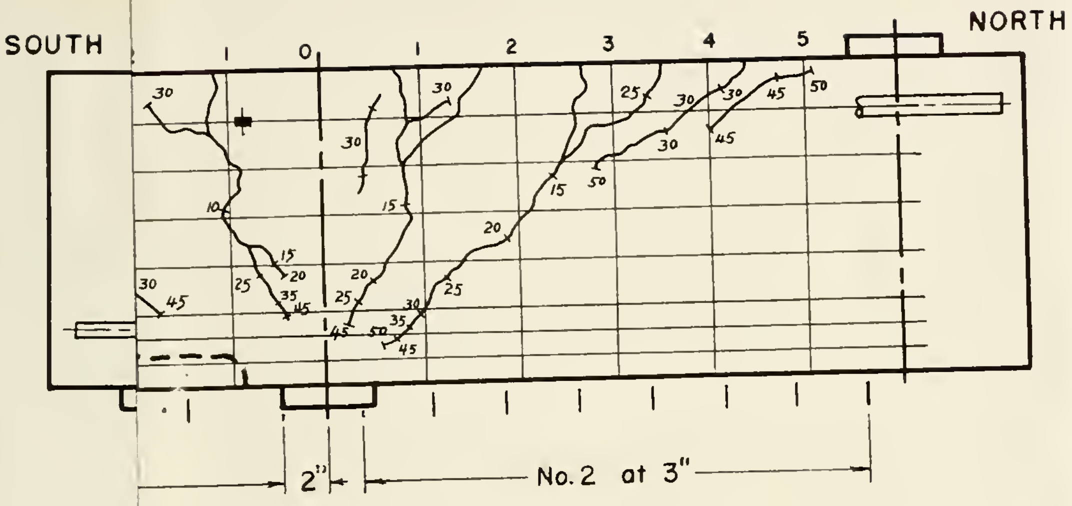
SOUTH
NORTH
1 0 1 2 3 4 5
2"
No.2 at 3"

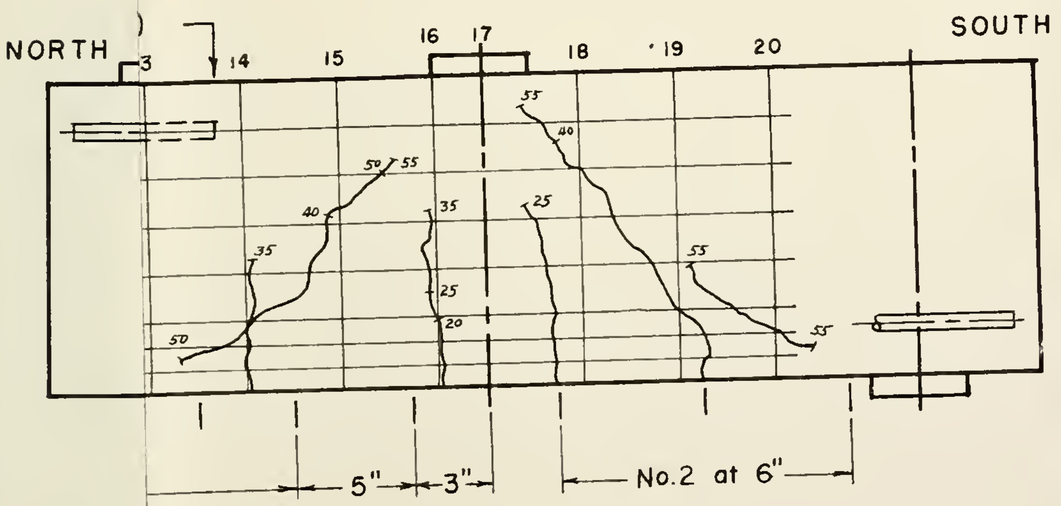
NORTH
SOUTH
13 14 15 16 17 18 19 20
5"
3"
No.2 at 6"

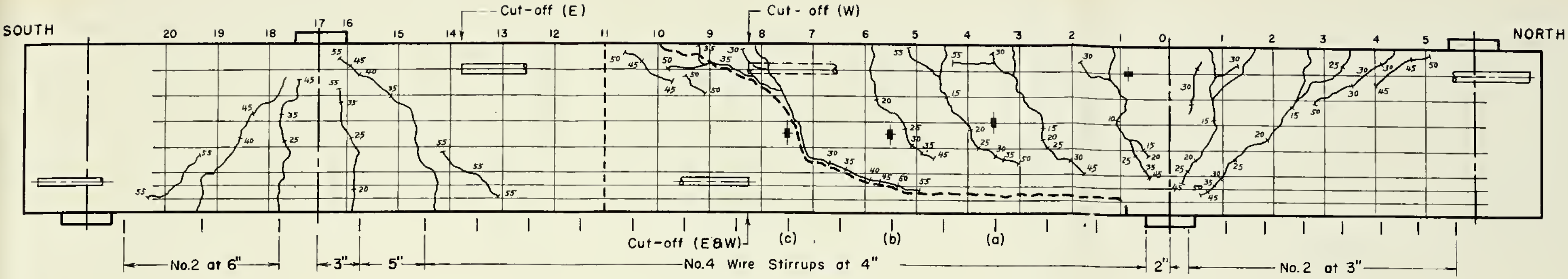

EAST SIDE

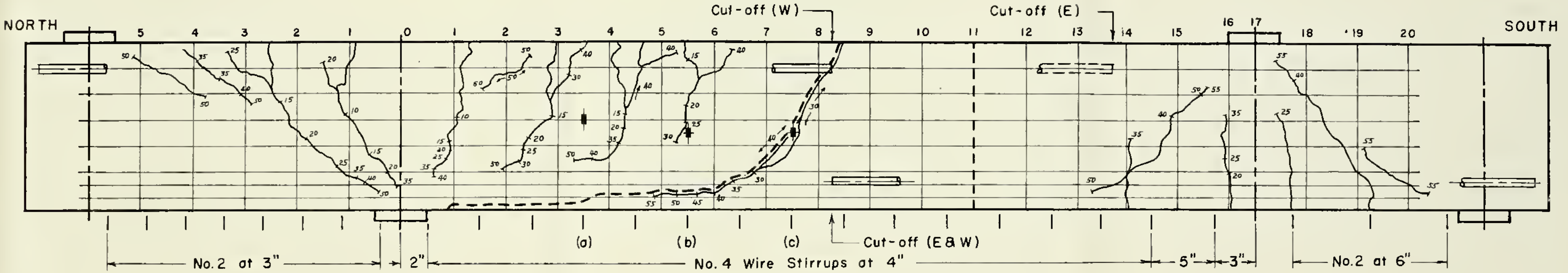

WEST SIDE

SR-4 Gage Locations:

No. 6 Bar — 3 1/2" from support (E)
Stirrup (a) — 7" from bottom (E)
" (b) — 6" " " (W)
" (c) — 6" " " (E)

Whittemore Gage Locations:

0", 1/2", 1 1/2", 2 1/2" from bottom (E&W)

FIGURE 49. BEAM IIIB-5

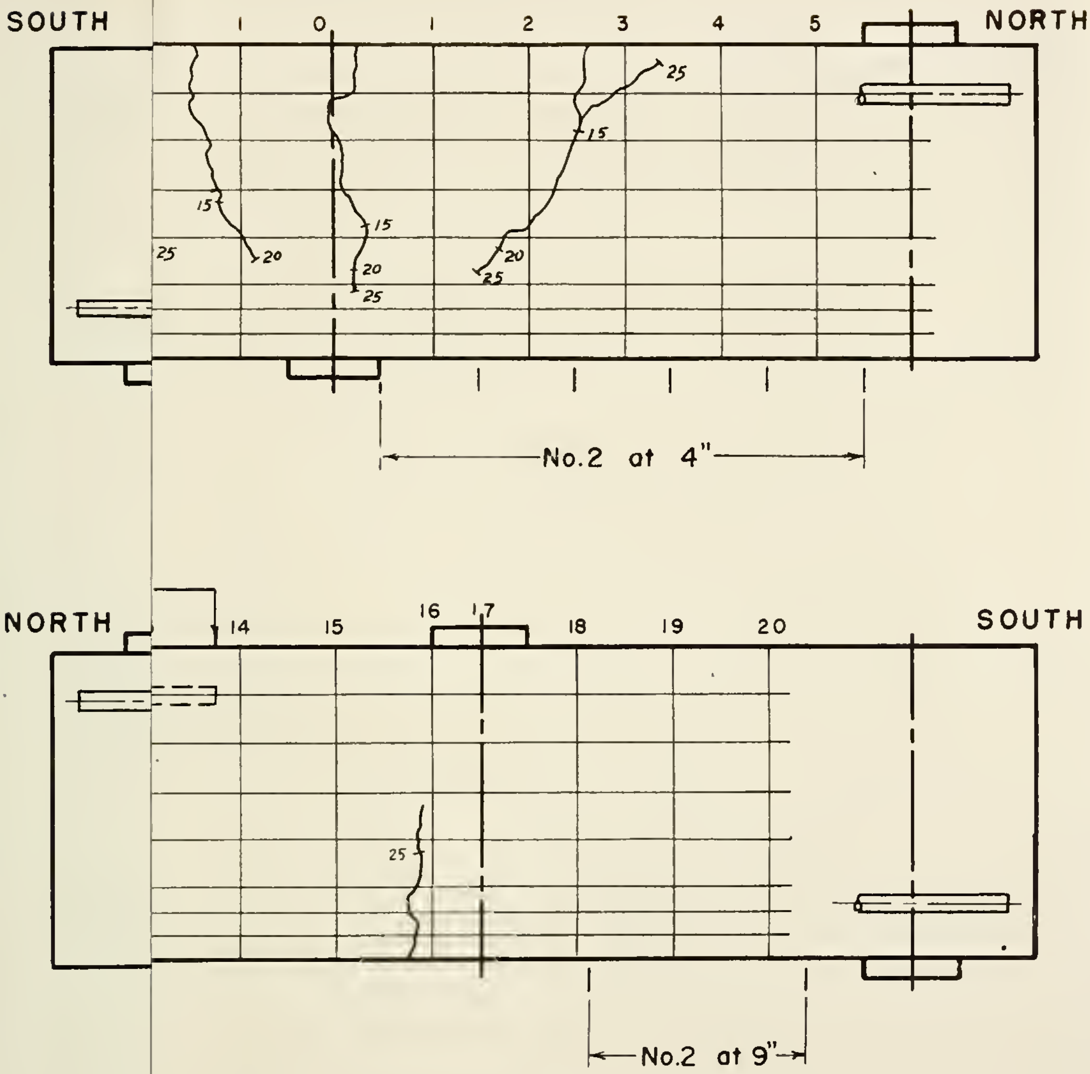

o

lly

5),

6)

er

d

I

ally

n

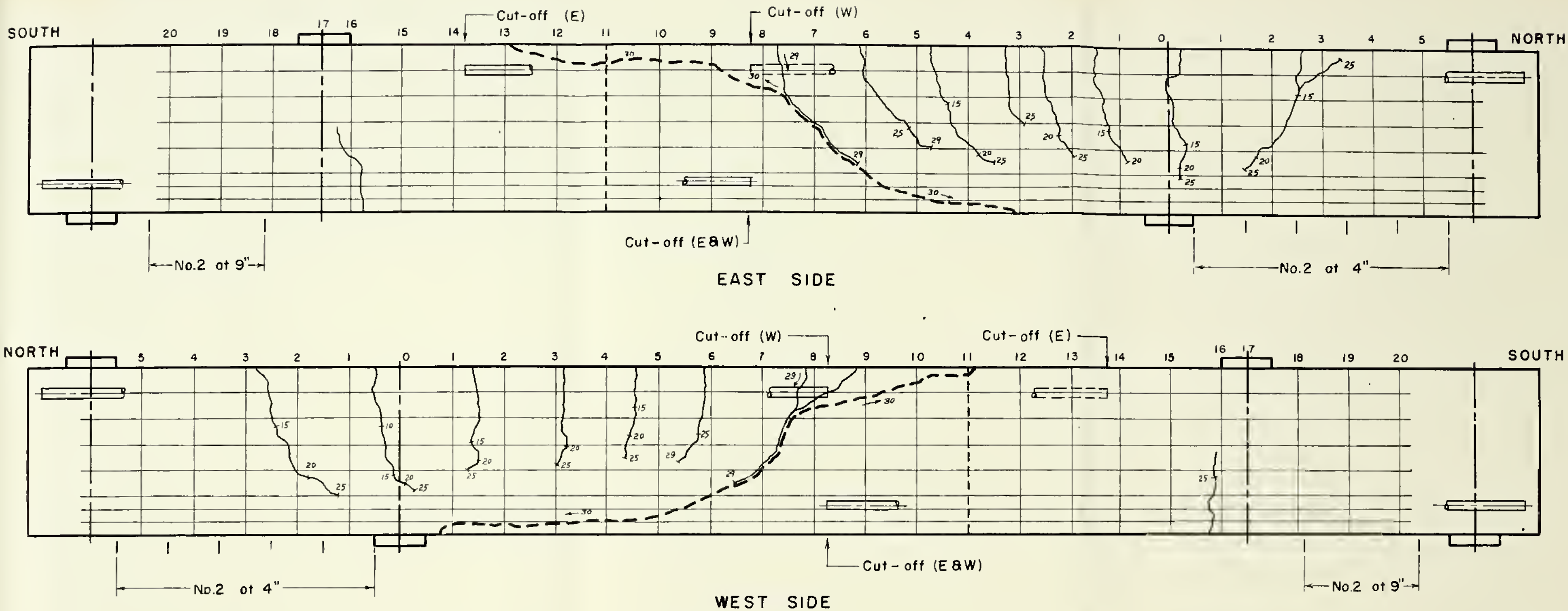

FIGURE 50. BEAM IIIB-6

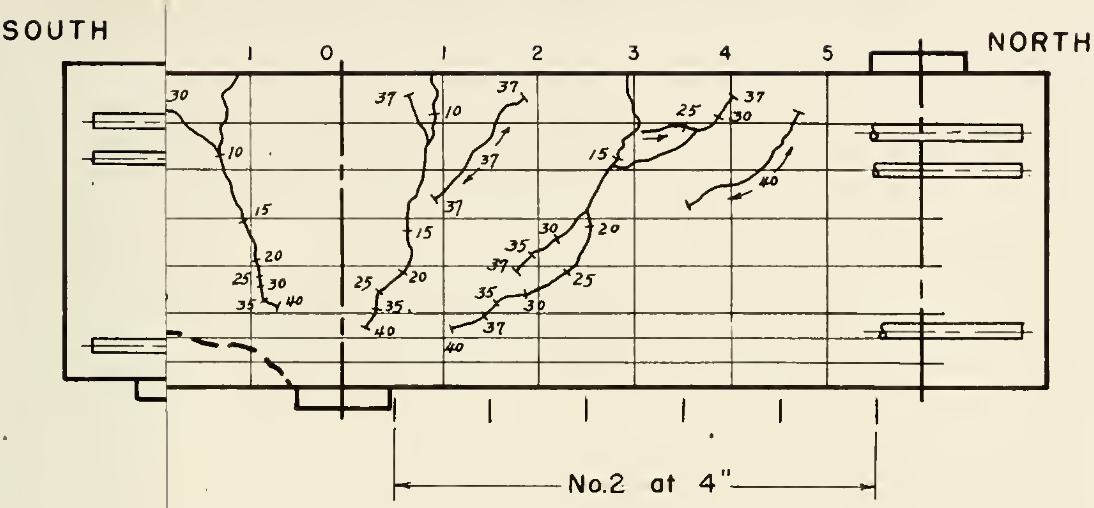

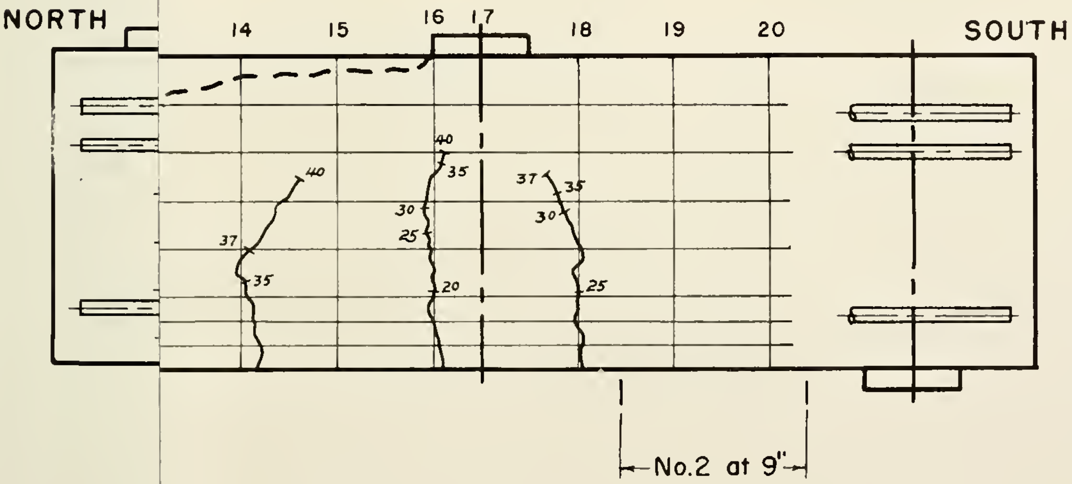

o

lly

5),

6)

er

d

I

ally

n

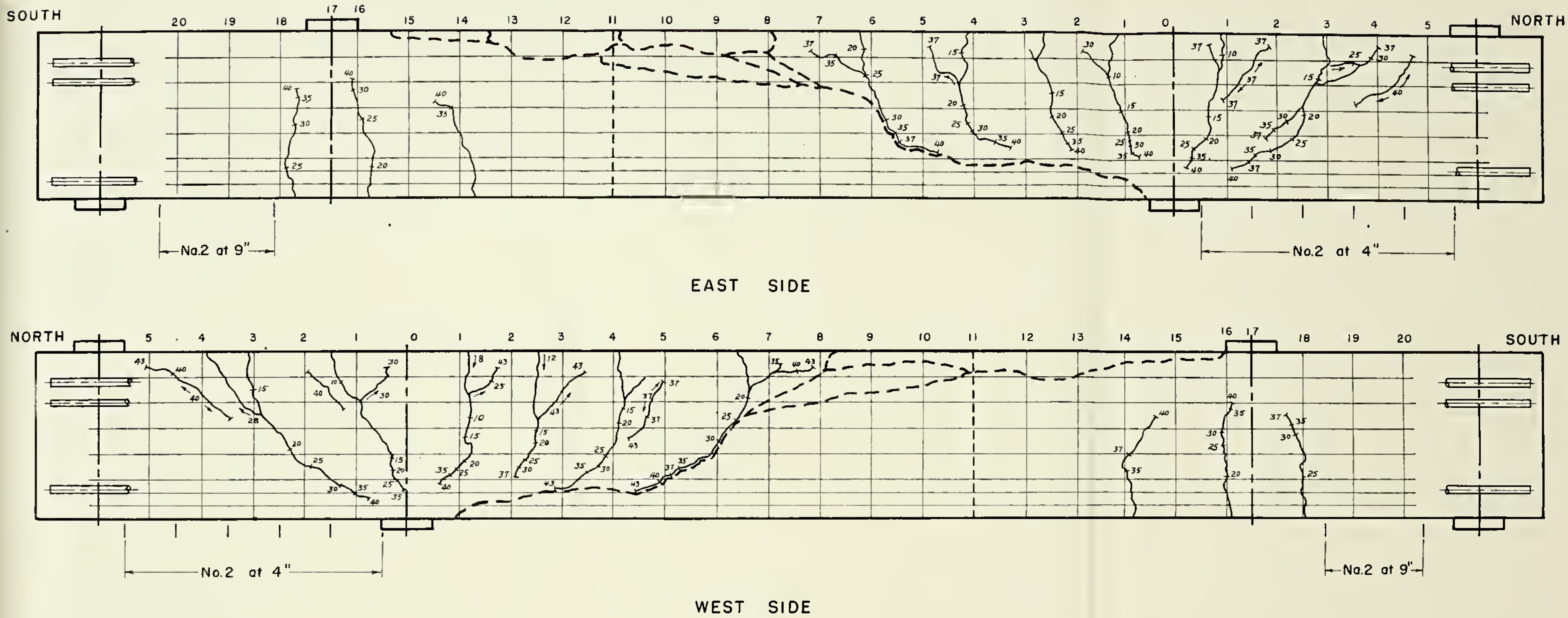

FIGURE 51. BEAM IIIA-1

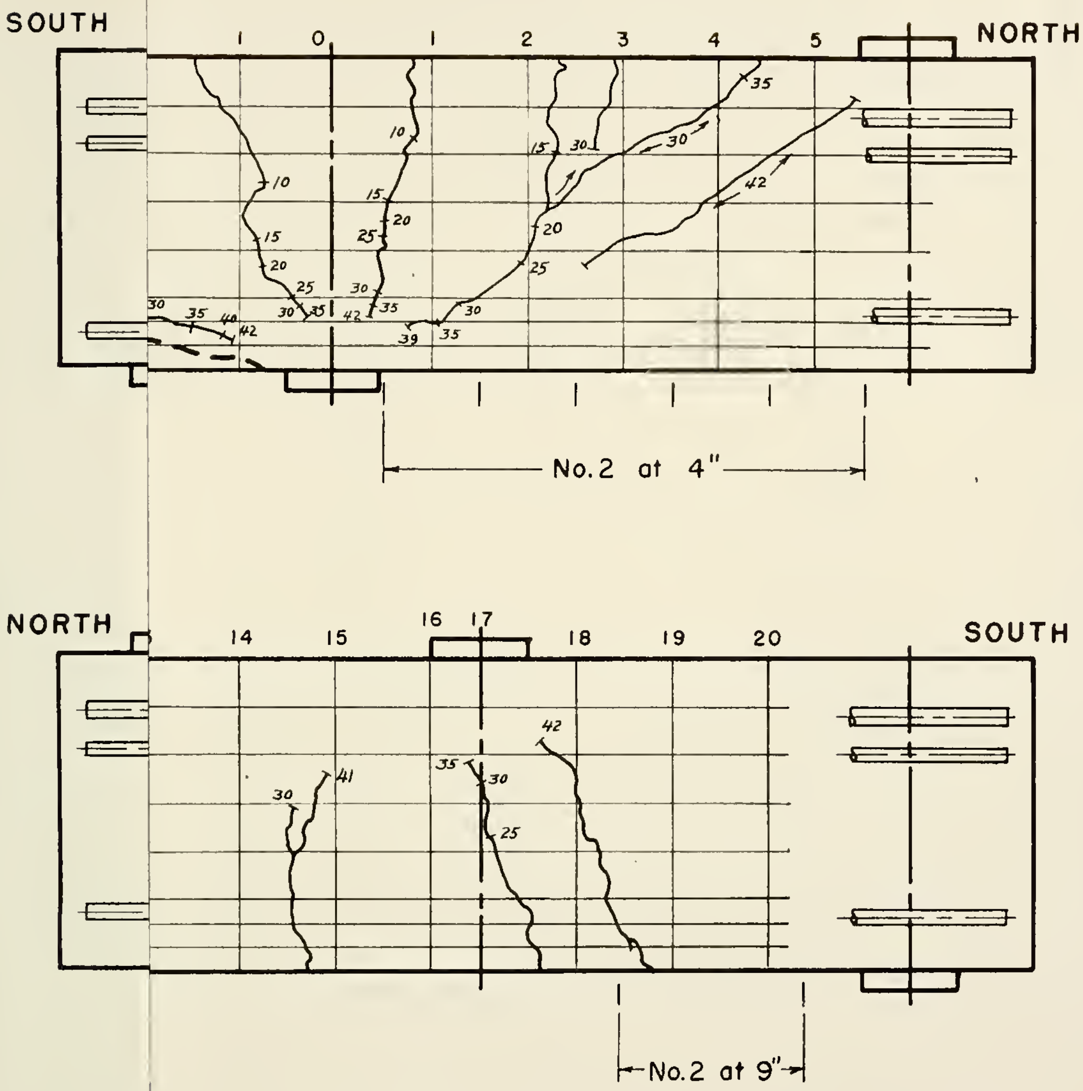

o

lly

5),

6)

er

d

I

ally

n

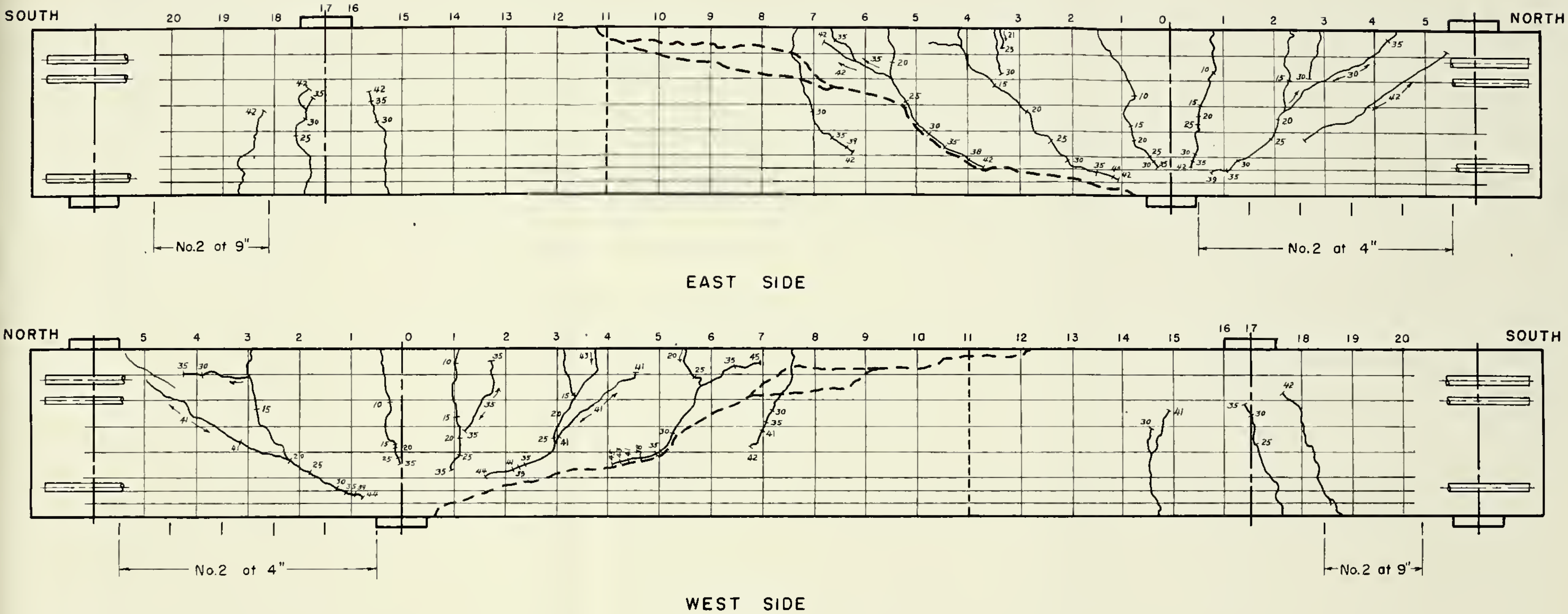

FIGURE 52. BEAM III A-2

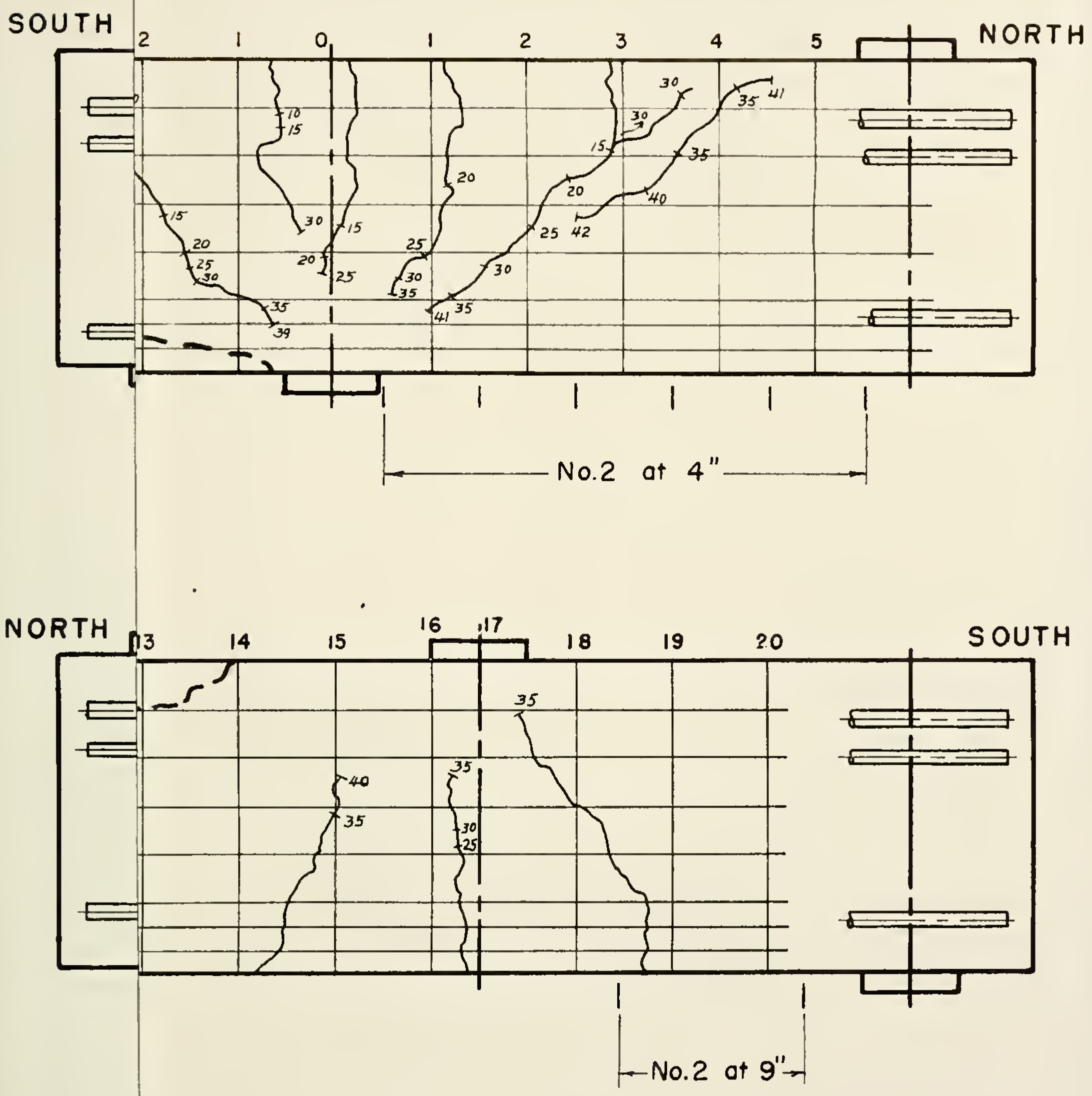

o

lly

5),

6)

er

d

I

ally

n

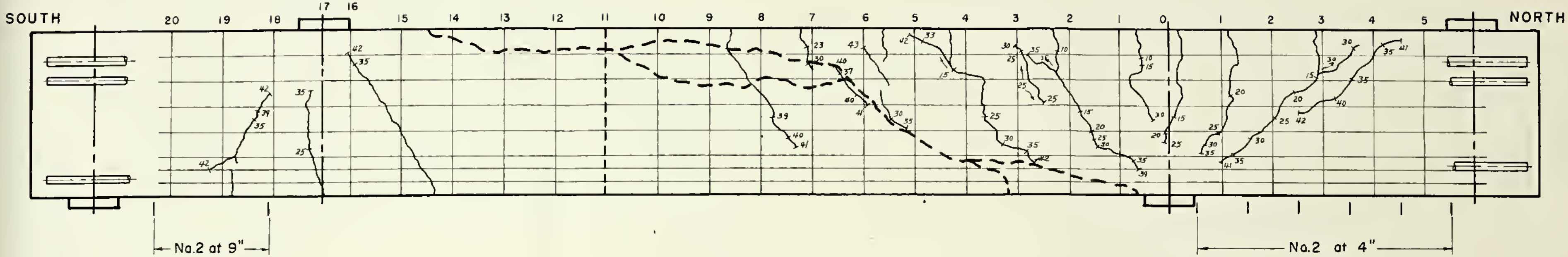

EAST SIDE

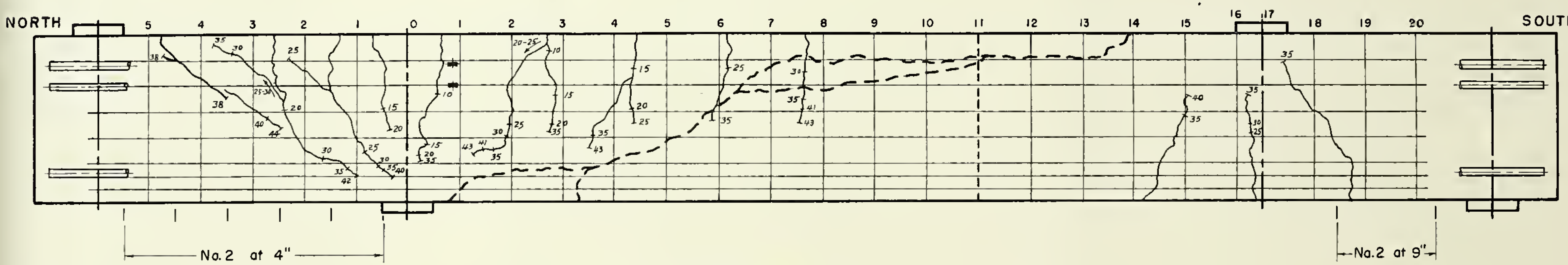

WEST SIDE

SR-4 Goge Locations:
No. 5 Bar — 3 1/2" from suppart (W)
No. 4 Bar — " " " "

FIGURE 53. - BEAM IIIA-3

DISCUSSION OF TEST RESULTS

Modes of Failure

Beams Without Stirrups

The behavior and mechanism of failure for beams with no web reinforcement in the critical shear span agreed generally with that described by other investigators. (6), (23), (25), (28, (29). Previous tests by both Morrow (25) and Bower (6) indicated shear-compression failure for a/d ratios below approximately 3.4 and sudden diagonal tension failure for a/d greater than 3.4.

Series III beams of this investigation had nominal a/d ratios of 4.0 and 4.4. Failure of the five beams without web reinforcement in Series III was sudden, occurring either simultaneously with or at slightly greater load than the formation of the diagonal crack.

The beams of Series I had nominal a/d ratios of 2.2 and 2.4 and those of Series II had an a/d ratio of 2.9. With two exceptions (Beams IA-4 and IIB-5), all beams of Series I and II without stirrups sustained a failure load substantially greater than the diagonal cracking load. Crack penetration into the compression zone was gradual, and a substantial

redistribution of strains was observed. Splitting along the top steel throughout the shear span followed diagonal cracking in each of these beams. Ultimate failure was caused by crushing of the concrete at the end of the diagonal tension crack.

The two exceptions noted above were beams IA-4 and IIB-5. Beam IA-4 was identical to both IA-2 and IA-3 except that two strain gages were placed on the tension steel in the shear span (at 18" and 24" from the support). While IA-2 and IA-3 failed by shear-compression at loads much greater than the diagonal cracking loads, Beam IA-4 did not experience any significant strain redistribution, and a diagonal tension type failure occurred almost immediately after the diagonal crack first penetrated the compression zone. Beam IIB-5 was the companion to IIB-1 with the tension steel cut-off in accordance with moment requirements. Not only did the diagonal tension crack form at a greatly reduced load, but also the mode of failure was by sudden diagonal tension.

Beams With Web Reinforcement

Some beams in Series II and III were provided with stirrups in the critical shear span. The mechanism of failure in Series II beams with tension steel throughout the length of the beam was that of shear compression adjacent to the

support, following yield of the stirrups crossed by the crack. With tension steel cutoff (Beam IIB-4) the critical diagonal tension crack was located much farther out in the shear span. Failure was similar to the diagonal tension failure immediately after the stirrups reached yield strains.

In Series III beams with stirrups both the shear compression and the diagonal tension modes of failure were observed. Beam IIIB-2 with a relatively light amount of web reinforcement failed essentially in the same manner as its companion beam without web reinforcement, IIIB-1. Formation of the critical diagonal crack occurred at the same load and in the same location. The ultimate load, of course, was substantially greater, but the mechanism of failure following yield of the stirrups was the same. Beams IIIB-3 and IIIB-4 were provided with higher percentages of web steel and were expected to develop strengths near the ultimate bending capacity of the section. The diagonal tension failure experienced in IIIB-1 and IIIB-2 was effectively prevented. Collapse was by crushing of the concrete adjacent to the support following substantial yielding of the tension steel.

Beam IIIB-5 was identical to IIIB-4, but with the longitudinal steel cutoff. Both the cracking load and the ultimate

strength were again significantly reduced when compared to the companion beam with extended steel.

Factors Affecting Beam Behavior

Four major variables have been noted to affect the strength of reinforced concrete beams in shear: concrete strength; percentage of tension reinforcement; shear span to depth ratio; and the amount of web reinforcement. Throughout the present investigation the first two of these were maintained reasonably constant. With the exception of two beams the concrete cylinder strength was maintained between 4000 and 4600 psi. For all practical purposes the amount of tension steel was also held constant. (p = 1.3 percent and p = 1.7 percent.)

While the major differences in behavior for the beams included in this study can be attributed directly to differences in a/d ratio and in amount of stirrups, the presence of three additional factors seem significant enough to merit separate discussion. These additional factors are the arrangement of the longitudinal tension steel, the tension steel cutoff, and the location of the diagonal tension crack.

Shear Span to Depth Ratio

The results tabulated in Table 5 indicate that the average shearing stress at diagonal cracking generally decreases

with increasing a/d ratio. For beams with identical tension steel arrangements and with nearly the same concrete strengths the tests show the following:

Beams	a/d	Average v_c^* (psi)
IA-2, 3, 4	2.4	193
IIIA-1,2,3	4.4	173
IB-2	2.2	156
IIB-1, 2, 3	2.9	162
IIIB-1, 2	4.0	135

$^*v_c$ = V/bd at diagonal tension cracking

More significant than this, however, is the difference in behavior after diagonal cracking for beams of different a/d ratio. The beams of Series I and II without stirrups were able to accept the deep penetration of the diagonal crack into the compression zone and carry substantially more load until ultimately failing in compression. It can be seen that for these beams the diagonal tension crack was an extension of a vertical tension crack located generally at d = 11" from the support. The beams of longer shear span, Series III, could withstand little or no load beyond the point where the crack first penetrated the compression zone. Failure was a

a brittle type diagonal tension failure. The critical crack in these beams was always located farther away from the support. Consider, for example, IIIB-1. The diagonal crack was an extension of the flexural crack at about 24" from the support.

The location of the critical crack appears to be somewhat random. Considering again IIIB-1, one could reason that the critical crack forms as an extension of the flexural crack farthest from the support, because of increased resistance to penetration offered by higher bending stresses at sections closer to the support. However, in Beams IIIA-2 and IIIA-3 the diagonal crack was located in the same position as in IIIB-1, even though a flexural crack had formed farther out.

The difference in failure mechanisms associated with the long and short shear spans may be primarily due to the local compression induced by the concentrated loads and support reaction. In Series I and II beams the diagonal crack penetrated into the compression zone nearly to the edge of the support block. The vertical compression at this point would definitely tend to reduce the principle tension below the end of the crack, and thereby delay or stop the progression of the crack.

Percentage of Web Reinforcement

Series II Beams. The effects of stirrups on the redistribution of strains following diagonal cracking are shown clearly by the load deformation curves, Figures 25 through 30, together with the cracking patterns, Figures 30 through 35. Without stirrups (IIB-1) the redistribution was apparent immediately following diagonal cracking at 36^k. Loss of bond throughout the span was complete at a load of 40^k. The resulting transformation from beam action to tied-arch action can be seen by the sharp increase of compressive strains at 1" above the bottom fiber, while a decrease in strains occurred at the extreme fibers.

Although the diagonal tension crack penetrated into the compression zone at about the same load in Beams IIB-2 and IIB-3, its progression at greater loads was significantly restrained. Strain redistribution was delayed until all stirrups crossed by the crack had yielded. Comparisons of the strains in the compression zone (Figures 27, 28, and 29) for IIB-1, IIB-2, and IIB-3 show that the increased strains at distances above the extreme fibers are definitely associated with the observed splitting and resulting loss of bond along the tension steel. In Beam IIB-2 splitting was prevented until all stirrups were yielding ($P = 46^k$). As loading was increased from this point, the concrete strains at 1/2" above the bottom fiber began increasing rapidly relative to those at the extreme fibers.

<u>Series III Beams</u>. The beams of this series were of particular interest because they revealed an indication that the diagonal tension type failure occurring in long beams is transformed with increasing amounts of web steel to the shear-compression mode of failure. As discussed previously, the beam with relatively light web reinforcement (IIIB-2) failed in essentially the same manner as the beam with no stirrups. However, as stirrups were spaced more closely (IIIB-3 and IIIB-4), the critical diagonal tension crack was shifted closer to the support. The deep penetration of the crack resulted in a concentration of strain in the uncracked compression zone similar to that observed in the shorter shear spans. Failure was by crushing of this zone and was preceded by definite yielding of the tension steel.

To the writer's knowledge very few systematic studies of relatively long-span beams with varying amounts of web reinforcement have been reported in the literature. One recent investigation, however -- reported by Bresler and Scordelis (7) -- included test specimens quite similar to the beams of Series III. Beams of the same shear-span to depth ratio as that of Series III ($a/d = 4$) were tested with web reinforcement ratios, $Krf_y = 0, 50, 75$, and 100. (Beams IIIB-1, IIIB-2, IIIB-3, IIIB-4 of the study reported herein had Krf_y values of 0, 57.8, 84.2, and 115.8, respectively. See Table 1.)

From Reference (7) the beam with no web reinforcement ($Krf_y = 0$) failed by sudden diagonal tension in the same manner

as beam IIIB-1. With the addition of web reinforcement the tests of Reference (7) indicated that the mode of failure was shear compression for all beams with stirrups. While the results of beams IIIB-3 and IIIB-4 (Krf_y = 84.2 and 115.8) agree with this finding, beam IIIB-2 (Krf_y = 57.8) failed in diagonal tension. The only notable difference between beam IIIB-2 and the beam of Reference (7) with Krf_y = 50 was the stirrup-spacing-to-depth ratio. In beam IIIB-2 s/d = .73, while in the beam of Reference (7) s/d = $\frac{1}{2}$.

Hence, it may be that use of smaller stirrups at closer spacing in the long-span beam is more effective, because of the greater strengths generally associated with the shear-compression mode of failure.

Arrangement of Tension Steel

Comparisons of the beams with a double-layered arrangement of tension steel to those with one layer (See Table 5) indicate a significant increase in shear strength, when a larger number of smaller bars are placed in multiple layers. Comparing the strengths of IA beams with IB beams and of IIIA with IIIB shows the effect of this variable alone. ("A" had two bars in one layer and "B" had four bars in two layers.)

Beams	Average v_c^* (psi)
IA - 2,3,4	193
IB - 2	156

IIIA - 1,2,3	173
IIIB - 1,2	135

* $v_c = \frac{V}{bd}$ at diagonal tension cracking.

Hence, the diagonal cracking strengths of the beams with the double-layered arrangement were 1.24 and 1.27 times those of the beams with steel in a single layer for Series I and III, respectively.

This increased resistance is believed due to the increased ability of the beam to carry shear by dowel action.

Bar Cut-Off

Beams IIB-4, IIB-5, IIIB-5, and IIIB-6 indicate a serious reduction in shear strenth when bars are terminated within the tension zone.

The bars were cut off in accordance with the provisions of the "Standard Specifications for Highway Bridges" (4). The cut-off points are shown for each of these beams on the crack pattern sheets (Figures 34, 35, 49 and 50.)

All four beams had companion specimens with extended steel. The reduction in both diagonal cracking loads and ultimate strength can be seen from Tables 5 and 6.

In all cases the diagonal tension crack was initiated at the cut-off point, and the mode of failure was that of diagonal tension. As would be expected, the effect of bar cut-off was

more serious for the two beams without stirrups (Beams IIB-5 and IIIB-6). Fialure was very sudden in these cases as both top bars pulled out and the beam collapsed in two pieces.

TABLE 6

EFFECT OF STEEL CUT-OFF

Beam with Cut-off Steel	Companion Beam with Extended Steel	Diagonal Cracking Load $\frac{P_c \text{ (cut-off)}}{P_c \text{ (extended)}}$	Ultimate Load $\frac{P_u \text{ (cut-off)}}{P_u \text{ (extended)}}$
IIB-4	IIB-3	1.00	0.88
IIB-5	IIB-1	0.74	0.61
IIIB-5	IIIB-4	----	0.85
IIIB-6	IIIB-1	0.83	0.81

Diagonal Crack Location

As discussed previously, the location of the diagonal crack has a definite effect on the beam behavior and mechanism of failure. The difference in modes of failure between the long and short-span beams was definitely associated with the position of the crack relative to the support. In the beams with the tension bars cut off, the critical crack was shifted farther from the support than in the companion beams with extended steel. The results were not only a reduction in strength, but also a change in the mode of failure.

Further indication of this influence is shown by comparison of beam IA-4 with IA-2 and IA-3. The latter two beams failed in shear-compression at loads greatly in excess of those at diagonal cracking. Beam IA-4 failed suddenly upon formation of the diagonal crack with essentially no redistribution of strains. While the influence of the strain gages out in the shear span very likely was a factor, it is of interest that a slight difference in crack location would have such an extreme effect on the ability of the beam to resist penetration of the diagonal crack.

ANALYSIS OF TEST RESULTS

Nominal Shearing Stress at Diagonal Cracking

Several semi-empirical expressions for predicting the resistance to diagonal tension cracking have been reported. (1), (7), (10), (24), and (25). The equation recommended by ACI-ASCE Committee 326 (1) has been shown to give good results under a variety of conditions. The equation is:

$$v_c = \frac{V_c}{bd} = 1.9 \sqrt{f'_c} + 2500 \frac{pVd}{M} \qquad \text{(Eq'n. 4)}$$

This equation is intended to predict the average shearing stress required to produce diagonal cracking at the section considered. For the beams of this investigation the critical section for application of this formula is at a distance of one effective depth, d, from the section of maximum moment. Hence $\frac{V}{M} = \frac{1}{a-d}$ for the beams of this investigation. Test results are compared with values predicted by this equation in Table 7.

For beams with tension reinforcement in a single layer (B-designation) this equation gives a good prediction of the diagonal cracking load for all except those with the steel cut off. Three of thefour beams with the steel cut off in

the tension zone cracked at 80% of calculated load. With tension steel in a double layer (A-designation) the equation tends to give a more conservative estimate.

Ultimate Shear Strength

The test results are compared with calculated ultimate strengths in the last column of Table 7. For beams without web reinforcement Committee 326 recommended that the load-producing the diagonal tension crack should be considered in design as the ultimate load capacity in shear. This requirement results in a greatly conservative estimate for the beams of shorter shear span, where failure is by shear-compression. However, until the conditions under which this additional strength can be depended upon can be firmly established, this requirement is justified. Had the loads and reactions been introduced as shears to the sides of these beams, it is questionable shether these higher strengths would have been developed.

For beams with stirrups Committee 326 (1) recommends the following formula for ultimate shear strength

$$v_u = \frac{V_u}{bd} = v_c + v_s$$

where v_s is the portion of the total unit shear assumed to be carried by the stirrups, as given by the truss analogy. Thus:

$$v_s = k \frac{A_v}{bs} f_{vy} \text{ or } Krf_{vy}, \text{ where } K = 1 \text{ for vertical stirrups.}$$

TABLE 7.
COMPARISON OF TEST STRENGTHS WITH
ACI-ASCE COMMITTEE 326 RECOMMENDATIONS (1) (3)

Beam	Diagonal Cracking Strength			Ultimate Shear Strength			
	v_c test (psi)	v_c calc.* (psi)	$\frac{v_c \text{ test}}{v_c \text{ calc.}}$	v_u test (psi)	Krf_{vy} (psi)	v_u calc. ** (psi)	$\frac{v_u \text{ test}}{v_u \text{ calc.}}$
IA-1	173	136	1.27	235	---	136	1.73
IA-2	198	151	1.31	280	---	151	1.85
IA-3	202	154	1.31	277	---	154	1.80
IA-4	181	150	1.21	192	---	150	1.28
IB-1	158	141	1.12	221	---	141	1.57
IB-2	156	152	1.03	302	---	152	1.99
IIB-1	157	143	1.10	221	---	143	1.54
IIB-2	167	142	1.18	292	77.2	219	1.33
IIB-3	163	146	1.12	312	132.5	279	1.12
IIB-4	163	141	1.16	275	132.5	274	1.00
IIB-5	116	143	0.81	135	---	143	0.94
IIIA-1	164	137	1.20	177	---	137	1.29
IIIA-2	171	134	1.28	183	---	134	1.37
IIIA-3	185	135	1.37	185	---	135	1.37
IIIB-1	136	134	1.01	140	---	134	1.04
IIIB-2	134	139	0.96	179	57.8	197	0.91
IIIB-3	---	138	----	263	84.2	222	1.18
IIIB-4	---	139	----	258	115.8	255	1.01
IIIB-5	111	138	0.80	221	115.8	254	0.87
IIIB-6	111	139	0.80	111	---	139	0.80

* $v_c = \frac{V_c}{bd} = 1.9 \sqrt{f'_c} + 2500 \frac{p\,vd}{M}$

** $v_u = \frac{V_u}{bd} = v_c + Krf_{vy}$ for beams with stirrups,

$v_u = v_c$ for beams without stirrups

Hence,

$$v_u = 1.9 \sqrt{f'_c} + 2500 \frac{pVd}{M} + Krf_{vy} \qquad \text{(Eq'n. 5)}$$

As shown in Table 7, test values agreed reasonably well with the strengths calculated by use of this equation.

In Table 8 test results are also compared with the allowable shear strengths given by the design criteria of the current "Standard Specifications for Highway Bridges" (4). Under these requirements the allowable shearing stress (v_a) for beams without stirrups - computed by $v_c = \frac{V}{bjd}$ - is 0.03 f'_c or 90 psi maximum. For beams with vertical stirrups the allowable shearing stress is given by

$$v_a = \frac{V}{bjd} = 90 + r\, f_v \qquad \text{(Eq'n. 3)}$$

where f_v is the working stress for the stirrup steel. The steel used in all test beams was of structural grade according to the ASTM yield strength requirements. Hence the allowable stirrup stress was f_v = 18,000 psi.

For the beams of shorter shear span (Series I and II) the stresses computed on this basis were found to be safe and generally quite conservative. Emphasizing that these calculated values are intended to be safe working stresses, it is noted that four beams of Series III have factors of safety less than two with respect to shear failure. Beam IIIB-6, which had no web reinforcement, failed with a ratio of only

TABLE 8.

COMPARISON OF TEST STRENGTHS WITH
AASHO "STANDARD SPECIFICATIONS FOR HIGHWAY BRIDGES" (4)

Beam	v_u test** (psi)	$r\,f_v$ (psi)	v_a* (psi)	$\frac{v_u \text{ test}}{v_a}$
IA-1	268	----	90	2.98
-2	320	----	90	3.56
-3	316	----	90	3.51
-4	220	----	90	2.44
IB-1	252	----	90	2.80
-2	346	----	90	3.84
IIB-1	252	----	90	2.80
-2	334	37.0	127	2.63
-3	356	65.1	155	2.30
-4	314	65.1	155	2.02
-5	154	----	90	1.71
IIIA-1	202	----	90	2.24
-2	209	----	90	2.32
-3	212	----	90	2.36
IIIB-1	160	----	90	1.78
-2	204	28.4	118	1.73
-3	300	41.4	131	2.29
-4	295	56.9	147	2.00
-5	252	56.9	147	1.71
-6	127	----	90	1.41

** $v_u \text{ test} = \frac{V_u}{bjd}$ or practically $\frac{8V_u}{7bd}$

* $v_a = 90$ psi for beams without stirrups;

$v_a = 90 + r\,f_v$ for beams with stirrups.

1.4. It is noted that this beam was one which had the tension steel cut off in accordance with the design specifications.

Moment at Shear-Compression Failure

Noting a similarity with the mode of failure in pure bending, it has been hypothesized that failure in shear-compression could also be predicted on the basis of a limiting moment criterion. This has been supported by the fact that in several instances the crushing occurring at the end of a diagonal tension crack has been observed to take place at nearly the same moment, regardless of the moment to shear ratio. (21), (6).

The ultimate moment criterion is much the same as that used for the ultimate strength in pure bending. For the case of beams without stirrups, the analysis is as follows:

Assumptions:

A. Failure occurs at the section of maximum moment by crushing of the concrete in compression above the end of the diagonal crack.

B. The compressive stress block at failure may be defined by three empirical parameters k_1, k_2, k_3.

$$k_3 = \frac{\text{maximum stress at crushing}}{f'_c}$$

$$k_1 = \frac{\text{average stress over the depth } c}{k_3\ f'_c}$$

k_2c = distance from extreme fiber to the resultant compressive force.

C. No shear is carried by "dowel action" of the longitudinal reinforcement.

The following derivation refers to Figure 54.

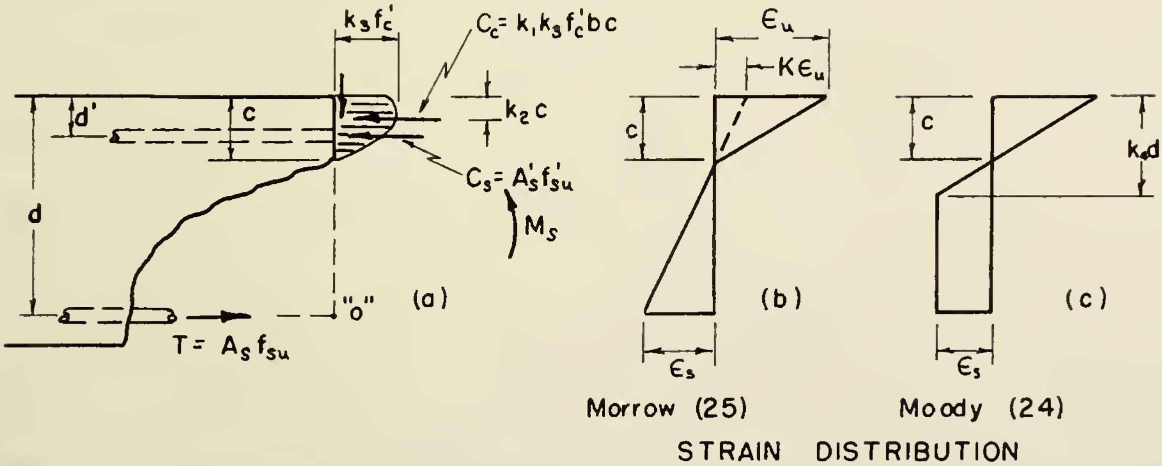

FIGURE 54. CRITERION FOR SHEAR-MOMENT CAPACITY

Summing horizontal forces:

$$k_1 k_3 f_c' \, bc + A_s' \, f_{su}' - A_s f_{su} = 0 \qquad \text{(Eq'n. 6)}$$

Summing moments about "O":

$$M_s = k_1 k_3 f_c' \, bc \, (d - k_2 c) + A_s' \, f_{su}' \, (d - d') \qquad \text{(Eq'n. 7)}$$

Assuming further that the compression zone is reduced sufficiently by the penetration of the crack such that the strain in the compression reinforcement is negligible, Equations (6) and (7) combine to yield:

$$\frac{M_s}{f'_c\, bd^2} = \frac{p\, f_{su}}{f'_c}\left(1 - \frac{k_2}{k_1 k_3}\;\frac{p\, f_{su}}{f'_c}\right) \text{ where } p = \frac{A_s}{bd} \qquad \text{(Eq'n. 8)}$$

where f_{su} and the properties of the stress block $\frac{k_2}{k_1 k_3}$ are the unknowns. For flexural compression failures (over-reinforced beams) the problem of finding f_{su} is simplified by two facts: 1) The distribution of strain across the section is linear; 2) Crushing strain of concrete in flexure has been found to vary over a rather narrow range and is primarily a function of f'_c. For under-reinforced beams, where the tension steel has a well-defined yield point, the ultimate moment criterion is further simplified by the fact that $f_{su} = f_y$. The stres block parameters have been evaluated empirically by many investigators and are known to be primarily functions of f'_c.

For the shear-compression failure, however, the inclination of the diagonal tension crack results in a concentrated rotation about the compression zone, producing a non-linear strain distribution. In addition, splitting along the tension steel in many cases results in a further redistribution, in which the maximum compressive strain is no longer at the extreme fiber. These two facts have been indicated by the strain measurements of this study. (Figures 27-29 and 42-44).

Moody (24) and Morrow (25) assumed strain distributions as shown in Figure 54. On this basis each investigator developed empirical expressions for the steel stress at failure. Moody's equations are based on a series of simple and restrained beams under one and two concentrated loads. Simple beams and knee-frames form the basis of Morrow's equations.

The ultimate moments for the beams failing in shear-compression in this study are compared with the values predicted by these two formulas in Tables 9 and 10. Moody extended his criterion to include beams with web reinforcement, while Morrow considered only beams without stirrups. Moody's equation was found to over-estimate the strength of all beams of this study. The correlation seemed to be somewhat better for beams without web reinforcement. Morrow's equation gave a very good prediction for beams IA-2 and IA-3, each of which contained a double layer of tension steel.

For beams IB-1 and IIB-1 the measured steel stress at failure was substituted into the basic shear-moment equation, using the stress block parameters from both Moody and Morrow. In each case a much better prediction of the actual shear-compression strength was obtained. This is an indication that the basic criterion of a limiting moment is valid, but the major problem is that of accurately predicting the steel stress at failure.

The strain measurements as shown in Figures 27-29 and 42-44 indicate a similarity with the strain distributions

TABLE 9.
MOMENT AT SHEAR-COMPRESSION FAILURE
(Test vs. Calculated from Equations of Ref. 24)

Beam	(Calculated - Moody) f_{su} (psi)	M_s (in-kips)	P_{calc} * (kips)	Measured f_s ** (psi)	P_{test} (kips)	$\frac{P_{test}}{P_{calc.}}$	Calculated (using measured f_s) M_s (in-kips)	$\frac{P_{test}}{P_{calc.}}$
IA-2	43,400	417	54.8	----	49.5	0.90	-----	-----
IA-3	43,800	411	54.0	----	48.0	0.89	-----	-----
IB-1	46,200	412	54.2	36,600	42.0	0.77	332	0.96
IIB-1	54,500	496	53.2	51,500	48.0	0.90	481	0.93
IIB-2	----	755.5	81.0	----	63.0	0.78	-----	-----
IIB-3	----	807	86.5	----	67.0	0.78	-----	-----
IIIB-3	----	861	83.0	----	71.3	0.86	-----	-----
IIIB-4	----	919	88.5	----	70.0	0.79	-----	-----

* $P_{calc.}$ - based on M_s developed at edge of support block. (See Figure 5)

Series I: $P = \frac{M_s}{7.61}$ Series II: $P = \frac{M_s}{9.32}$ Series III: $P = \frac{M_s}{10.38}$

** Measured $f_s = (30 \times 10^6)\,\epsilon_{su}$

(Neglecting influence of compression steel)

Beams without stirrups:

$$M_s = p\, f_s \left(1 - \frac{k_2}{k_1 k_3} \frac{p\, f_s}{f'_c}\right) bd^2 \quad \text{--------- Eqn. (3a) Ref. 24}$$

$$k_2 = .42, \quad k_1 k_3 = 1.121 - 0.0485 \frac{f'_c}{1000} \quad \text{-- Eqns. (5a) and (5b) Ref. 24}$$

$$f_s = \frac{3\frac{M}{vd} - 0.45}{3\frac{M}{vd} + 0.55} \left[6.9 \times 10^{-4} E_s \left(-1 + \sqrt{1 + \frac{1450}{p\, E_s/k_1 k_3\, f'_c}}\right) \right] \quad \text{- Eqn. (6a) Ref. 24}$$

Beams with vertical stirrups:

$$M_s = A_1 M'_s + A_2 A_3 (r\, f_{vy}) \left(\frac{a''}{2}\right)^2 bd^2 \quad \text{---- Eqn. (7) Ref. 24}$$

where M'_s = shear moment capacity of same beam without stirrups.

$A_1 = 1.38$, $A_2 A_3 = .08$ which are empirical constants

a'' = the distance from the section of maximum negative moment to the section of maximum positive moment.

TABLE 10.
MOMENT AT SHEAR-COMPRESSION FAILURE
(Test vs. Calculated from Equations of Ref. 25)

Beam	Calculated (Morrow) f_{su} (psi)	Calculated (Morrow) M_s (in-kips)	Calculated (Morrow) $P_{calc.}$ (kips)	Measured f_s (psi)	Measured P_{test} (kips)	$\frac{P_{test}}{P_{calc.}}$	Calculated using measured f_s: M_s (in-kips)	Calculated using measured f_s: $P_{calc.}$ (kips)	Calculated using measured f_s: $\frac{P_{test}}{P_{calc.}}$
IA-2	37,500	365	48.0	---	49.5	1.03	---	---	---
IA-3	37,500	356	46.8	---	48.0	1.02	---	---	---
IB-1	40,600	365	48.0	36,600	42.0	0.88	332	43.6	0.96
IIB-1	41,800	390	41.9	51,500	48.0	1.15	473	50.8	0.95

(Neglecting influence of compression steel)

$$M_s = p\ f_s \left(1 - \frac{k_2}{k_1\ k_3}\ \frac{p\ f_s}{f'_c}\right) bd^2$$

$$\frac{k_2}{k_1\ k_3} = 0.44\ , \qquad k_1\ k_3 = \frac{800 + f'_c}{70 + f'_c}$$

$$f_s = \frac{1}{2} E_s\ K\epsilon_u \left(-1 + \sqrt{1 + \frac{4k_1 k_3 f'_c}{p\ E_s\ K\epsilon_u}}\right)$$

$$10^4\ K\ \epsilon_u = \frac{1.116\ a/d + .174}{a/d - .872}$$

suggested by both Moody and Morrow. However, the factors which could influence the distribution of strains are numerous: extent of splitting along the tension steel, inclination of the diagonal crack, amount and spacing of web reinforcement, arrangement of tension steel.

Ultimate Strength in Flexure

Strains in the tension steel of Beams IIIB-3 and IIIB-4 indicated the section was at or near its ultimate capacity in bending. By Whitney's ultimate strength criterion (taking f_y = 75,000 psi and f'_c = 4500 psi)

$$M_u = q\,(1 - .59q)\,bd^2 f'_c \text{ where } q = p\,\frac{f_y}{f'_c} \qquad \text{(Eq'n. 9)}$$

$$M_u = 636{,}000''\# \quad \text{(neglecting the compression steel)}$$

For ultimate crushing adjacent to the support block this yields for beams IIIB-3 and IIIB-4:

$$P_u = \frac{636}{10.38} = 61.3 \text{ kips}$$

While the Load vs. Steel Strain curves for both beams (Figures 34 and 35) indicate definite signs of yielding at this load, the ultimate crushing loads were significantly higher (test $P_u = 71.3^k$ and 70^k for IIIB-3 and IIIB-4 respectively). This difference is believed to be primarily due to the fact that the high strength steel used had little or no definite yield plateau. Steel strains at which crushing occurred were

definitely in the work-hardening range. (ϵ_{su} = 10,000 MII for both beams)

In an attempt to obtain a better estimate, the steel stress-strain curve in this work-hardening range was approximated by a straight line, as shown in the sketch below.

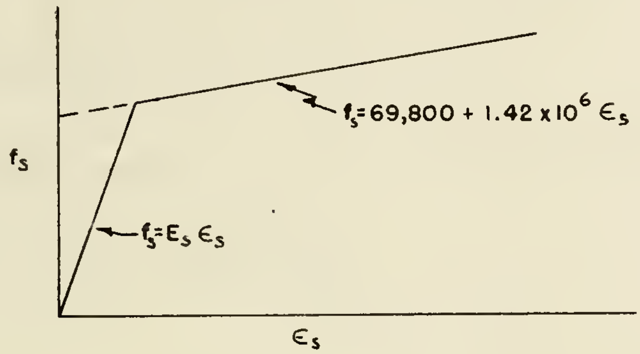

From the results of four tension coupons an average equation for the steel stress in this range was taken to be

$$f_s = 69{,}800 + 1.42 \times 10^6 \epsilon_s$$

Returning to the basic equilibrium equations derived earlier, along with the assumption of a linear distribution of strain across the section, the following was obtained:

$$\epsilon_{su} = \left(\frac{d-c}{c}\right) \epsilon_{cu}$$

where ϵ_{su} and ϵ_{cu} are the maximum steel and concrete strains at failure and $f_{su} = 69{,}800 + 1.42 \times 10^6 \left(\frac{d-c}{c}\right) \epsilon_{cu}$.

Substituting into Equation (6) (neglecting the compression steel)

$$k_1k_3\, f'_c\, bc = A_s\, f_{su} = 69{,}800\, A_s + 1.42 \times 10^6 \left(\frac{d-c}{c}\right) \epsilon_{cu}\, A_s$$

The properties of the stress block for $f'_c = 4500$ psi were taken from Reference (20), Table 2.

$$k_1k_3 = .715\ , \quad k_2 = .445\ , \quad \epsilon_{cu} = .0034$$

Solving the above equation $c = 3.65''$

and substitution into

$$M_u = k_1k_3\, f'_c\, bc\, (d - k_2c)$$

yields

$$M_u = 669{,}000 \text{ in. lbs.}$$

Hence

$$P_u = \frac{669}{10.38} \quad \text{or} \quad P_u = 64.4 \text{ kips}$$

While this is slightly closer to the observed ultimate loads, it must be remembered that the effects of the diagonal tension crack were clearly indicated in both of these beams.

SUMMARY AND CONCLUSIONS

1. The beam tests reported herein indicate two general modes of shear failure in reinforced concrete beams without shear reinforcement:

   A. A "shear compression" failure occurring at the section of maximum moment and shear at loads substantially greater than the load at which the diagonal crack first penetrated the compression zone. Collapse was by crushing of the concrete in the reduced compression zone adjacent to the support, following a significant redistribution of internal strains.

   B. A "diagonal tension" failure occurring generally at some distance away from the support at a load equal to or only slightly greater than the load at which the critical diagonal tension crack formed. These failures were sudden, occurring with very little warning.

2. In the absence of stirrups indications were that the mode of failure was definitely associated with the relative

position of the diagonal tension crack within the shear span. The position of the crack, in turn, was related to the length of shear span to depth ratio. In beams of relatively short shear spans (a/d = 2.2 and 2.9) the crack formed close to the support and progressed gradually into the compression zone to points adjacent or above the support block. For a/d = 4 the crack formed generally near the middle of the shear span and split almost completely through the beam before reaching the support.

An explanation for the difference in location of the crack in the two cases cannot be offered. It seems logical, however, to reason that the difference in failure mechanism is due to differences in restraint to the crack's propagation as it crosses the neutral axis. Adjacent to the support not only are the bending stresses larger, but also there is a high local compression due to concentration of the support reaction. In the case of the long-span beam the crack is located farther out, where the bending stresses are lower and the local compression is absent.

3. Short-span beams with web reinforcement failed basically in the same manner as did the companion beams without stirrups, following yielding of all stirrups crossed by the crack. Splitting along the tension steel and the resulting strain redistribution observed in beams without stirrups was effectively delayed until the stirrups had yielded.

The long span beam with light web reinforcement also failed in the same manner as its companion beam without stirrups. The diagonal crack formed in the same location at the same load. Diagonal tension failure followed yield of the stirrups.

In long span beams with a high percentage of web steel the diagonal tension type failure out in the middle of the shear span was prevented. Stirrups near the support yielded first. Redistribution of strains adjacent to the support was followed by crushing in this region.

4. Both the diagonal cracking load and the ultimate shear strength were increased when a given amount of tension steel was provided by smaller reinforcing bars placed in two layers. It is believed that the increased rigidity of the double-layered arrangement allows a greater portion of the total shear to be carried by "dowel action".

5. Beams with longitudinal steel cut off at the point where it is no longer needed to resist tension suffered a reduction in both the diagonal cracking load and ultimate shear strength. This held true even in beams with closely spaced stirrups. The two beams without stirrups failed suddenly upon formation of the diagonal crack. Each collapsed completely as the bars were stripped out of the concrete.

6. Test strengths, when compared to the maximum allowable shearing stress permitted by the AASHO "Standard Speci-

fications for Highway Bridges" (4), indicated factors of safety of at least two for 15 of the 20 beams tested. Of the beams with lower factors of safety, four had long shear spans (a/d = 4). The lowest factor of safety was 1.41. This particular beam had a long shear-span, no stirrups, and the tension steel cut off.

7. For the beams with extended steel in one layer, the new ACI-ASCE Committee 326 equation predicted the load at diagonal cracking with good accuracy. The ratio of test strength to calculated strength varied from 0.96 to 1.18. When the tension steel was provided in two layers, the equation was slightly more conservative. However, for three of the beams with the tension steel cut off, the test strength was 80% of the calculated value.

8. Test results indicate that a criterion for shear-compression failure based on a limiting moment capacity may be valid, providing an accurate estimate of the steel stress at collapse can be made.

SUGGESTIONS FOR FURTHER RESEARCH

1. The results of the particular beams tested indicate that the manner in which the loads and reactions are carried to the beam may have a large effect of the ultimate shear strength and mode of shear failure. High local compressive forces in the vicinity of the concentrated support reaction seemed to be responsible for the development of the shear-compression type failure, experienced in beams of short shear spans. In many monolithic frames loads and reactions are carried to the beam or girder as distributed shears from other members framing into its sides. Hence, further tests should include beams with: a) loads and reactions similar to the beams of this study, but distributed over larger areas; and b) loads and reactions distributed over the full depth of the beams rather than concentrated on the top and bottom.

2. To provide light percentages of web reinforcement at practical stirrup spacings the use of small diameter, smooth wire stirrups was required for the beams of this study. While adequate anchorage was provided by wrapping the stirrups around the tension steel, there may have been some difference in behavior had deformed bar stirrups been used. To conform more closely with practical beam designs, test beams in the

future should be proportioned such that the larger size, deformed bars can be used.

3. Four beams of this study indicate a definite lack of safety in the present AASHO "Standard Specifications for Highway Bridges" with respect to allowing longitudinal bars to be cut off in the tension zone. This reduction in shear strength, associated with bar cut-off, has been reported in other studies of rectangular beams. (14), (27) Need of further study of this effect has definitely been indicated.

As most bridge girders are monolithic with the deck slab and are actually T-beams, the situation may be somewhat alleviated in the bridge structure. Further tests should include companion specimens of both rectangular and T-sections.

Also, this reduction in strength may not be so severe when the tension steel consists of a larger number of smaller bars. In beams with extended steel the difference in strengths between the single and double-layered arrangements was substantial.

Hence, in studying the bar cut-off effect, a variety of steel arrangements might be considered.

BIBLIOGRAPHY

BIBLIOGRAPHY

1. ACI-ASCE Committee 326, "Shear and Diagonal Tension" ACI Journal, Jan., Feb. 1962 <u>Proceedings</u> Vol. 59.

2. ACI Committee 318, "Building Code Requirements for Reinforced Concrete (ACI 318-56)" ACI Journal, May 1956 <u>Proceedings</u> Vol. 52, pp. 913.

3. ACI Committee 318, "Building Code Requirements for Reinforced Concrete (ACI 318-63)" ACI Standard, June 1963.

4. American Association of State Highway Officials, "Standard Specifications for Highway Bridges."

5. Al-Alusi, A.F., "Diagonal Tension Strength of Reinforced Concrete T-Beams with Varying Shear Span", ACI Journal, May 1957, <u>Proceedings</u>, Vol. 53, pp. 1067.

6. Bower, J.E. and Viest, I.M., "Shear Strength of Restrained Concrete Beams without Web Reinforcement", ACI Journal, July 1960, <u>Proceedings</u>, Vol. 57, pp. 73.

7. Bresler, B. and Scordelis, A.C., "Shear Strength of Reinforced Concrete Beams." ACI Journal, Jan. 1963, <u>Proceedings</u> Vol. 60, pp. 51.

8. Bryant, R.H., Bianchioni, A.C., Rodriguez, J.F., Kesler, C.E., "Shear Strength of Two-Span Continuous Reinforced Concrete Beams with Multiple Point Loading." ACI Journal, Sept. 1962, Proceedings Vol. 59, pp. 1143.

9. Clark, A.P., "Diagonal Tension in Reinforced Concrete Beams," ACI Journal, Oct. 1951, Proceedings Vol. 43, pp. 145.

10. de Cossio, R.D., and Siess, C.P., "Behavior and Strength in Shear of Beams and Frames without Web Reinforcement," ACI Journal, Feb. 1960, Proceedings, Vol. 56, pp. 145.

11. Elstner, R.C., and Hognestad, E., "Laboratory Investigation of Rigid Frame Failure," ACI Journal, Jan. 1957, Proceedings Vol. 53, pp. 637.

12. Ferguson, P.M., and Thompson, J.N., "Diagonal Tension in T-Beams without Stirrups," ACI Journal, Mar. 1953, Proceedings Vol. 49, pp. 665.

13. Ferguson, P.M., "Some Implications of Recent Diagonal Tension Tests," ACI Journal, Aug. 1956, Proceedings Vol. 53, pp. 157.

14. Ferguson, P.M., and Matloob, F.N., "Effect of Bar Cut-off on Bond and Shear Strength of Reinforced Concrete Beams," ACI Journal, July 1959, Proceedings Vol. 56, pp. 5.

15. Guralnick, S.A. "Shear Strength of Reinforced Concrete Beams," ASCE, Vol. 85, STI Jan. 1952, Paper 1909.

16. Guralnick, S.A. "High Strength Deformed Steel Bars for Concrete Reinforcement," ACI Journal, Sept. 1960, Proceedings Vol. 57, pp. 241.

17. Hanson, J.A. "Shear Strength of Lightweight Reinforced Concrete Beams," ACI Journal, Sept. 1958, Proceedings Vol. 55, pp. 387.

18. Hognestad, E. "Fundamental Concepts in Ultimate Load Design of Reinforced Concrete Members," ACI Journal, June 1952, Proceedings Vol. 48, pp. 809.

19. Hognestad, E. "What Do We Know About Diagonal Tension and Web Reinforcement in Concrete?" Circular Series No. 64, University of Illinois Engineering Experiment Station, Mar. 1952.

20. Hognestad, E., Hanson, N.W., and McHenry, D. "Concrete Stress Distribution in Ultimate Strength Design," ACI Journal, Dec. 1955, Proceedings Vol. 52, pp. 455.

21. Laupa, A., Siess, C.P., Newmark, N.M. "Strength in Shear of Reinforced Concrete Beams," Bulletin No. 428, University of Illinois Engineering Experiment Station, 1955.

22. Mathey, R.G., and Watstein, D. "Shear Strength of Beams without Web Reinforcement Containing Deformed Bars of Different Yield Strength," ACI Journal, Feb. 1963, Proceedings Vol. 60, pp. 183.

23. Moody, K.G., Viest, I.M., Elstner, R.C. "Shear Strength of Reinforced Concrete Beams," ACI Journal, Dec. 1954, Jan., Feb. 1955, Proceedings Vol. 51, pp. 317, 417, 525.

24. Moody, K.G., and Viest, I.M., "Shear Strength of Reinforced Concrete Beams," Part 4 - Analytical Studies, ACI Journal, Mar. 1955, Proceedings Vol. 51, pp. 697.

25. Morrow, JoDean, and Viest, I.M. "Shear Strength of Reinforced Concrete Frame Members without Web Reinforcement," ACI Journal, Mar. 1957, Proceedings Vol. 53, pp. 833.

26. Rensaa, E.M. "Shear, Diagonal Tension, and Anchorage in Beams," ACI Journal, Dec. 1958, Proceedings Vol. 55, pp. 695.

27. Rodriguez, J.J., Bianchioni, A.C., Viest, I.M., Kesler, C.E. "Shear Strength of Two-Span Continuous Reinforced Concrete Beams," ACI Journal, April 1959, Proceedings Vol. 55, pp. 1089.

28. Taub, J., and Neville, A.M. "Resistance to Shear of Reinforced Concrete Beams," Parts 1, 2, 5, ACI Journal, Aug., Sept., Dec. 1960, Proceedings Vol. 59, pp. 193, 315, 715.

29. Watstein, D., and Mathey, R.G. "Strains in Beams having Diagonal Cracks," ACI Journal, Dec. 1958, Proceedings Vol. 55, pp. 717.

30. Zowyer, E.M., and Siess, C.P. "Ultimate Strength in Shear of Simply-Supported Prestressed Concrete Beams without Web Reinforcement," ACI Journal, Oct. 1954, Proceedings Vol. 51, pp. 181.

31. Hognestad, E., Hanson, N.W., Magura, D.D., and Mass, M.A. "Shear Strength of Slender Continuous Reinforced Concrete T-Beams," PCA Journal, Vol. 5, No. 3, Sept. 1963.

APPENDIX A

STRESS-STRAIN PROPERTIES OF THE REINFORCEMENT

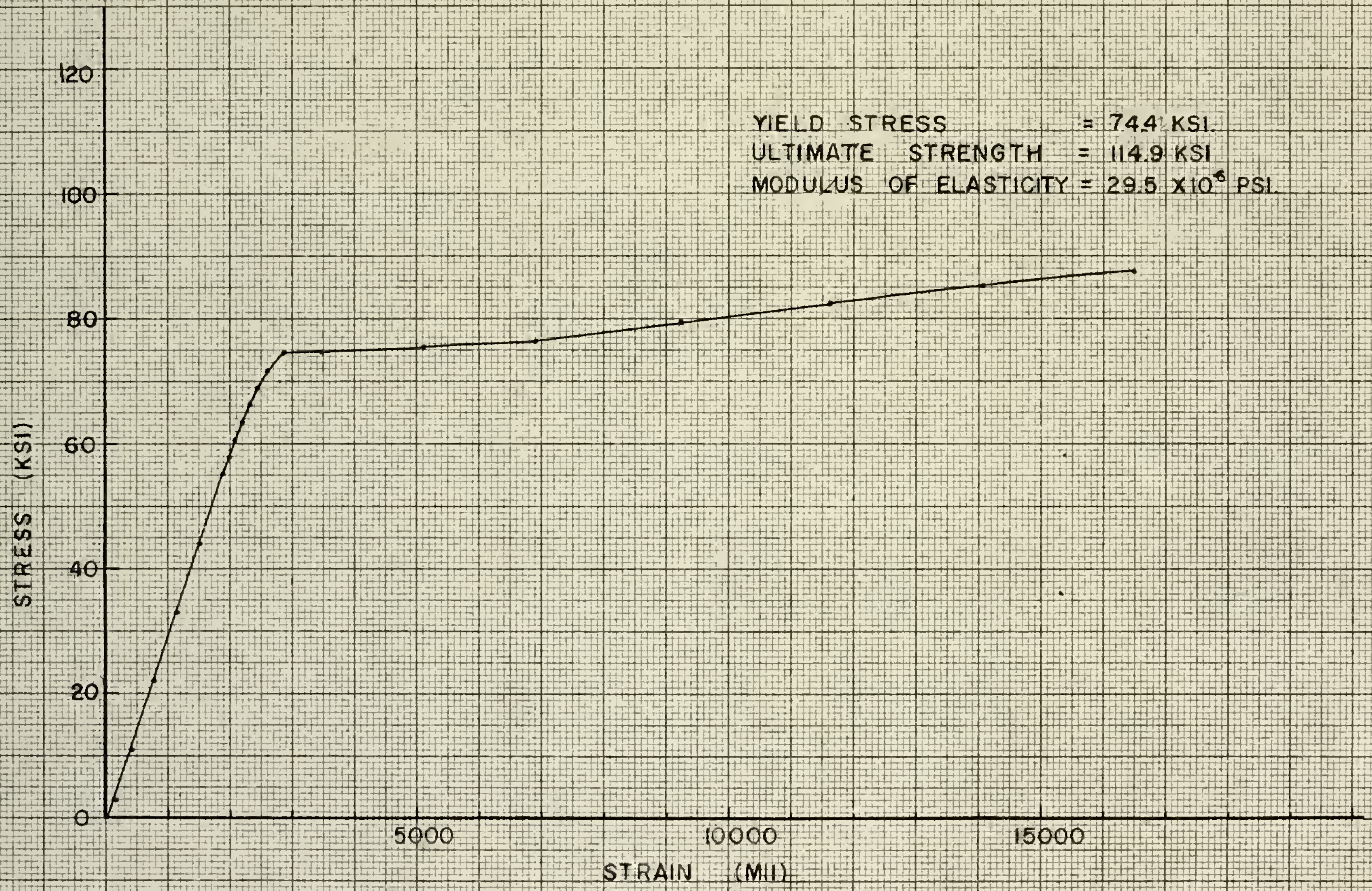

FIGURE 55. TYPICAL STRESS—STRAIN PROPERTIES — LONGITUDINAL STEEL

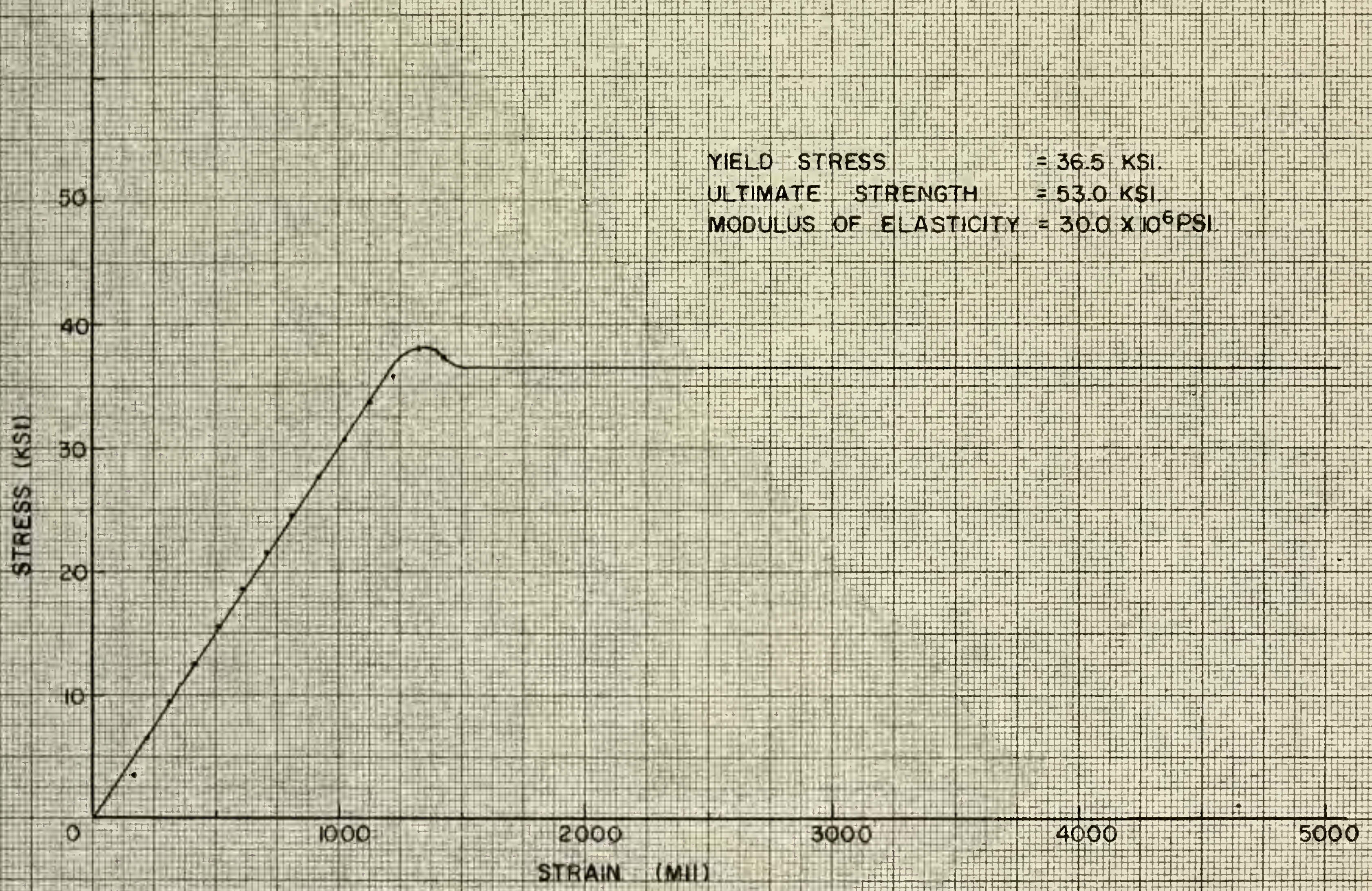

FIGURE 56. TYPICAL STRESS - STRAIN PROPERTIES — STIRRUP STEEL

APPENDIX B

PROCEDURES FOR APPLICATION AND WATERPROOFING OF THE SR-4 STRAIN GAGES

APPENDIX B

PROCEDURES FOR APPLICATION AND WATERPROOFING OF THE SR-4 STRAIN GAGES

Type A-18, SR-4 electric strain gages were used for all beam specimens. The installation procedures used were in general, those recommended by the manufacturer and are given as follows.

Surface Preparation

Placement of gages on the deformed bars required the removal of a small portion of two of the lugs to allow space for the gage. The lugs and mill scale were removed with a file. Emery cloth of medium coarseness was then used to obtain a smooth surface.

The area was finally cleansed with carbon tetrachloride and methyl-ethyl keytone.

Application

The gage was placed and held in position by taping the leads to the bar. The leads were insulated from the bar by placing a small piece of electrical tape under the leads and tip of the gage. A liberal amount of Duco household cement was then applied both to the bar and to the gage. Pressure to

the gage was applied through a small neoprene pad wrapped firmly with heavy string. After applying the cement, a piece of cellophane tape, wrapped around one end of the gage with the sticky side out, held both the gage and neoprene pad in place. The string was wrapped, starting at the center of the gage and working both ways.

Pressure was applied for approximately 20 minutes, after which time the pad and tape were removed to allow proper curing of the cement. The cement was then cured at air temperature for three hours, at 110°-120°F for 2 hours, and at 160°-170°F for an additional eight hours.

Upon completion of curing No. 18 Gencaseal insulated copper wire leads were soldered directly to the terminal wires of the gage and were taped to the bar. The resistance of the gage and the resistance to ground were then checked to insure proper functioning of the gage.

Waterproofing

To provide protection against both moisture and against possible damage to the gage during placement of the concrete a tough, but pliable asphaltic material* was used. The bar was completely covered in the vicinity of the gage (generally over a length of 2 1/2" to 3"). The asphalt was poured hot

---

* "Petrolastic" asphalt No. 155 obtained from the American Bitumuls and Asphalt Company, 200 Bush Street, San Francisco, California.

over the bar in two layers. Prior to application the bar was heated in the vicinity of the gage to prevent the asphalt from cooling too quickly. After the first layer had cooled, the leads were lapped back across the gage to obtain embedment over a substantial length of the wire. The first layer of asphalt was pressed and kneaded while still soft to remove air pockets which usually formed, particularly around the leads.

APPENDIX C

LOAD - STRAIN DATA

TABLE 11.
STEEL AND CONCRETE STRAINS - BEAM IB-1*

Load (kips)	No. 6 Bar (MII) 3 1/2" from Support	No. 6 Bar (MII) 16" from Support	No. 6 Bar (MII) 24" from Support	Compression Zone 3 1/2" from Support Bottom		Remarks
				East	West	
5	49	18	0	150	50	
10	210	32	0	300	100	
15	444	52	0	450	250	
20	615	72	0	600	350	
24	747	252	0	650	450	
26	812	316	0	750	500	
28	875	399	0	800	550	
30	937	466	0	900	600	
32	1003	527	10	1000	750	
34	1066	604	20	1100	850	
34.8	1084	909	430	1100	850	
36.4	1074	---	---	1150	900	
35.6	----	1054	---	----	---	Load dropped due to splitting
35.0	----	----	900	----	---	along tension steel.
37	1095	1104	1000	800	650	
38	1120	1134	1030	750	650	
39	1144	1157	1060	700	600	
40	1169	1184	1090	650	550	
41	1197	1214	1120	650	550	
42.0	----	1244	1160	600	500	Ultimate Load

* See Figure 17 for gage locations.

TABLE 12.
STEEL AND CONCRETE STRAINS - BEAM IB-2*

Load (kips)	No. 6 Bar (MII) 3 1/2" from Support	Compression Zone, 3 1/2" from Support: Bottom East	Bottom West	1" from Bottom East	1" from Bottom West	Remarks
5	40	---	---	---	50	
10	163	---	150	50	200	
15	394	350	250	150	300	
20	624	400	300	200	300	
25	796	450	250	150	250	
30	976	400	400	150	450	
32	1034	600	---	---	---	
34	1098	---	----	---	---	
35	1125	---	250	500	450	
37	1169	---	---	---	---	
38	1195	450	---	550	---	
39.7	---	800	600	700	1200	
41	---	800	600	850	1200	
42	1236	---	---	---	---	
44	1294	---	---	---	---	
46	1345	---	---	---	---	
48	1401	---	---	---	---	
50	1465	---	---	---	---	
51	---	1050	1100	900	1150	
52	1510	---	---	---	---	
54	1561	1050	---	1050	---	
56	1611	---	---	---	---	
58.1	---	---	---	---	---	Ultimate Load

* See Figure 18 for gage locations.

TABLE 13.
CONCRETE STRAINS - BEAM IA-2*

Load	Compressine Zone, 3 1/2" from Support (Mu)						Remarks
	Bottom		1 1/2" from Bottom		3" from Bottom		
(kips)	East	West	East	West**	East	West	
5	50	150	50	---	50	50	
10	150	350	100	---	100	150	
15	200	450	150	---	150	200	
20	250	550	150	---	150	250	
25	300	750	150	---	150	300	Crack penetrated between 1 1/2" and 3" gage points
30	350	800	200	---	150	150	
35	650	1100	200	---	200	50	
37	550	1300	-300***	---	250	0	
38	500	1300	-300	---	400	150	
39	500	1300	-450	---	250	150	
42	500	1300	-450	---	250	15	

* See Figure 20 for gage locations

** Gage Point Lost

*** (-) denotes tensile strain

TABLE 14.
CONCRETE STRAINS - BEAM IA-3*

Compression Zone, 3 1/2" from Support (MII)

Load	Bottom		1 1/2" from Bottom	
(kips)	East	West	East	West
5	100	150	100	50
10	200	250	200	100
15	300	400	250	200
20	400	550	300	300
25	450	600	350	400
30	550	750	600	500
35	850	950	700	550
38	900	1000	700	650
39	950	1000	---	700
42	950	1000	800	750
46	800	850	---	---

* See Figure 21 for gage locations.

TABLE 15.
STEEL STRAINS - BEAM IA-4*

Load (kips)	No. 5 Bar (MII) 3 1/2" from Support (East)	No. 5 Bar (MII) 3 1/2" from Support (West)	No. 5 Bar (MII) 18" from Support	No. 5 Bar (MII) 24" from Support	Remarks
2	15	17	6	0	
5	42	40	14	0	
10	223	252	28	2	
15	428	462	43	7	
20	603	649	91	17	
25	767	809	152	20	
30	935	961	398	108	
32	1007	1019	584	398	
33	1052	1054	626	520	
34.0					Ultimate Load

* See Figure 22 for gage locations

TABLE 16.
CONCRETE STRAINS - BEAM IA-4*

Compression Zone, 3 1/2" from Support

Load	Bottom		1" from Bottom		2" from Bottom		
(kips)	East	West	East	West	East	West	Remarks
2	50	50	50	---	50	---	
5	150	100	200	50	100	50	
10	300	200	300	100	200	100	
15	450	300	400	200	250	150	
20	550	400	450	250	300	200	
25	650	550	550	300	350	250	
30	800	650	650	350	400	250	
32	950	750	750	400	450	250	
33	1150	800	800	200	450	250	
34	950						

* See Figure 22 for gage locations.

TABLE 17.
STEEL AND CONCRETE STRAINS - BEAM IIB-1 *

Load (kips)	No. 6 Bar 3 1/2" from Support	Compression Zone, 3 1/2" from Support: Bottom East	Bottom West	1" from Bottom East	1" from Bottom West	2" from Bottom East	2" from Bottom West	Remarks
5	45	---	50	---	---	---	150	
10	188	150	150	100	150	---	250	
15	473	---	---	---	---	---	---	
20	728	400	400	350	300	200	200	
25	938	---	---	---	---	---	---	
27	1020	---	---	---	---	---	---	
29	1109	---	---	---	---	---	---	
30	1148	700	700	550	450	400	325	Crack between gage points at 2" from bottom at 34^k - 36^k.
32	1218	---	---	---	---	---	---	
34	1298	900	950	550	550	-200**	400	
36	1367	900	1150	1000	500	-800	- 50	
37	1392	---	---	---	---	---	---	
38	1428	---	---	---	---	---	---	
39	1448	650	950	1400	750	-1200	-600	
40	Load dropped off suddenly							
36.5	1318	---	---	---	---	---	---	
40	1435	---	---	---	---	---	---	
41	1470	---	---	---	---	---	---	
42	1508	500	900	3400	1200	-950	---	
43	1542	---	---	---	---	---	---	
46	1650	---	---	---	---	---	---	
48	1720	400	700	5400	1500	500	---	Ultimate Load.

* See Figure 31 for gage locations.

** (-) denotes tensile strain.

TABLE 18.

STEEL AND CONCRETE STRAINS - BEAM IIB-2*

Load (kips)	No. 6 Bar (MII) 3 1/2" from Support	Stirrups (MII) (a)	(b)	(c)	Compression Zone, 3 1/2" from Support Bottom East	Bottom West	1/2" from Bottom East	1/2" from Bottom West	1" from Bottom East	1" from Bottom West	Remarks
5	132	0	0	0	---	---	---	---	---	---	
10	253	0	0	0	10	150	100	250	250	250	
15	460	0	50	0	---	---	---	---	---	---	
20	660	0	132	0	---	---	350	300	350	400	
25	859	0	205	0	---	---	---	---	---	---	
30	1061	21	340	10	600	600	550	500	450	450	
32	1132	50	380	19	---	---	---	---	---	---	
34	1208	107	453	50	---	---	---	---	---	---	
36	1292	875	1243	992	950	950	850	550	550	500	
37	1320	939		1081	---	---	---	---	---	---	
38	1351	981		1139	---	---	---	---	---	---	
39	1390	1050		1229	1050	1050	850	850	550	550	
40	1425	1101		1285	---	---	---	---	---	---	
42	1497	1240		1400	---	---	---	---	---	---	
44	1572	1400			1350	1300	1000	1000	700	550	
46	1549				---	---	---	---	---	---	
48	1722				1450	1400	1400	1200	800	550	
50	1792		Yielding		---	---	---	---	---	---	
52	1884				1700	1550	1650	1400	900	450	
54	1970				1600	1650	1900	1550	1200	450	
55	2020				---	---	---	---	---	---	
56	2068			Yielding	---	---	---	---	---	---	
57	2100	Yielding			---	---	---	---	---	---	
59	2200				1900	1800	2150	1700	1150	---	
61	---				2100	2150	2450	---	1250	---	
62	2388				---	---	---	---	---	---	
63	2500				---	---	3100	---	1500	---	Ultimate Load

* See Figure 32 for gage locations.

TABLE 19.

STEEL AND CONCRETE STRAINS - BEAM IIB-3*

Load (kips)	No. 6 Bar (MII) 3 1/2" from Support	Stirrups (MII) (a)	(b)	(c)	Compression Zone, 3 1/2" from Support: Bottom East	Bottom West	1/2" from Bottom East	1/2" from Bottom West	1" from Bottom East	1" from Bottom West	Remarks
5	40	0	0	0	150	150	150	50	100	100	
10	102	0	0	0	---	---	---	---	---	---	
15	431	0	0	0	200	400	250	250	150	200	
20	630	0	0	18	---	---	---	---	---	---	
25	802	0	0	81	450	500	400	400	350	350	
30	978	0	0	210	---	---	---	---	---	---	
35	1082	0	119	362	600	900	500	650	450	550	
40	1358	49	332	551	---	---	---	---	---	---	
45	1530	210	541	773	800	1100	700	750	600	650	
50	1700	570	1060	1300	---	---	---	---	---	---	
52	1770	634	1170		1100	1450	900	1050	800	850	
54	1839	690	1321		---	---	---	---	---	---	
56	1909	765	1400		---	---	---	---	---	---	
58	1978	842		Yielding	1600	1800	950	1150	1000	900	
60	2052	929			---	---	---	---	---	---	
62	2135	1050	Yielding		1750	2000	1000	1300	1150	950	
64	2237	1290			---	---	---	---	---	---	
66	2365	1590			1550	2500	1450	1800	1400	1150	
66	2730	Yielding			4350	6550	6450	4500	1800	1750	
67	2890 to 3250				---	---	---	---	---	---	Ultimate Load

* See Figure 33 for gage locations.

TABLE 20.
STEEL AND CONCRETE STRAINS _ BEAM IIB-4*

Load (kips)	No. 6 Bar (MII) 3 1/2" from Support	Stirrups (MII) (a)	Stirrups (MII) (b)	Compression Zone, 3 1/2" from Support: Bottom East	Bottom West	1/2" from Bottom East	1/2" from Bottom West	1" from Bottom East	1" from Bottom West	2" from Bottom East	2" from Bottom West	Remarks
5	50	0	0	50	50	---	50	---	---	100	100	
10	113	0	0	---	---	---	---	---	---	---	---	
15	342	0	0	200	300	---	200	250	150	200	150	
20	550	72	0	---	---	---	---	---	---	---	---	
25	730	190	22	400	450	400	350	350	300	250	200	
30	918	351	248-280	---	---	---	---	---	---	---	---	
35	1150	472	483	800	800	650	550	600	400	300	150	
40	1350	560	605	---	---	---	---	---	---	---	---	
45	1560	662	778	950	1000	750	700	650	550	350	200	
50	1780	812	962	---	---	---	---	---	---	---	---	
55	2010	960	1130	1350	1350	1000	950	850	700	450	150	
57	2105	Yielding	1270	---	---	---	---	---	---	---	---	
59	2192	Rapidly	Yielding Rapidly									Ultimate Load

* See Figure 34 for gage locations.

TABLE 21.
STEEL STRAINS - BEAM IIIB-1*

No. 6 Bars
(MII)

Load (kips)	3 1/2" from Support East	West	Remarks
5	70	70	
8	242	237	
10	382	370	
11	433	430	
12	485	492	
15	628	643	
16	672	685	
18	760	779	
20	850	863	
24	1018	1037	
28	1187	1210	
32	1342	1365	
36	1505	1527	
37.1			Ultimate Load

* See Figure 45 for gage locations.

TABLE 22.
STEEL AND CONCRETE STRAINS - BEAM IIIB-2*

Load (kips)	No. 6 Bars (MII) 3 1/2" from Support	Stirrups (MII) (a)	(b)	(c)	Compression Zone (MII) Bottom Center	Remarks
5	113	0	0	0		
10	343	0	6	0		
15	607	0	12	0		
20	829	0	37	20		Load Removed
23.4						
0	152	0	10	11	0	
5	337	0	20	17	100	
10	510	0	28	23	200	
15	693	0	37	28	300	
20	878	0	42	35	400	
25	1092	0	48	55	450	
30	1307	10	108	97	700	
32	1390	12	118	110	---	
34	1475	23	137	143	---	
36	1560	47	155	220	1000	Critical diagonal crack formed as 36^k was sustained.
36	1568	53	214	440	---	
37	1607	60	242	483	---	
38	1645	63	270	533	---	
40	1732	97	357	798	1200	
42	1818	120	395	908	---	
43	1860	138	413	965	1250	
44	1908	162	448	1082	---	
45	1945	180	488	1165	---	
46	1990	200	572	1280	1350	
47	2040	242	770	Yielding		Ultimate Load.
48	2050	320	1400	Rapidly		
			Yielding Rapidly			

* See Figure 46 for gage locations.

TABLE 23.
STEEL AND CONCRETE STRAINS - BEAM IIIB-3*

Load (kips)	No. 6 Bars (MII) 3 1/2" from support	Stirrups (MII) (a)	Stirrups (MII) (b)	Compression Zone, 3 1/2" from Support: Bottom Center	1/2" from Bottom East	1/2" from Bottom West	1 1/2" from Bottom East	1 1/2" from Bottom West	Remarks
5	59	0	10	150	200	200	150	200	
10	245	0	15	---	---	---	---	---	
15	603	0	18	450	350	450	250	350	
20	835	0	31	---	---	---	---	---	
25	1080	0	140	650	550	600	450	400	
30	1305	32	308	---	---	---	---	---	
32	1385	62	345	---	---	---	---	---	
34	1469	161	421	---	---	---	---	---	
36	1560	220	480	1050	850	900	600	700	
38	1651	310	541	---	---	---	---	---	
40	1739	398	612	---	---	---	---	---	
42	1838	481	685	1200	950	1000	650	650	
44	1929	570	749	---	---	---	---	---	
46	2029	640	792	---	---	---	---	---	
48	2138	738	838	---	----	---	---	---	
50	2278	839	880	1500	1600	1400	800	800	
54	2600	1060	1020	1650	1600	1500	1000	800	
56	2810	1165	1110	---	---	---	---	---	
58	3078 to 3185	1219-1250	1150-1180	2000	2050	1750	1150	1000	Initial Yielding
60	3390 to 3530	1280-1310	1208-1218	2500	2500	2100	1050	1000	No. 6 Bars at 58^k
62	3650 to 4120	1360	Yielding	2850	2950	2350	1100	1050	
63	4270	1400	Rapidly	3050	3750**	2550	1200	1100	
64	4420 to 4760	1440		3350	4100	2700	1200	1200	
65	4960 to 5130	1480		3600	5100	2900	---	---	
67	5700 to 5950	1580		5350	7150	3250	1550	1400	
70	8600	1700							
71.3	10260								Ultimate Load.

* See Figure 47 for gage locations.

** First visible signs of crushing at $P = 63^k$ on East side in lower 1/2".

TABLE 24.
STEEL STRAINS - BEAM IIIB-4*

Load (kips)	No. 6 Bars (MII) 3 1/2" from Support	Stirrups (MII) (a)	(b)	(c)	(d)	Remarks
5	55	0	0	0	0	
10	308	0	15	0	0	
15	570	32	42	0	0	
20	818	119	112	0	0	
25	1080	210	191	48	0	
30	1305	278	279	139	15	
35	1528	350	370	332	151	
40	1742	429	728	400	260	
45	1958	488	985	470	425	
50	2179	561	1250	546	648	
52	2279	599	1362	590	715	
54	2375	631	1458	613	752	
56	2482	668	Yielding	662	800	
58	2613	699		719	840	
60	2840	730		770	892	
62	3200	760		820	1001	Initial Yielding No. 6 Bar
62	4145	---		---	---	
64	6060	789		873	1130	
66	6725	825		910	Yielding	
68	7395	882		939		
68	8610	---		---		Crushing in compression zone
70	10980	970		1160		Ultimate Load

* See Figure 48 for gage locations.

TABLE 25.
CONCRETE STRAINS - BEAM IIIB-4*

Surface Strains (MII) - Compression Zone 3 1/2" from Support

Load	Bottom		1/2" from Bottom		1 1/2" from Bottom		2 1/2" from Bottom		Remarks
(kips)	East	West	East	West	East	West	East	West	
5	---	---	100	---	100	150	150	150	
15	350	300	250	300	150	200	250	100	
25	500	500	400	450	300	250	150	100	
40	1050	900	850	850	500	450	300	50	
50	1200	1300	1150	1250	650	450	250	50	
56	1550	1600	1400	1450	700	550	250	50	
60	1700	1900	1550	1700	850	750	350	100	
62	1900	2100	1850	1850	950	750	450	150	
64	1950	2300	1950	2050	1000	850	---	---	
66	2400	2700	2200	2350	1100	800	---	---	
68	2550	3200	2750	2850	1300	850	---	---	First visible signs of crushing at P = 68k
70	---	---	---	6550	2050	1150	---	---	

* See Figure 48 for gage locations.

TABLE 26.

STEEL AND CONCRETE STRAINS - BEAM IIIB-5*

Load (kips)	No. 6 Bars (MII) 3 1/2" from Support	Stirrups (MII) (a)	(b)	(c)	Bottom East	Bottom West	1/2" from Bottom East	1/2" from Bottom West	1 1/2 from Bottom East	1 1/2 from Bottom West	Remarks
5	60	0	0	0	250	100	100	500	250	200	
10	325	0	0	0	---	---	---	---	---	---	
15	570	0	0	0	400	350	250	300	300	300	
20	797	5	38	0	---	---	---	---	---	---	
25	1048	20	97	0	600	600	500	550	350	400	
30	1250	30	170	390	---	---	---	---	---	---	
35	1451	65	242	620	800	900	700	800	550	500	
40	1660	110	313	863	---	---	---	---	---	---	
45	1861	181	389	1129-1160	1050	1200	1000	1100	650	750	
50	2084	299	450	1365-1390	---	---	---	---	---	---	
55	2322	419	489	Yielding	1600	1450	1400	1400	700	700	
59.6	2435	---	---	Rapidly	---	---	---	---	---	---	Ultimate Load

* See Figure 49 for gage locations.

TABLE 27.
STEEL STRAINS - BEAM IIIA-3*

Load (kips)	No. 5 Bar (MII) 3 1/2" from Support	No. 4 Bar (MII) 3 1/2" from Support	Remarks
5	68	48	
10	280	240	
15	533	500	
20	784	730	
25	1005	940	
30	1229	1148	
35	1442	1348	
37	1525	1424	
39	1613	1508	
40	1660	1545	
41	1702	1583	
42	1745	1622	
43	1787	1662	
44	1837	1705	
45	1878	1743	
45.9			Ultimate Load

* See Figure 53 for gage locations.